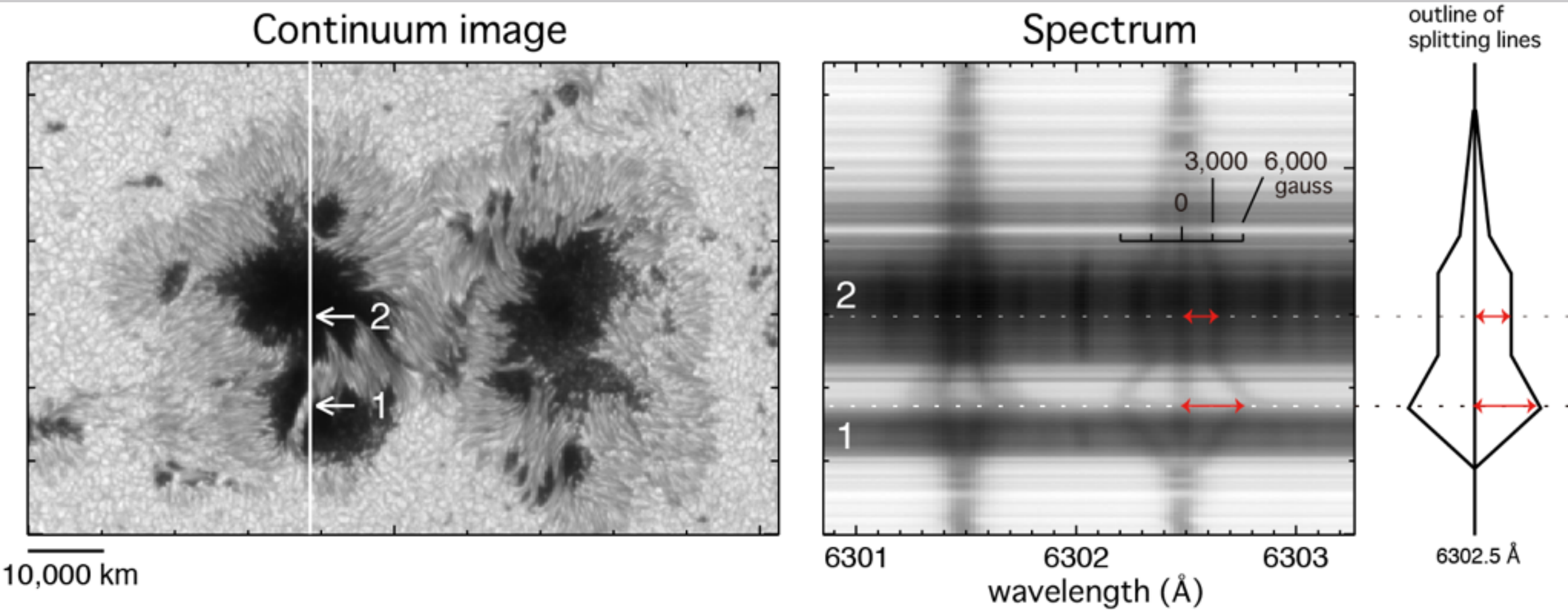


The Strongest Magnetic Fields in Sunspots and their Statistical Properties



Joten Okamoto
(NAOJ, Japan)

Motivation of This Study

What should we do, fully utilizing the performance of the high polarimetric accuracy of Hinode/SOT/SP ?

Motivation of This Study

What should we do, fully utilizing the performance of the high polarimetric accuracy of Hinode/SOT/SP ?

All papers with SP data published by Japanese researchers/students as first authors

Hinode/SOT has only SP now after Feb. 2016, using 54% telemetry of Hinode.

More papers with SP data are important for extension of Hinode mission and keeping our motivation of operation.

← → ↻ 🏠 ⓘ 🔒 https://hinode.nao.ac.jp/user/joten/paper_year_SOTSP.html

ver.	2019.02.22	paper	citation	19	18	17	16	15	14	13	12	11	10	09	08	07
#	Total	54		0	1	4	1	2	6	2	5	4	6	7	10	6
1	Ishikawa, R.	5	275									1	2	1	1	
2	Ichimoto, K.	3	173												1	2
3	Okamoto, T.	3	173		1									1	1	
4	Kubo, M.	7	152					1			1	1			2	2
5	Shimizu, T.	4	140					1			1		1	1		
6	Tsuneta, S.	1	131												1	
7	Kusano, K.	1	100								1					
8	Inoue, S.	3	89								2	1				
9	Toriumi, S.	3	75			1		1	1							
10	Fujimura, D.	1	75											1		
11	Katsukawa, Y.	3	74								1		1			1
12	Nagata, S.	1	73												1	
13	Shiota, D.	1	56								1					
14	Watanabe, H.	4	52						2					2		
15	Ito, H.	1	50										1			
16	Bamba, Y.	2	40						1	1						
17	Magara, T.	1	33												1	
18	Morinaga, S.	2	28												1	1
19	Shimojo, M.	1	15											1		
20	Iida, Y.	1	14										1			
21	Kanoh, R.	1	11				1									
22	Otsuji, K.	1	6					1								
23	Oba, T.	2	4			2										
24	Kano, R.	1	4						1							
25	Kawabata, Y.	1	1			1										

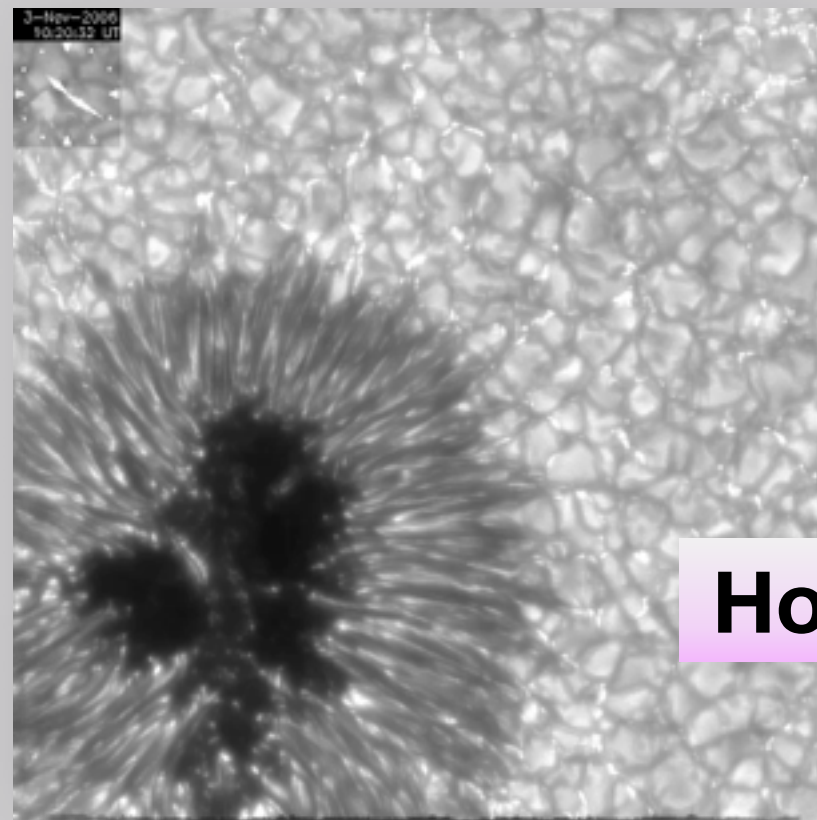
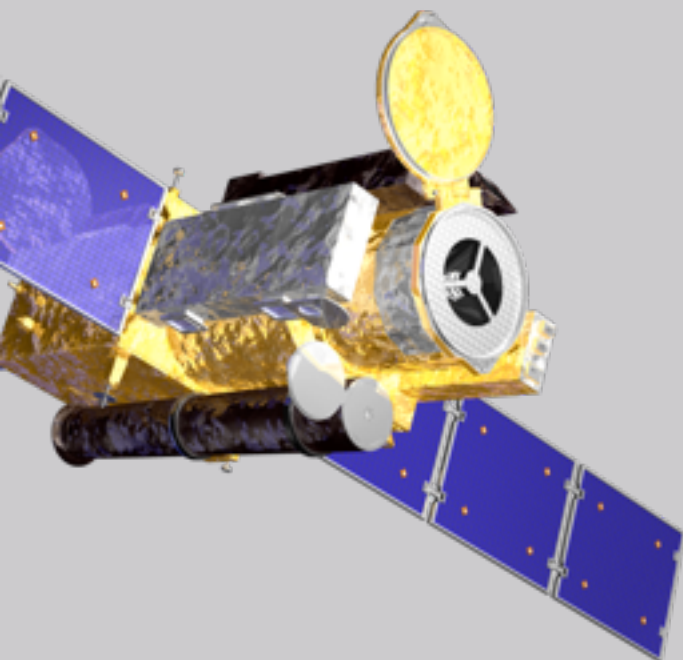
Motivation of This Study

What should we do, fully utilizing the performance of the high polarimetric accuracy of Hinode/SOT/SP ?

Hinode data accumulation for 10 years since 2006

SP data — highest polarimetric accuracy and constant data quality from space

good for statistical analysis



◀ sunspot field strength
typically 3,000 G

How large is the strongest ?

What I Did First

to investigate magnetic field strengths and their properties
of all sunspots observed by Hinode

[used data] SP level-2 data provided by HAO

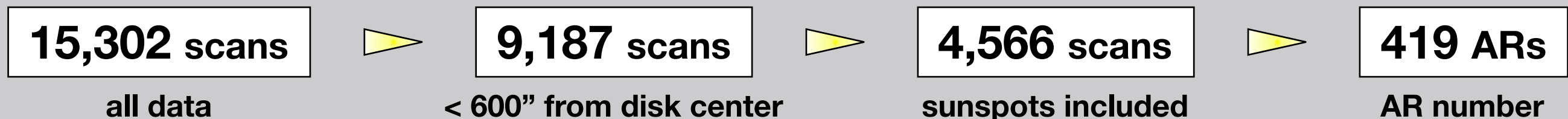
(field strength, azimuth, inclination, Doppler velocity, filling factor)

Oct. 25, 2006 – September 16, 2016

MERLIN inversion, limited field strength 5,000 G

partially used MEKSY inversion data (by NAOJ) for pixels > 5,000 G

= Milne-Eddington Katsukawa Shimojo Yokoyama
(submitted in 2008, and accepted as Yokoyama+2019 !)



What I Did First

419 ARs

- ▶ pick up the largest field strength of each AR
- ▶ extract physical parameters and locations of the strongest field

- location
- spectral shape
- close to PIL
- redshift at the location
- horizontal flow toward the location
- fitting result
- filling factor

[umbra] [penumbra] in large sunspot
[umbra] [outside umbra] in small ss.
[light bridge]

→ **Ranking list of sunspot field strength**

Ranking Top 30

	AR number	date	coordinates	spectral shape	location	redshift			fitting	multi comp	strength	
						PIL	↓	flow	↓		MERLIN	MEKSY
1	AR 11967	2014.02.04	(+248 -115)	VVV	light br	o	o	o	O	-mul	6251 G	
2	AR 11882	2013.10.28	(-464 -225)	VVV	light br	o	o	o	O		5046 G	
3	AR 11302	2011.09.30	(+331 + 93)	_/	light br	o	o	o	X		4991 G	--> 4055 G
4	AR 12297	2015.03.12	(- 77 -168)	_/	light br	o	o	o	X		4985 G	--> 4049 G
5	AR 11944	2014.01.05	(-509 -111)	V	lb/p (s)	o	o	o	X	-mul	4915 G	--> 3306 G
6	AR 11974	2014.02.14	(+356 -112)	VVV	light br	o	o	o	X		4855 G	--> 4225 G
7	AR 10930	2006.12.09	(-410 - 93)	ww-IV	umbra				O		4836 G	
8	AR 11515	2012.07.05	(+437 -350)	ww-I	penumbra	o	o	o	X	-mul	4807 G	--> 3913 G
9	AR 12192	2014.10.25	(+275 -323)	ww-IV	umbra				O		4743 G	
10	AR 11899	2013.11.21	(+574 + 51)	ww-IV	umbra				O		4702 G	
11	AR 11045	2010.02.09	(+362 +461)	VVV	light br	o	o	o	O	-mul	4692 G	
12	AR 11560	2012.09.03	(+368 - 87)	_/	penumbra	o	o	o	X		4691 G	--> 3817 G
13	AR 12546	2016.05.22	(+418 -143)	ww-IV	umbra				N		4684 G	
14	AR 12209	2014.11.19	(-199 -307)	_/	penumbra	o	o	o	O	-mul	4673 G	
15	AR 12080	2014.06.07	(-222 -218)	V	penumbra	o	o	o	X	-mul	4542 G	
16	AR 11429	2012.03.07	(-491 +381)	_/	penumbra		o	o	X	-mul	4503 G	
17	AR 11476	2012.05.09	(-554 +220)	_/	light br	o	o	o	O		4477 G	
18	AR 11890	2013.11.10	(+337 -267)	_/	light br	o	o	o	X		4461 G	--> 3708 G
19	AR 11785	2013.07.07	(-114 -256)	_/	penumbra	o	o	o	X		4365 G	--> 3601 G
20	AR 11339	2011.11.06	(-387 +259)	_/	penumbra	o	o	o	X		4363 G	--> 3679 G
21	AR 12497	2016.02.12	(+340 +310)	VVV	light br	o	o	o	O		4349 G	
22	AR 12422	2015.09.27	(+221 -458)	_/	light br	o	o	o	X		4320 G	--> 4700 G
23	AR 11166	2011.03.10	(+339 +257)	_/	penumbra	o	o	o	X	-mul	4271 G	--> 3249 G
24	AR 12529	2016.04.12	(-283 +245)	ww-IV	umbra				N		4262 G	
25	AR 11748	2013.05.17	(-455 +193)	_/	light br	o	o	o	X	-mul	4241 G	--> 3629 G
26	AR 12222	2014.11.30	(-224 -350)	ww-IV	umbra				O		4178 G	
27	AR 10956	2007.05.19	(+ 10 + 61)	_/	lb/p (s)	o	o	o	O		4160 G	
28	AR 10923	2006.11.12	(-305 -114)	ww-IV	umbra				O		4137 G	
29	AR 11161	2011.02.19	(+271 +415)	_/	light br	o	o	o	O		4135 G	
30	AR 11263	2011.08.02	(-197 +171)	ww-IV	umbra				O		4099 G	

Ranking Top 30

	AR number	date	coordinates	spectral shape	location	redshift			fitting	multi comp	strength	
						PIL	↓ flow	↓	↓		MERLIN	MEKSY
1	AR 11967	2014.02.04	(+248 -115)	VVV	light br	o	o	o	O	-mul	6251 G	
2	AR 11882	2013.10.28	(-464 -225)	VVV	light br	o	o	o	O		5046 G	
3	AR 11302	2011.09.30	(+331 + 93)	_/	light br	o	o	o	X		3991 G	--> 4055 G
4	AR 12297	2015.03.12	(- 77 -168)	_/	light br	o	o	o	X		4985 G	--> 4049 G
5	AR 11944	2014.01.05	(-509 -111)	V	lb/p (s)	o	o	o	X	-m	4915 G	--> 3306 G
6	AR 11974	2014.02.14	(+356 -112)	VVV	light br	o	o	o	X		4855 G	--> 4225 G
7	AR 10930	2006.12.09	(-410 - 93)	ww-IV	umbra				O		4836 G	
8	AR 11515	2012.07.05	(+437 -350)	ww-I	penumbra	o	o	o		-mul	4807 G	--> 3913 G
9	AR 12192	2014.10.05	(- 975 - 899)	ww-IV	umbra				O		4743 G	
10	AR 11899	2013.11.10	(+337 -267)	_/	light br	o	o	o	O		4702 G	
11	AR 11045	2013.07.07	(-114 -256)	_/	penumbra	o	o	o	O	-mul	4692 G	
12	AR 11560	2013.07.07	(-114 -256)	_/	penumbra	o	o	o	X		4691 G	--> 3817 G
13	AR 12546	2016.04.12	(-283 +245)	ww-IV	umbra				N		4684 G	
14	AR 12209	2016.04.12	(-283 +245)	ww-IV	umbra				O	-mul	4673 G	
15	AR 12080	2016.04.12	(-283 +245)	ww-IV	umbra				X	-mul	4542 G	
16	AR 11429	2013.05.17	(-455 +193)	_/	light br	o	o	o	X	-mul	4503 G	
17	AR 11476	2013.05.17	(-455 +193)	_/	light br	o	o	o	O		4477 G	
18	AR 11890	2013.11.10	(+337 -267)	_/	light br	o	o	o	X		4461 G	--> 3708 G
19	AR 11785	2013.07.07	(-114 -256)	_/	penumbra	o	o	o	X		4365 G	--> 3601 G
20	AR 11339	2011.11.06	(-387 +259)	_/	penumbra	o	o	o	X		4363 G	--> 3679 G
21	AR 12497	2016.02.12	(+340 +310)	VVV	light br	o	o	o	O		4349 G	
22	AR 12422	2015.09.27	(+221 -458)	_/	light br	o	o	o	X		4320 G	--> 4700 G
23	AR 11166	2011.03.10	(+339 +257)	_/	penumbra	o	o	o	X	-mul	4271 G	--> 3249 G
24	AR 12529	2016.04.12	(-283 +245)	ww-IV	umbra				N		4262 G	
25	AR 11748	2013.05.17	(-455 +193)	_/	light br	o	o	o	X	-mul	4241 G	--> 3629 G
26	AR 12222	2014.11.30	(-224 -350)	ww-IV	umbra				O		4178 G	
27	AR 10956	2007.05.19	(+ 10 + 61)	_/	lb/p (s)	o	o	o	O		4160 G	
28	AR 10923	2006.11.12	(-305 -114)	ww-IV	umbra				O		4137 G	
29	AR 11161	2011.02.19	(+271 +415)	_/	light br	o	o	o	O		4135 G	
30	AR 11263	2011.08.02	(-197 +171)	ww-IV	umbra				O		4099 G	

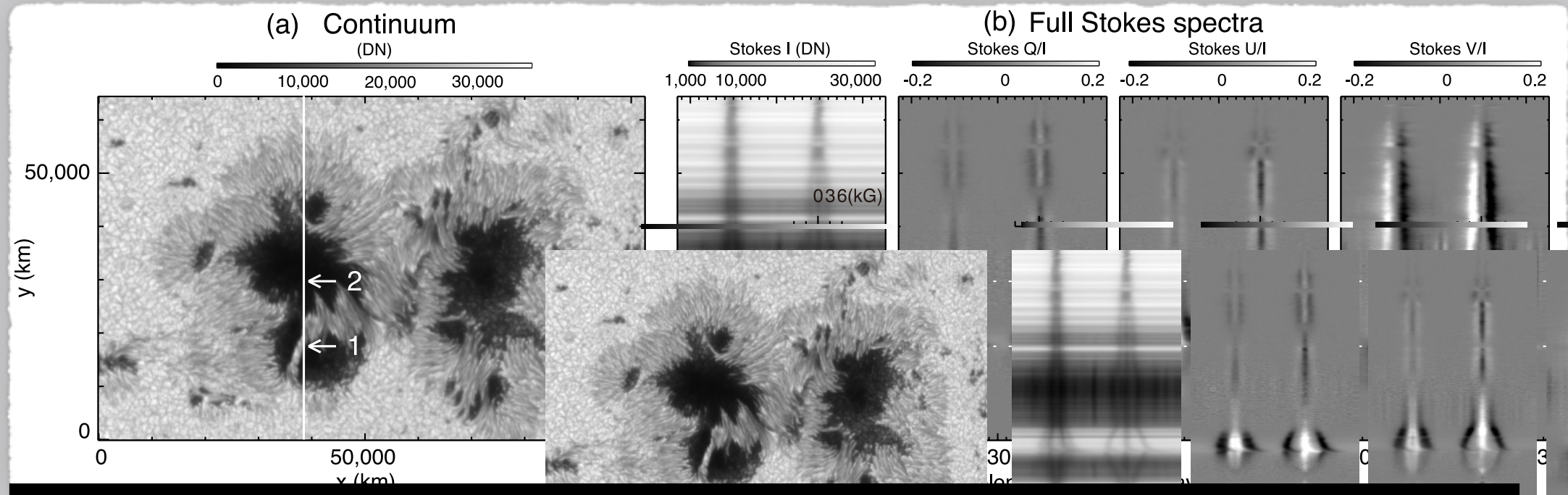
How large is the strongest ?

Answer : 6,250 G

Sunspot with Strongest Magnetic Field

Okamoto & Sakurai 2018, ApJ

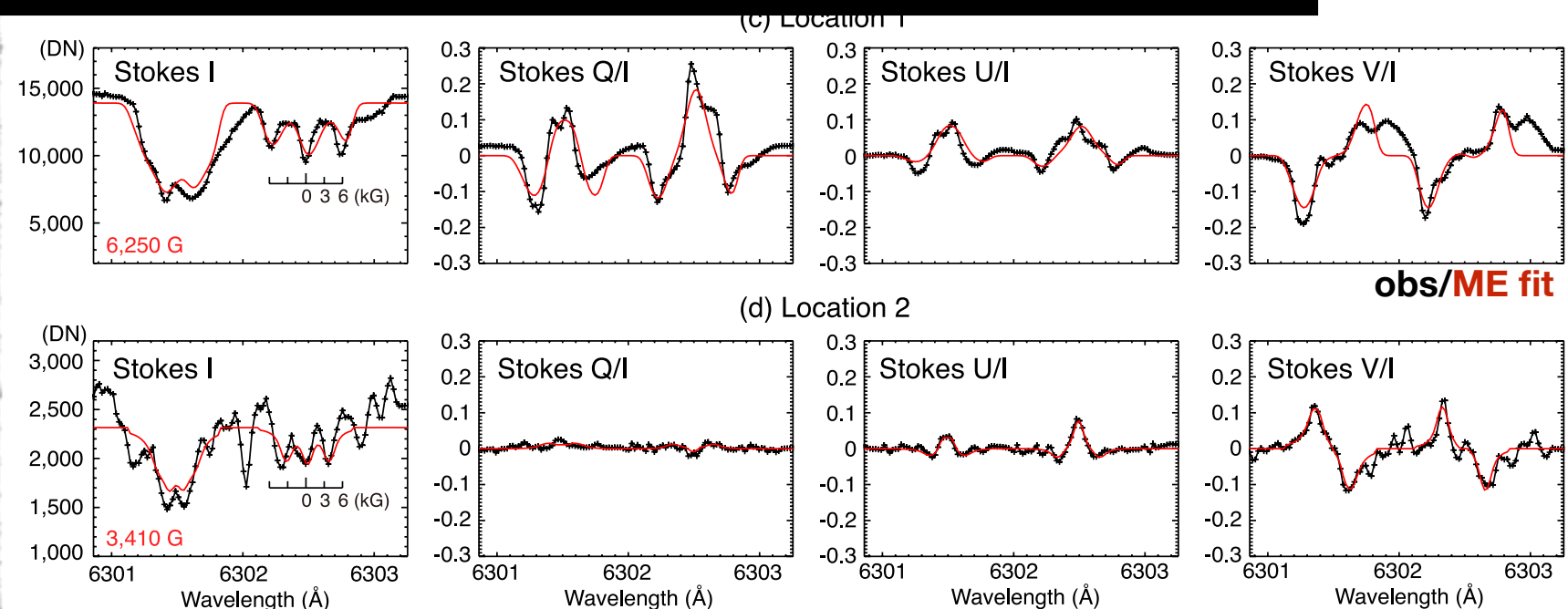
February 4, 2014 (AR 11967)



Why does a so-strong field exist outside an umbra ?

clear Zeeman splitting
in the light bridge

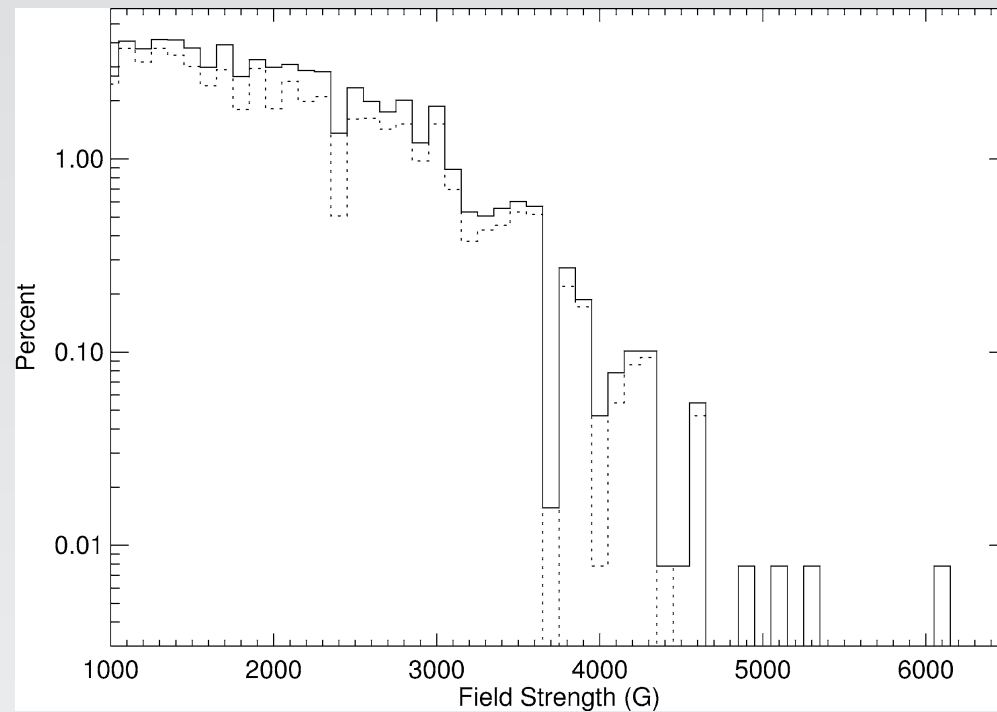
easy to derive the strength
even without inversion
6,250 G



not so strong in the umbra, no more than 4,300 G

Previous Researches

Livingston+2006



1917 – 2004

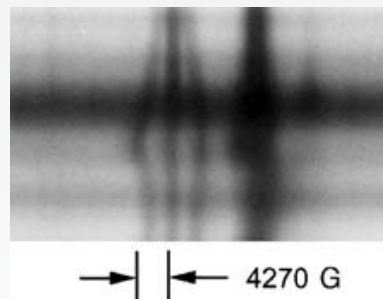
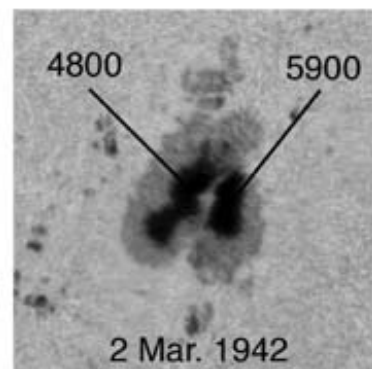
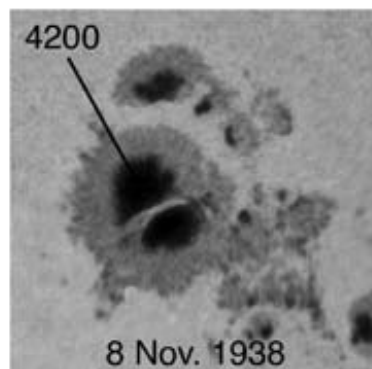
Mt. Wilson Observatory

visible light, Stokes-I

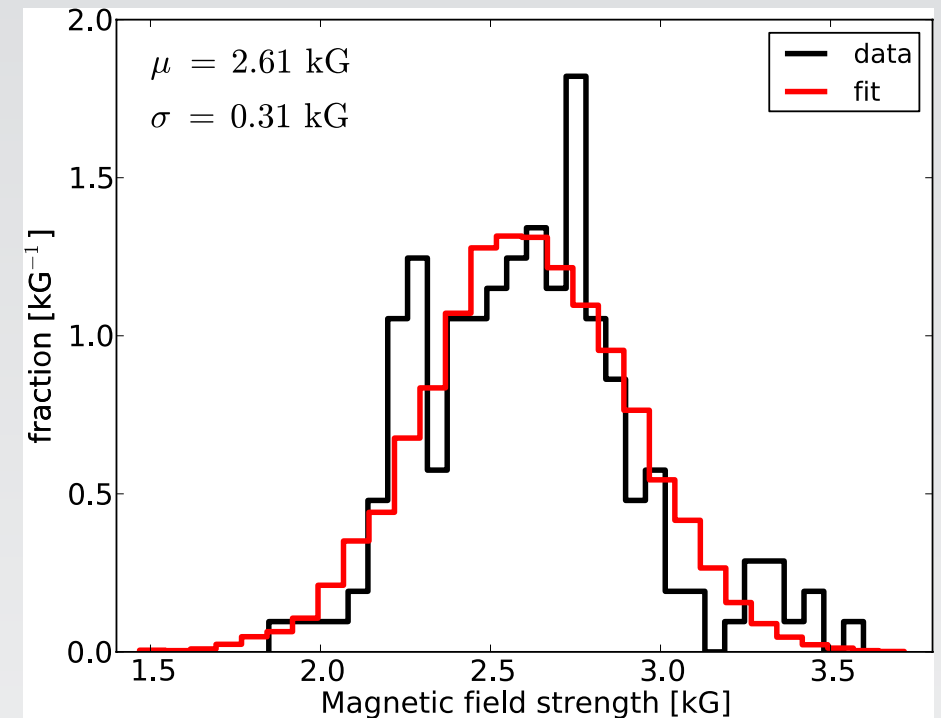
strongest field – 6,100 G (1942)

only 4 examples over 5,000 G

under 5,000 G after 1972



Rezaei+2012

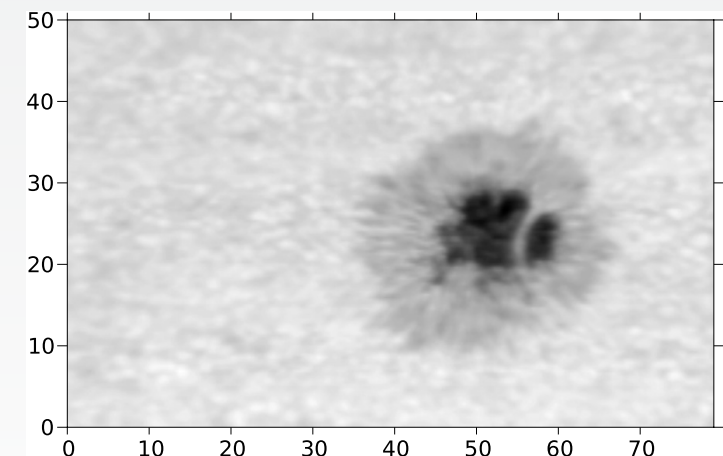


1999 – 2011

VTT/TIP

infrared, Stokes-V

strongest field – 3,600 G



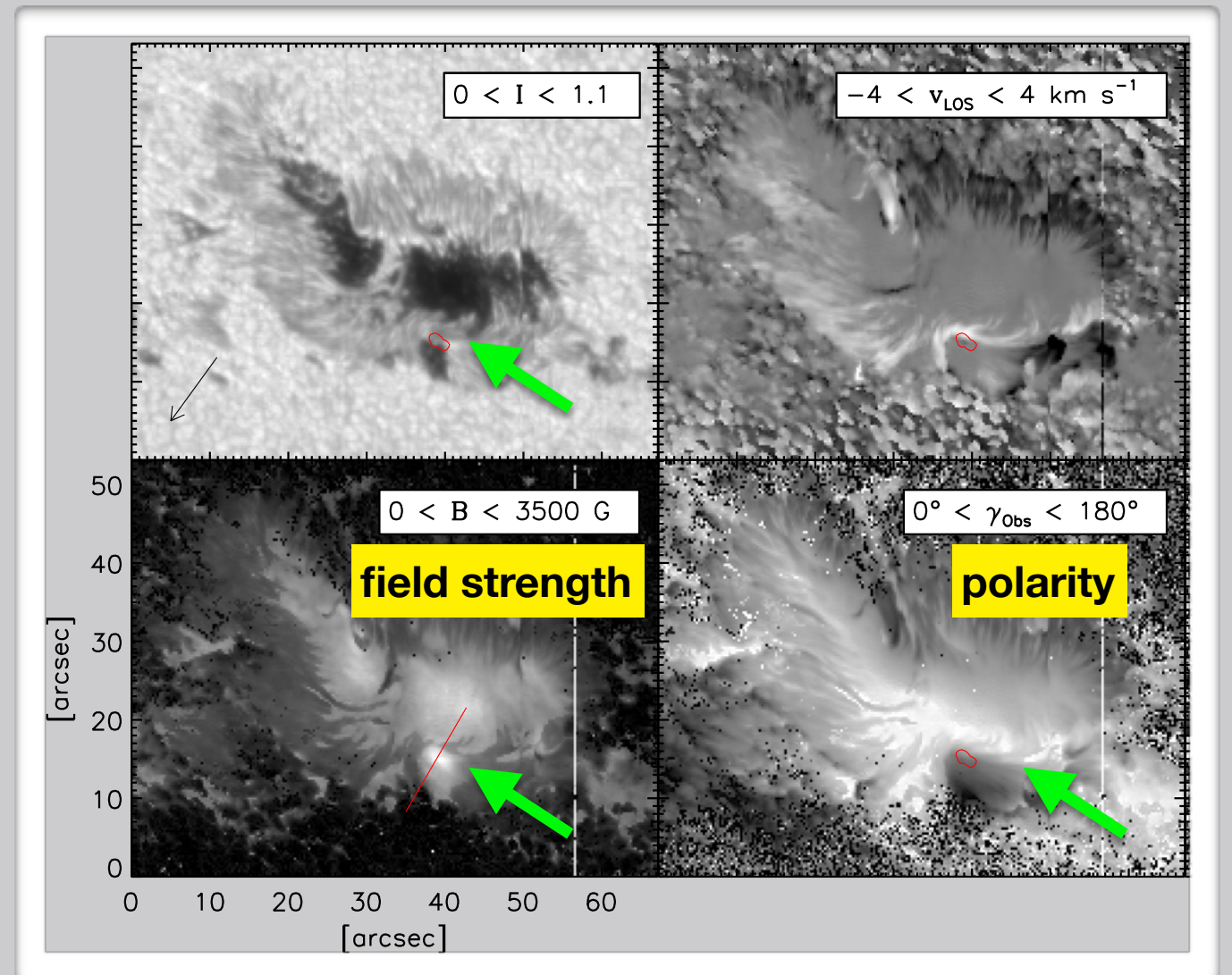
Previous Researches

often observed stronger fields
in light bridges and penumbrae
sandwiched by opposite-polarity
regions

(Tanaka 1991, Zirin+1993, Lites 2002)

unknown mechanism to generate
such a stronger field

Jaeggli 2016



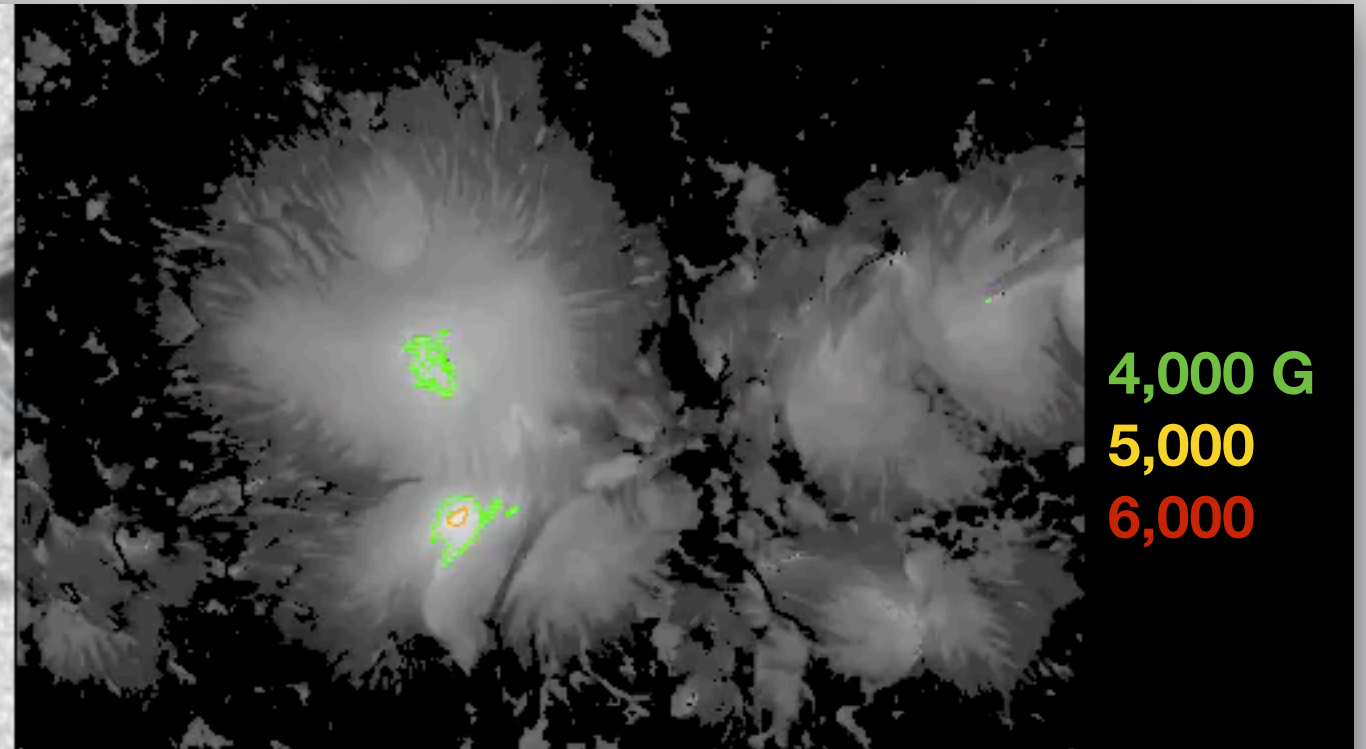
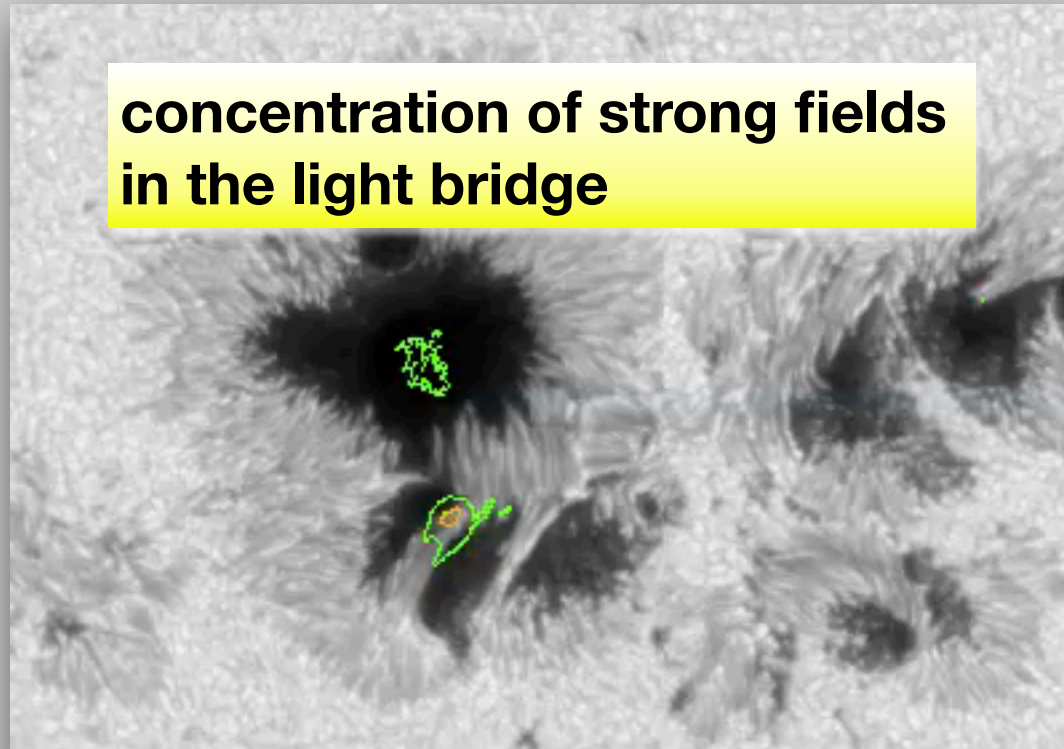
We can investigate the temporal evolution of strong fields existing
under the similar conditions.

Field Strength in Each Scan

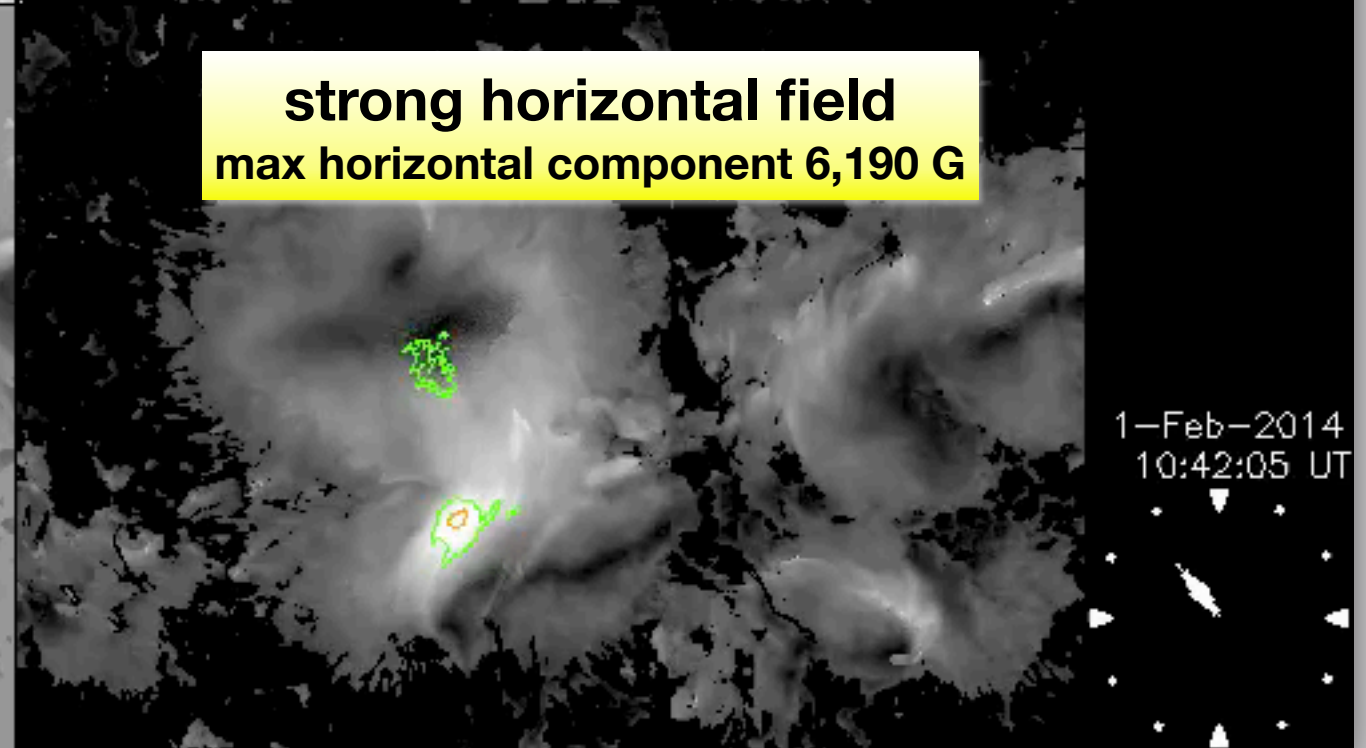
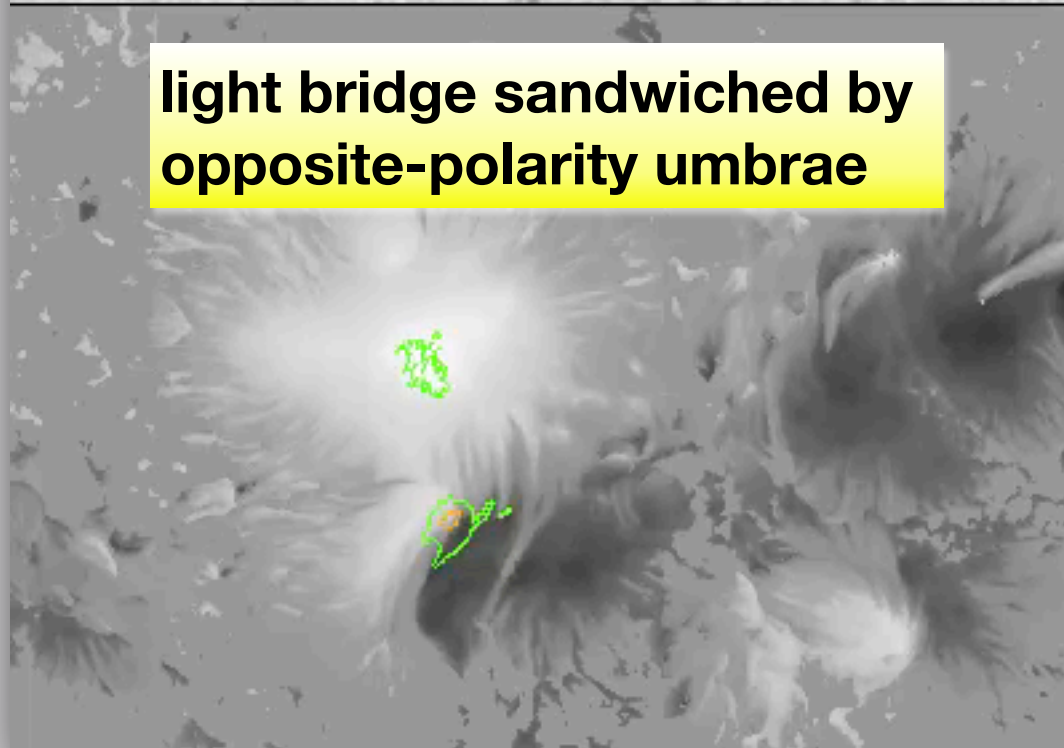
31 scans in February 1-6, 2014

Continuum

Absolute field strength $|B|$



4,000 G
5,000
6,000



1-Feb-2014
10:42:05 UT

Vertical component B_{ver}

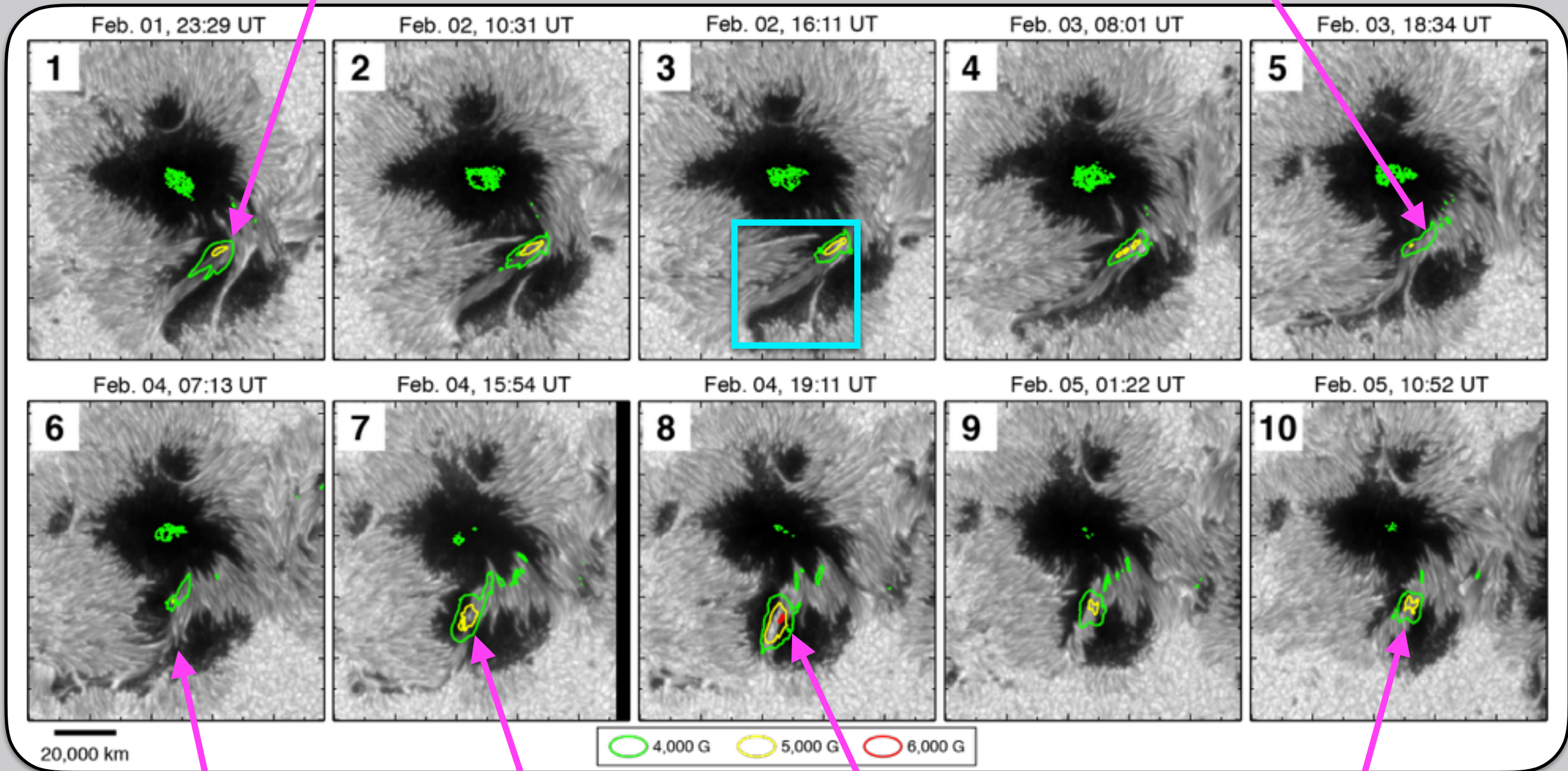
Horizontal component B_{hor}

180-deg ambiguity solved with AZAM (Lites+1995); vector field on local frame

Temporal Evolution of the Strong Field Region

northern part of the light bridge

gradual decay



changing orientation of the light bridge

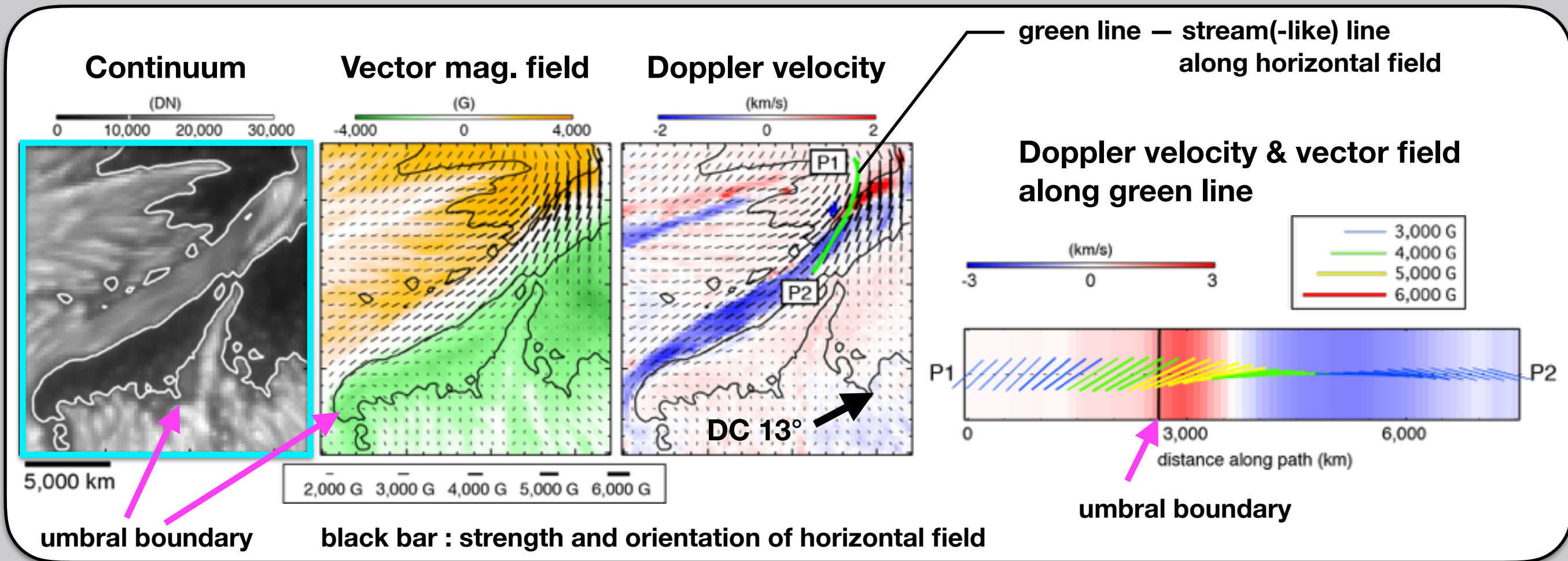
reappearance

over 6,000 G

decay again



Doppler Velocity and Field Strength



▶ horizontal field parallel to the light bridge

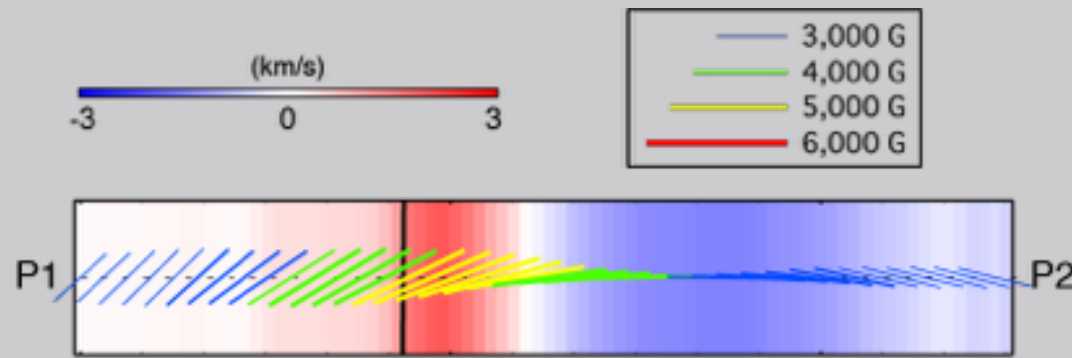
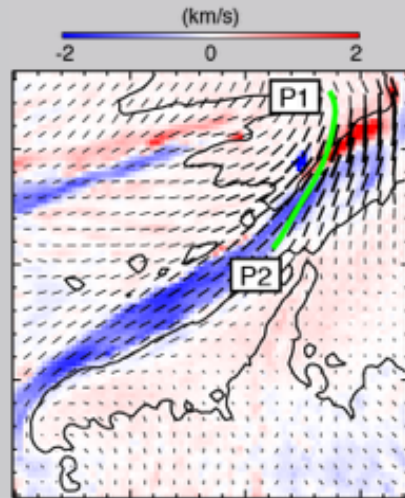
▶ coherent blueshift in the light bridge

7 km/s northward if assumed horizontal flow ~ Evershed flow (penumbra)

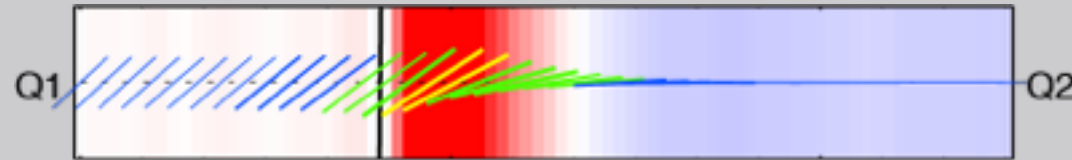
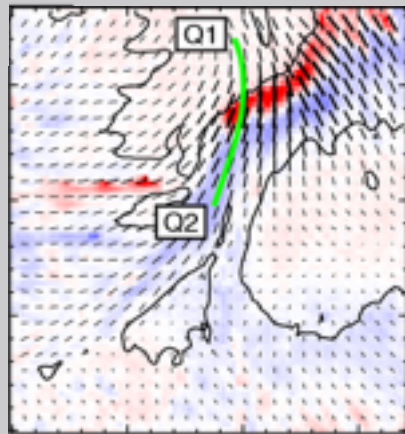
▶ redshift, increasing field inclination, and field enhancement at crosspoint of horizontal field and umbral boundary

Doppler Velocity and Field Strength

Feb. 02
16:11 UT

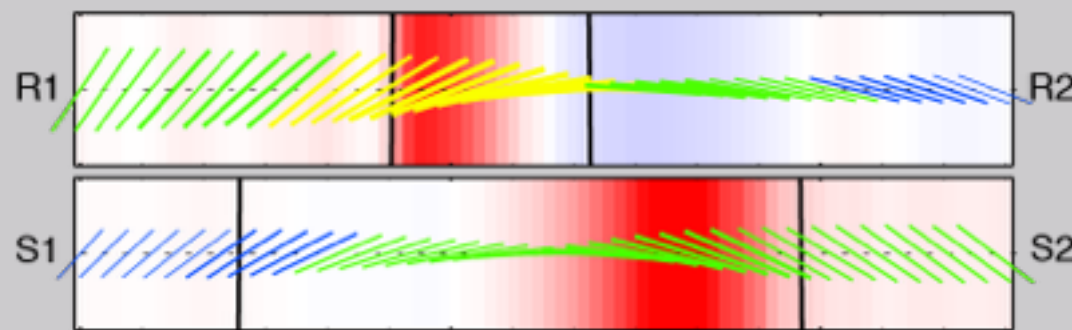
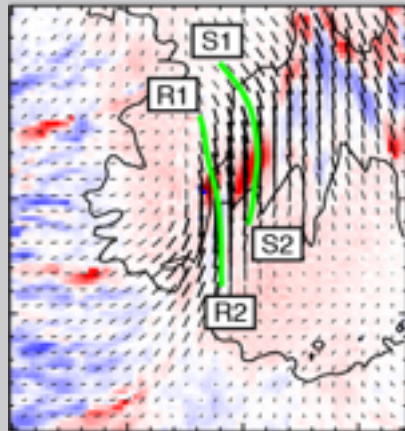


Feb. 03
18:34 UT



similar features seen during the observations

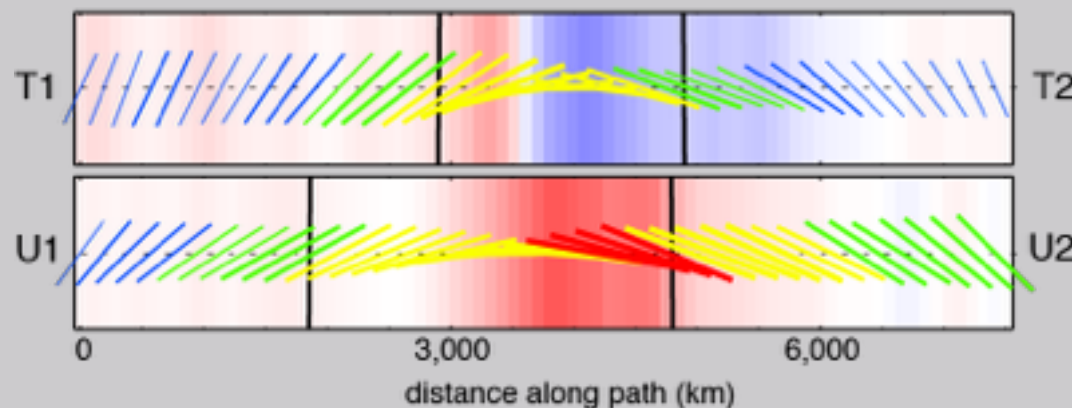
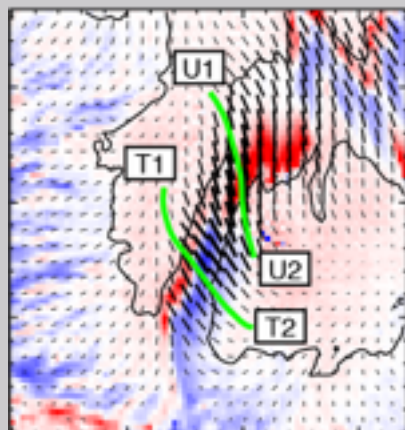
Feb. 04
15:54 UT



at the boundary

- blueshift → redshift
- inclination increased
- field strength enhanced

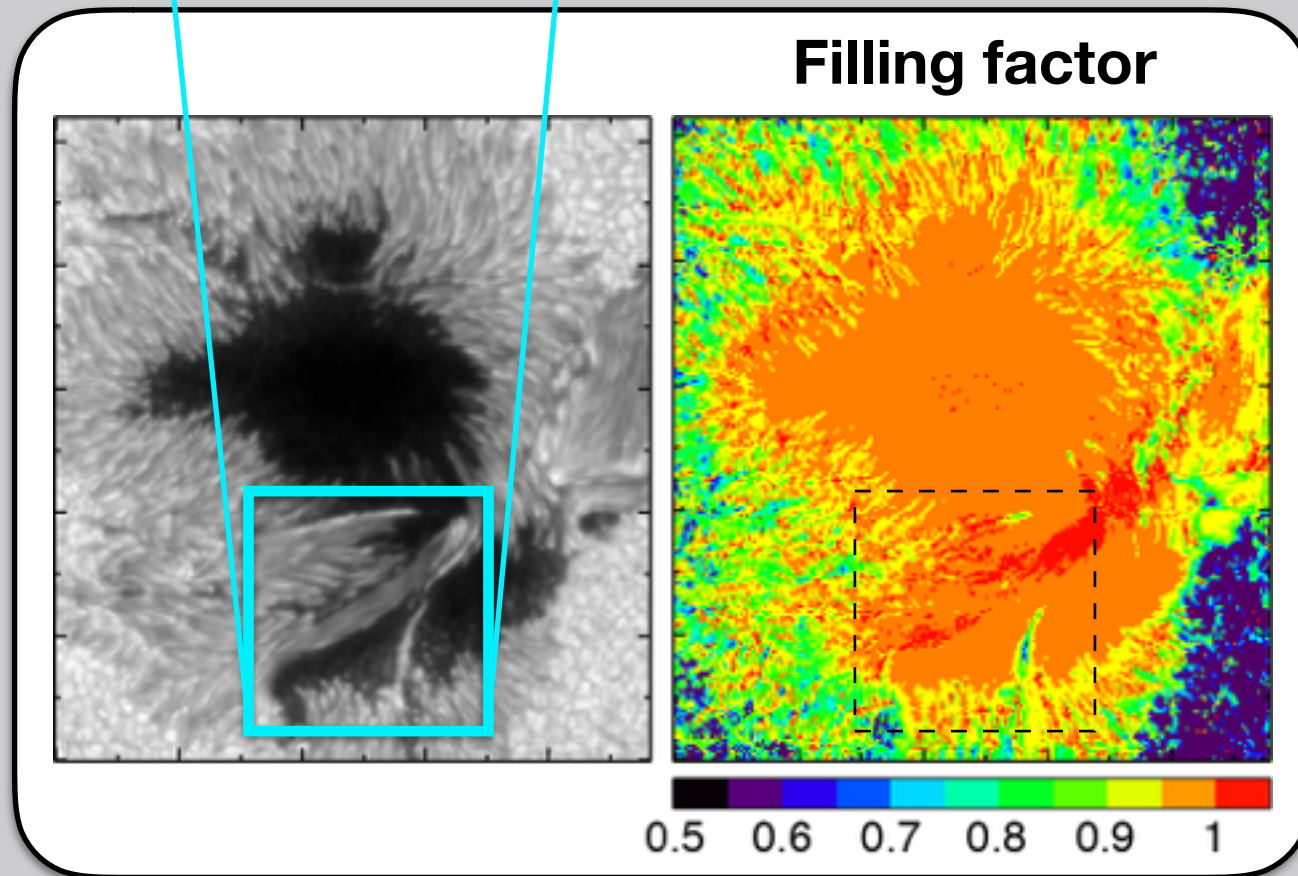
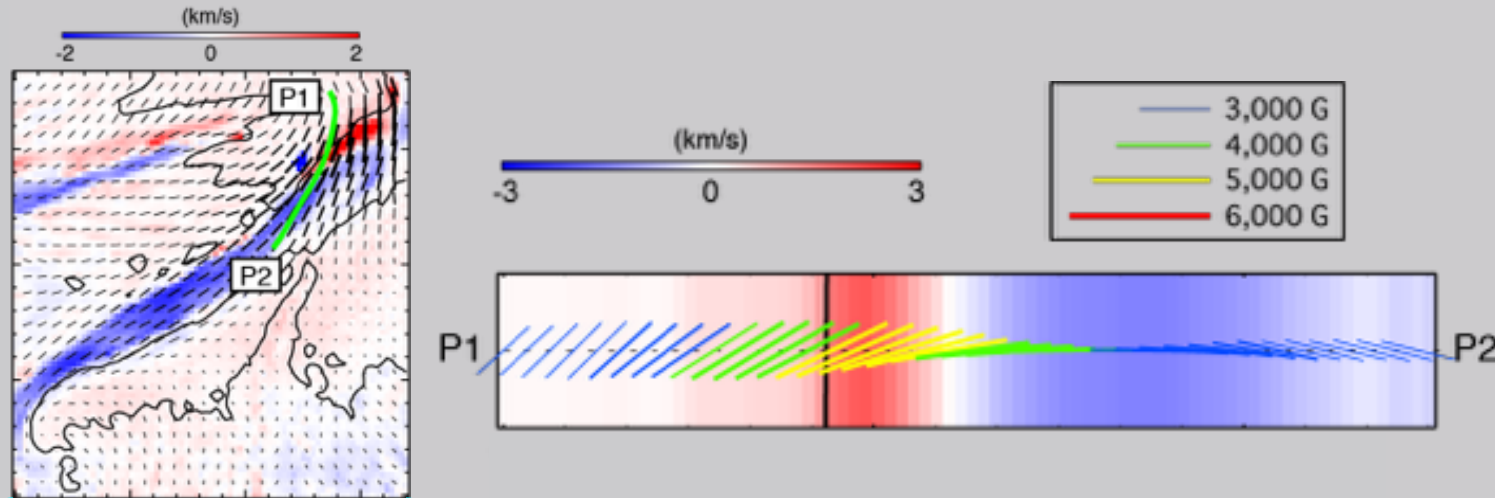
Feb. 04
19:11 UT



key structures

Filling Factor

Feb. 02
16:11 UT



**Filling factor is almost unity
in the light bridge.**

**smaller values in typical light bridges
(also mentioned in Leka 1997)**

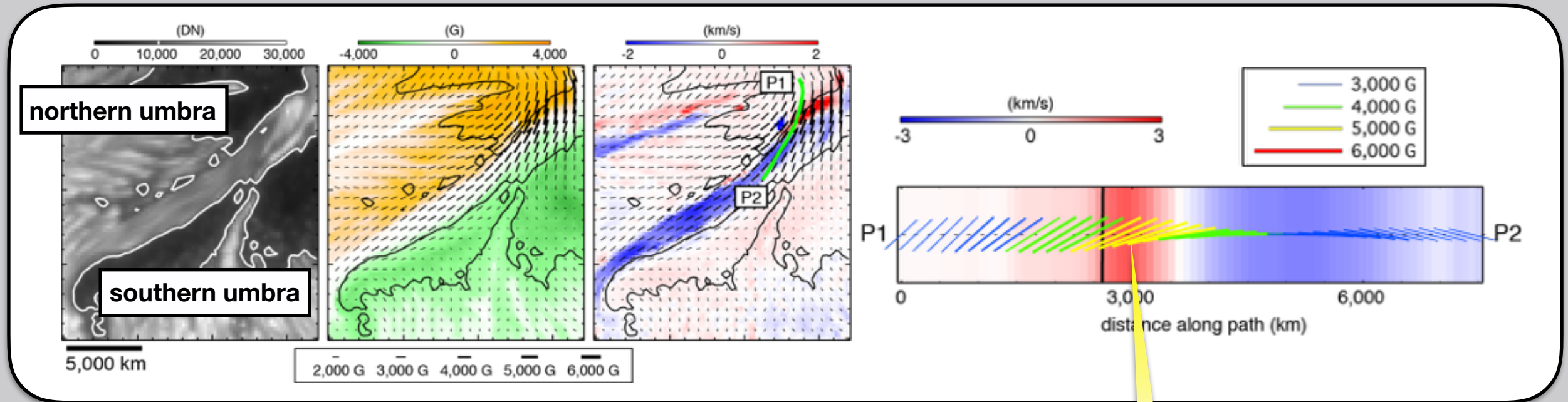
7 km/s horizontal flow

**The light bridge is actually a penumbra
belonging to the southern umbra.**

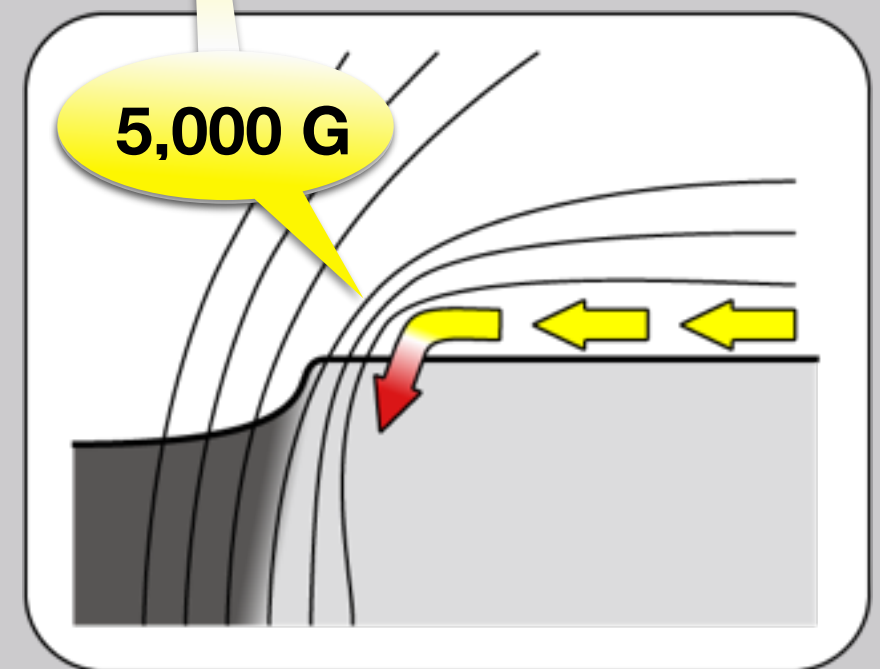
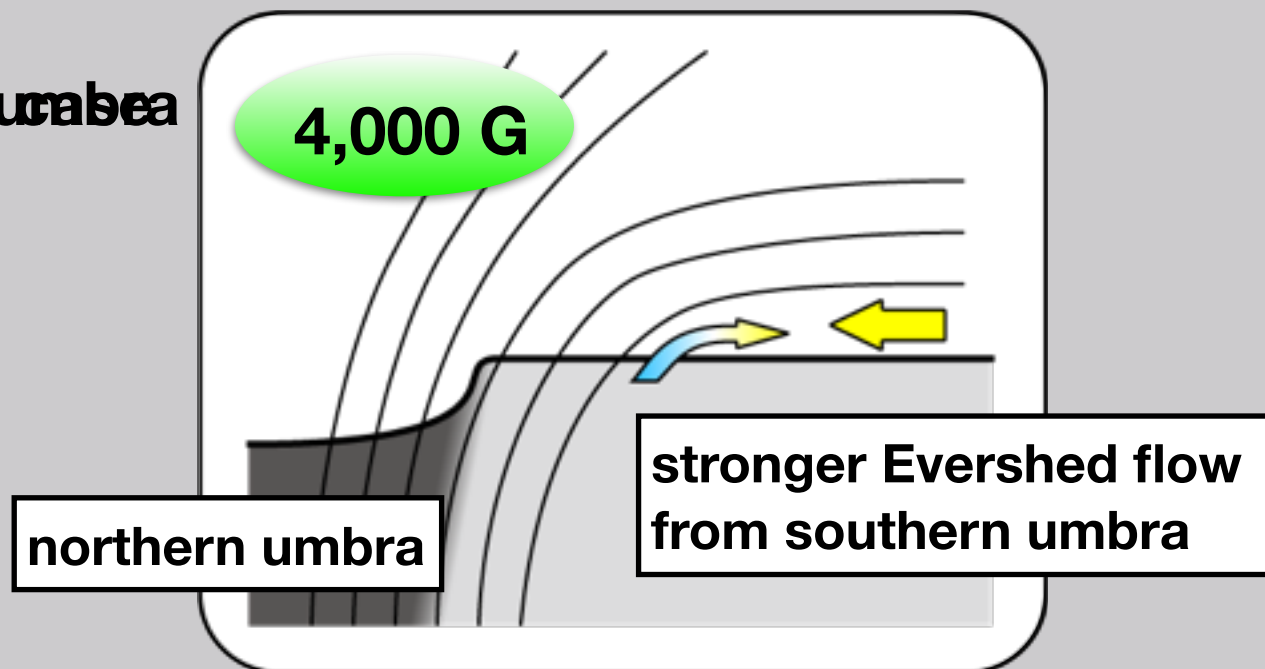
Interpretation

Fields are enhanced by compression of the northern umbra by the penumbral flow from the southern umbra.

The flow prevents the northern umbra from forming its penumbra on its southern side.



typical penumbra

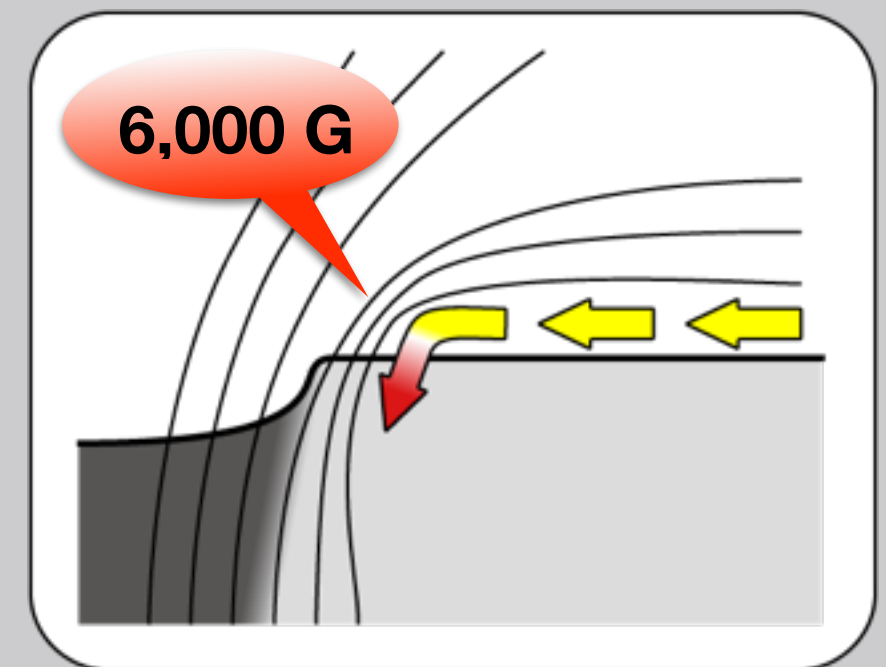
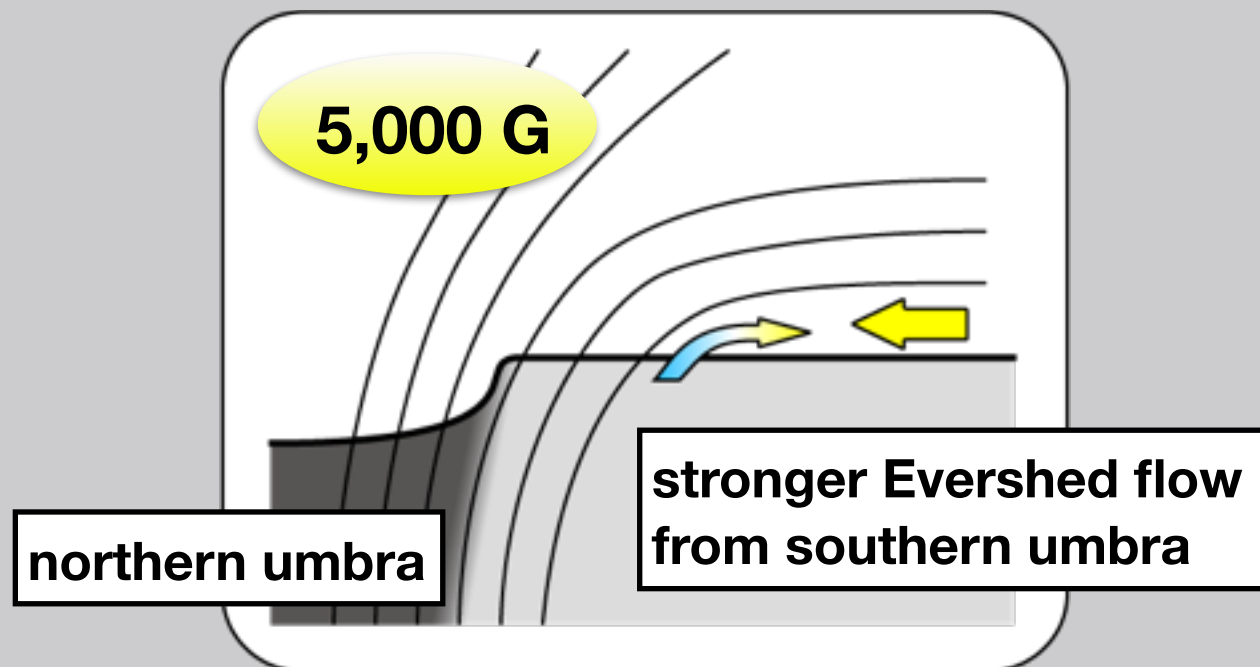
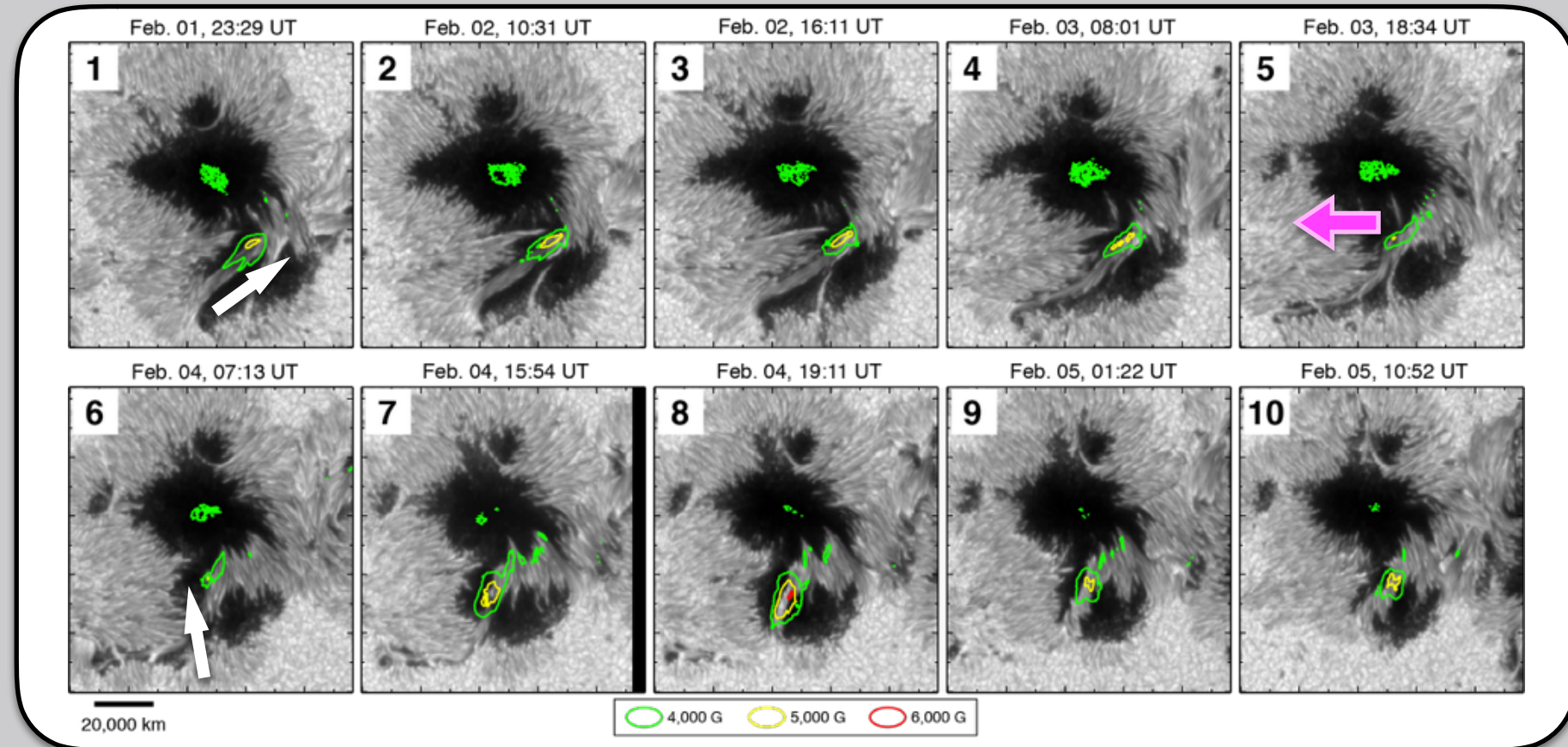


Interpretation

Enhanced fields are further intensified by changing configuration of two opposite-polarity umbrae.

5,000 G region at the northern umbra moved eastward.

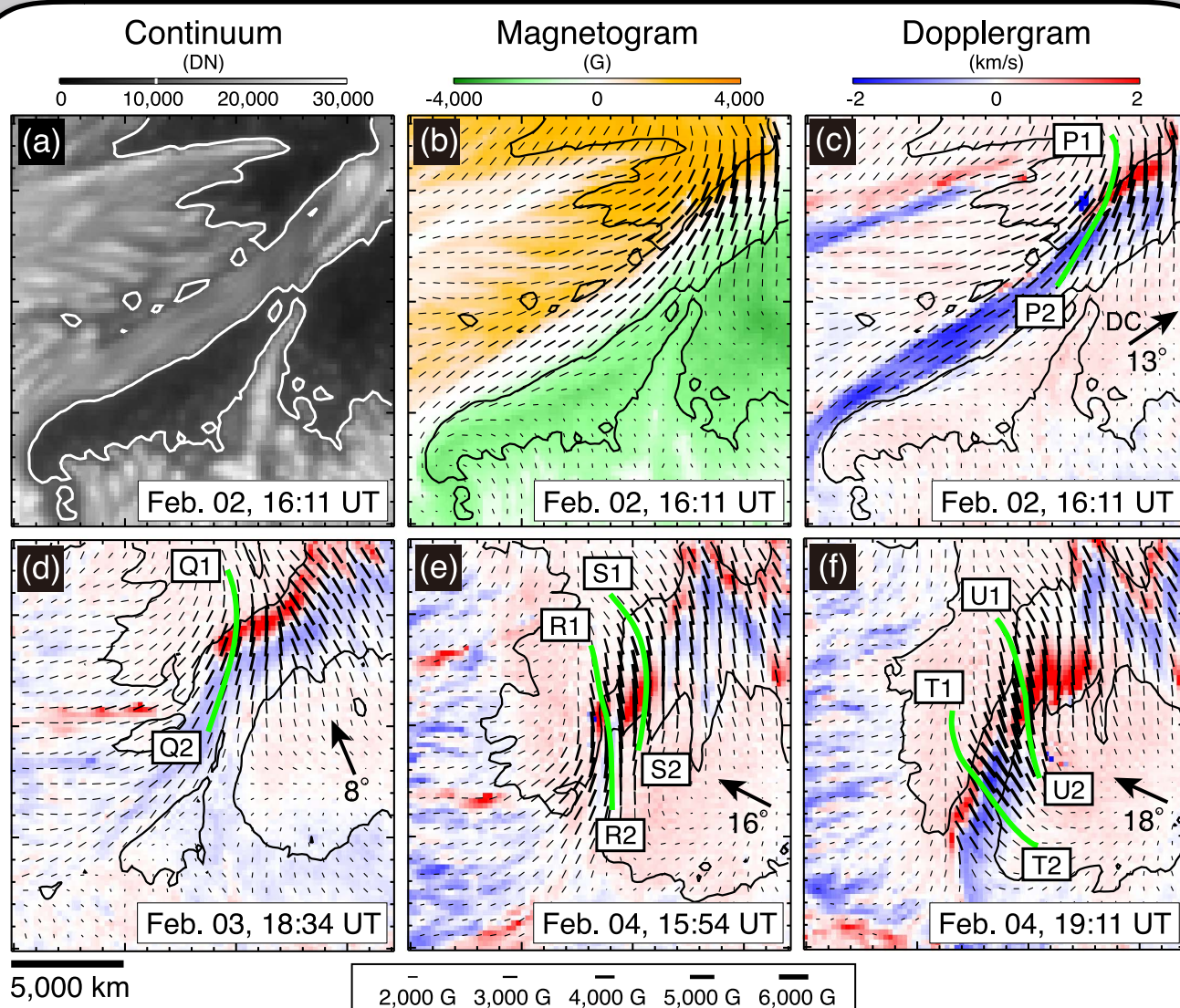
Orientation of the penumbra changes toward 5,000 G region. (N-ward from NW-ward)



Discussion 1

Is the strong field attributed to flux emergence ?

Sunspots and active regions are always formed by emerging magnetic flux coming from the solar interior.



Some apparent features are similar to those in the emerging flux scenario.

1-3 km/s blueshift
redshift at the end of the horizontal fields

But, 2 inconsistencies.

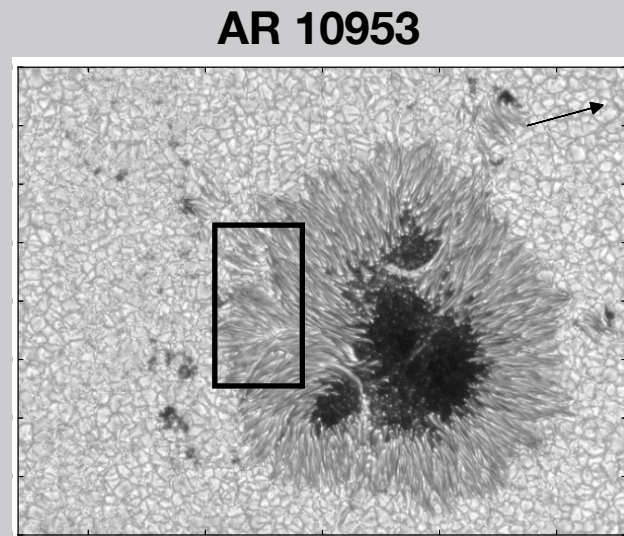
The duration of blueshift for 5 days is too long for the compact area of the light bridge (~30,000 km).

The Doppler velocity was larger when the sunspot was far from the DC, and smaller when close to the DC.

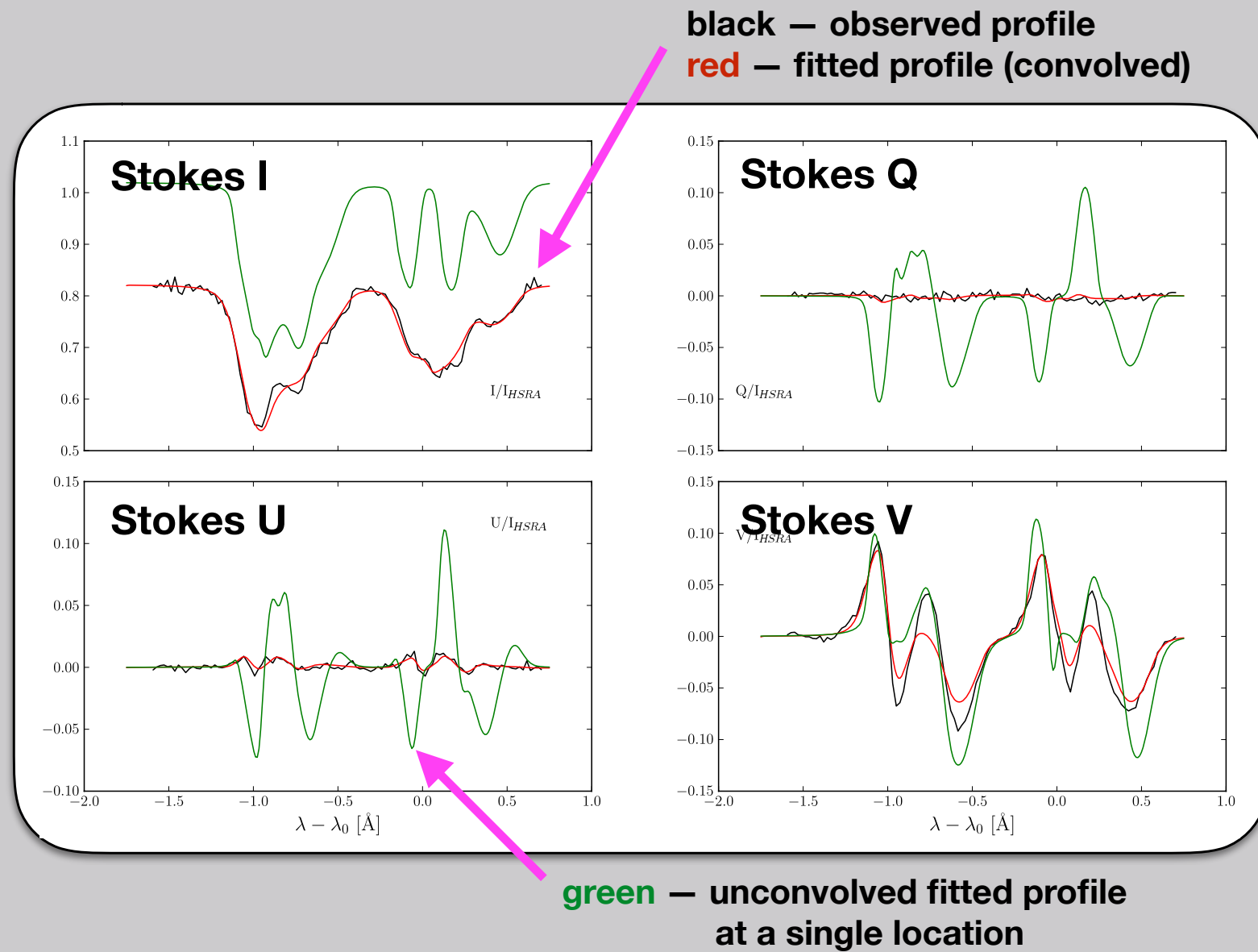
6.5 - 7.2 km/s at all times as horizontal flows

Discussion 2

7,500 G by van Noort+2013



- Hinode/SOT/SP
- simultaneous inversion over 2D region considered PSF
- SPINOR code, 3 node atmospheric model



The unconvolved Stokes Q and U profiles are far from the observed ones.

multi-components of Doppler velocity along LOS ?

spurious components with strong field made by image deconvolution ?

Discussion 2

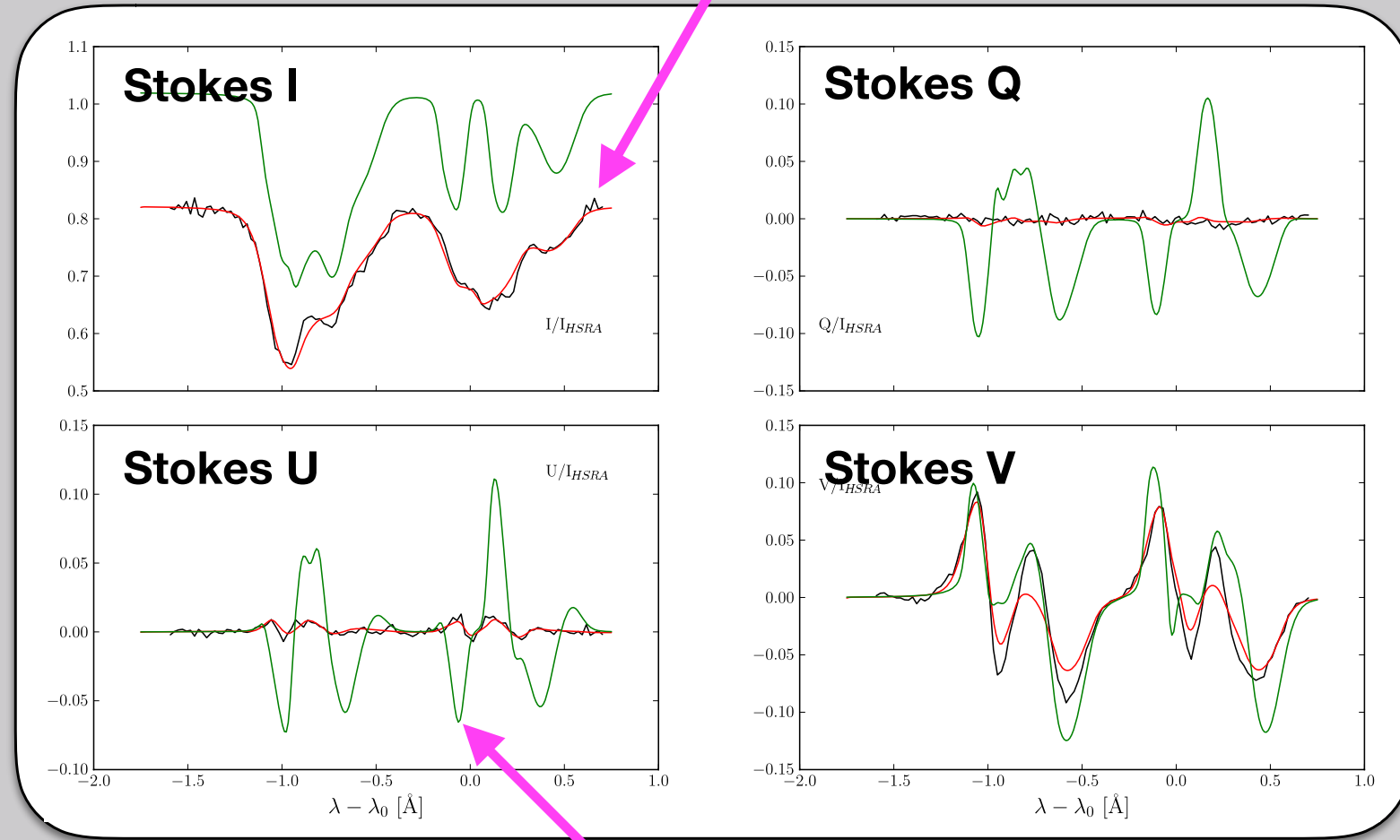
7,500 G by van Noort+2013



“The very high values of the magnetic field strength are predominantly based on the very broad wings of the Stokes V profiles that can only be produced by a strong magnetic field near optical depth unity.”

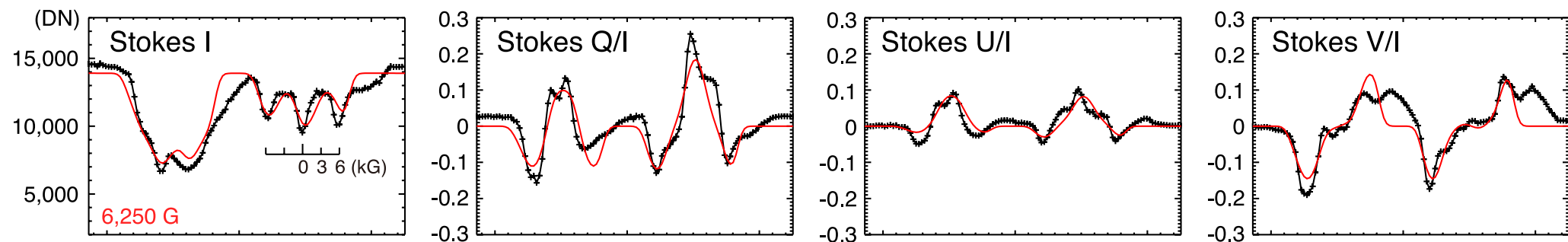
– SPINOR code, 3 node atmospheric model

black — observed profile
red — fitted profile (convolved)



green — unconvolved fitted profile at a single location

Okamoto+2018

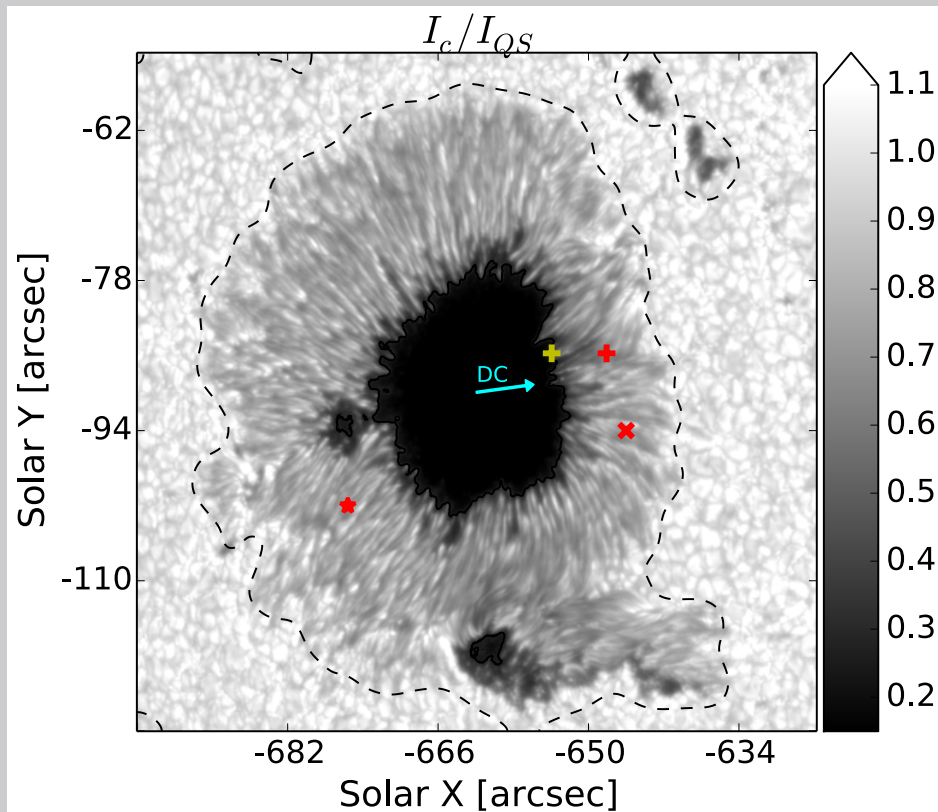


un-fitted high-velocity redshift component → hidden stronger component ?

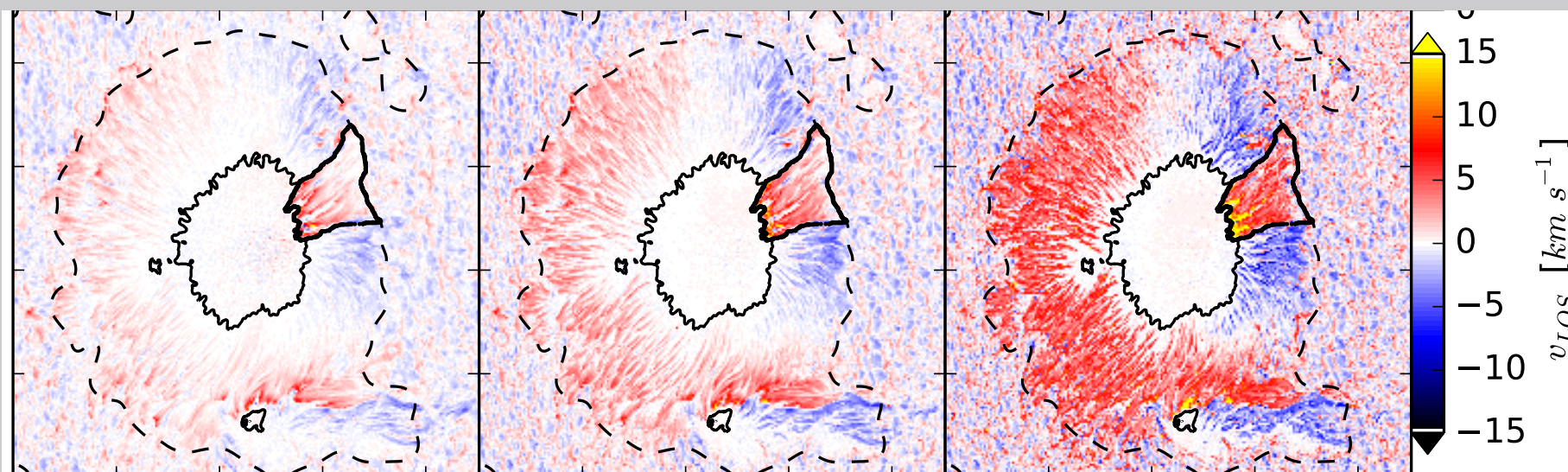
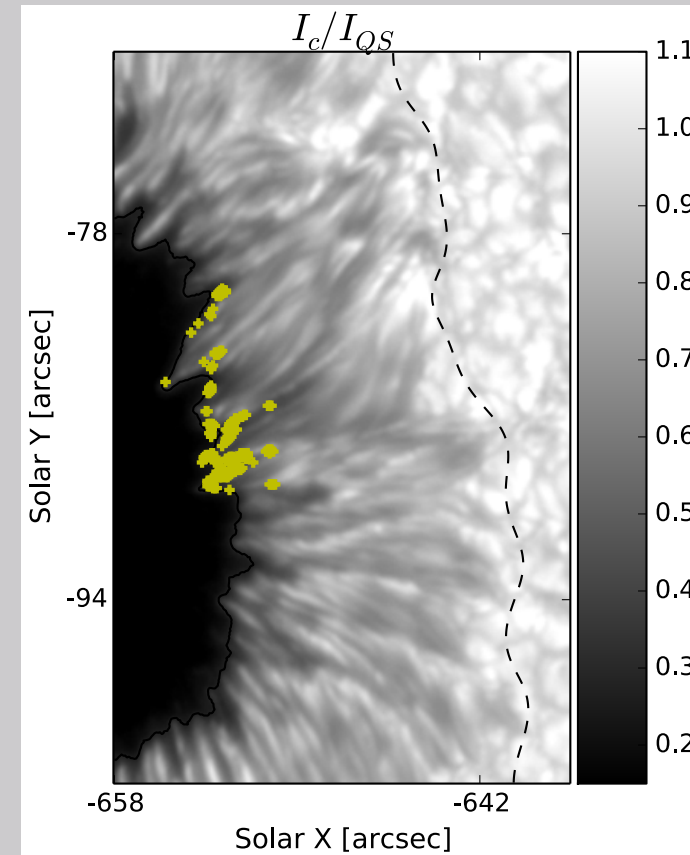
Discussion 3

Siu-Tapia+2017

Counter-Evershed flow



AR 10930

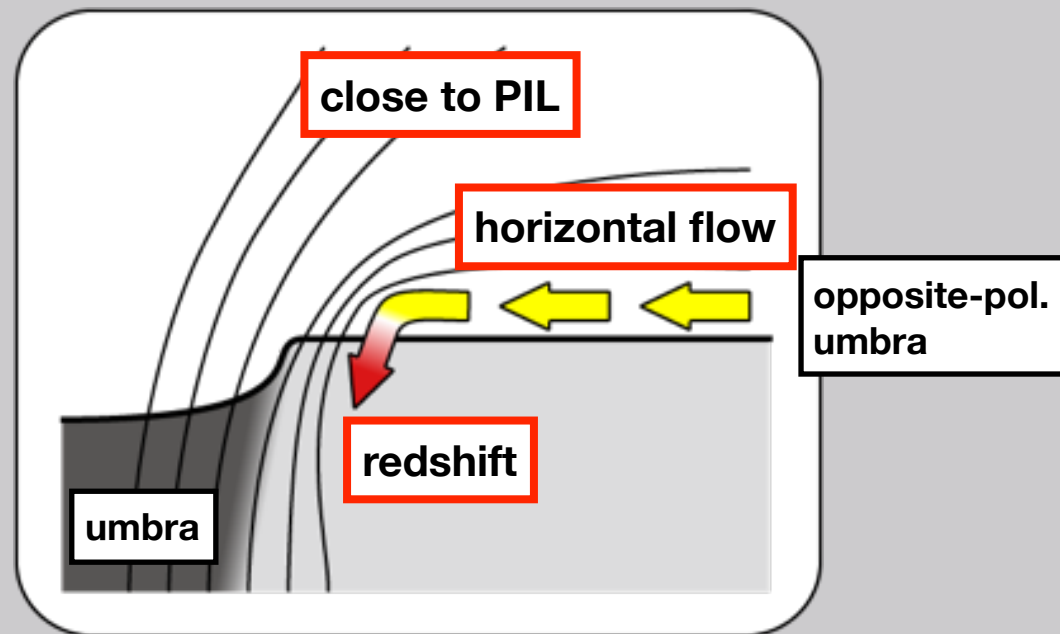


Umbral boundary shows the stronger field with more than 7 kG by SPINOR inversion.

Why does a so-strong field exist outside an umbra ?



Penumbral flows compress umbral fields to enhance the strength.



The above is a result from a few cases.

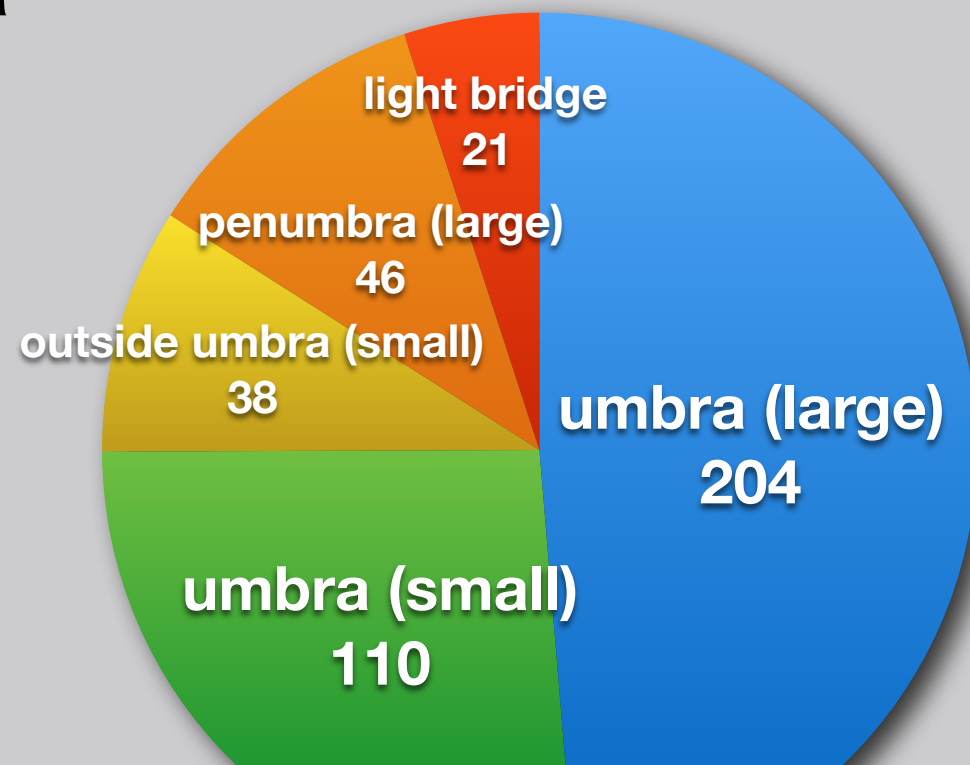
How about other sunspots ?

- statistical analysis-

Extracting Information

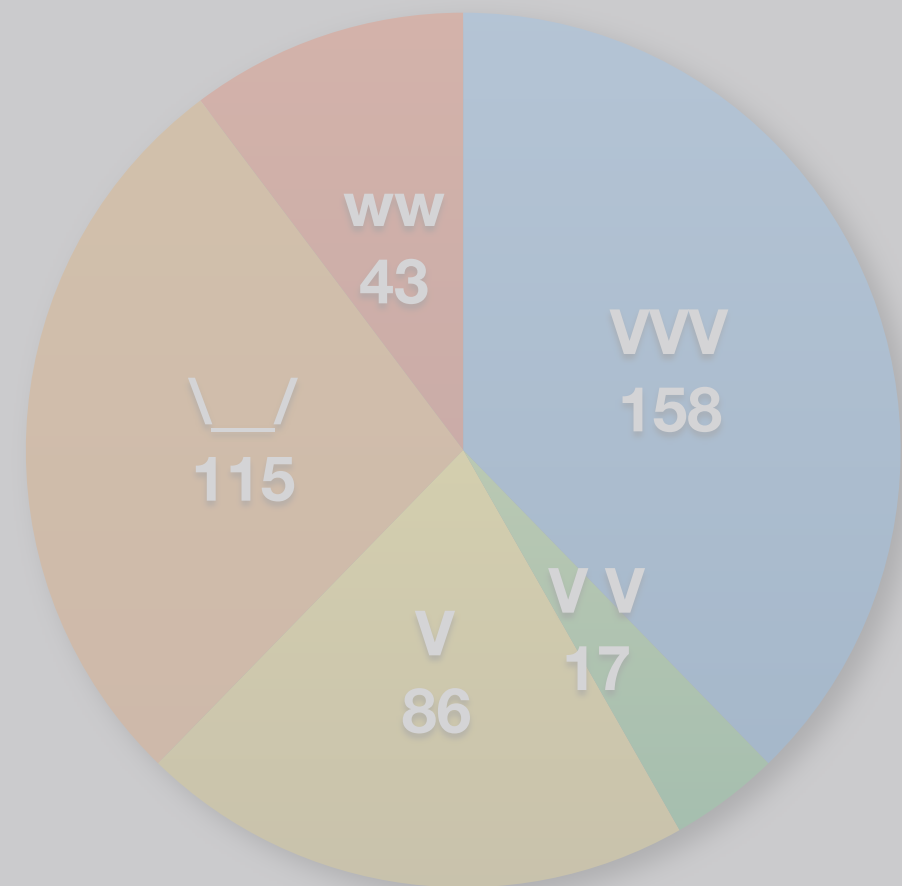
419 AR

Location

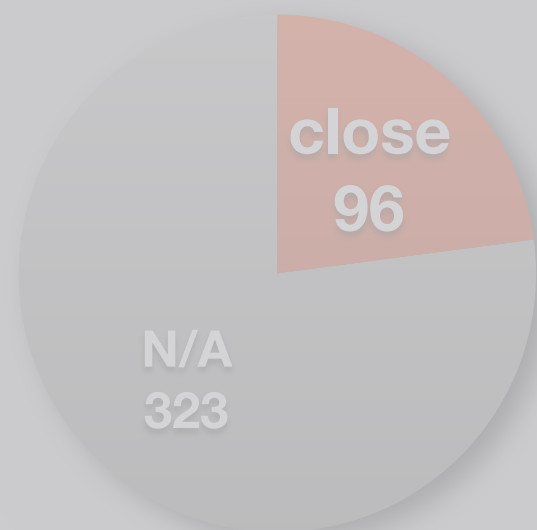


49% – umbra in large sunspots
75% – umbra

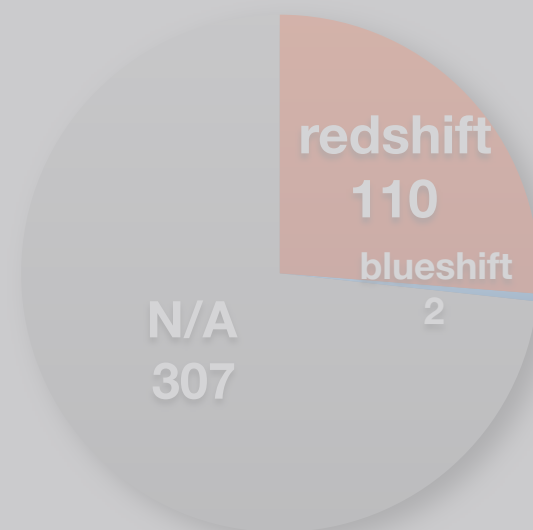
Spectral shape



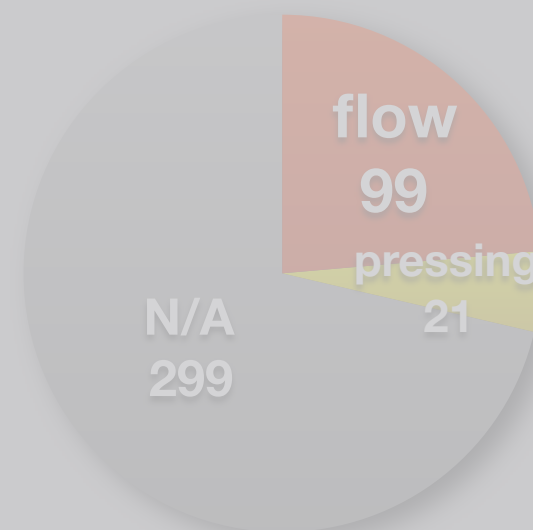
Close to PIL



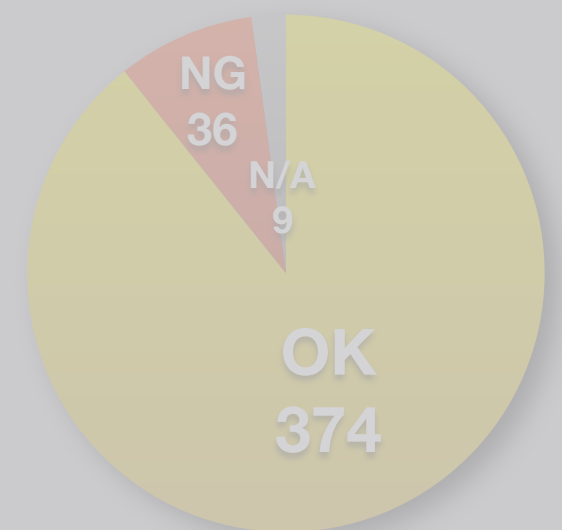
Redshift



Horizontal flow



Fitting result

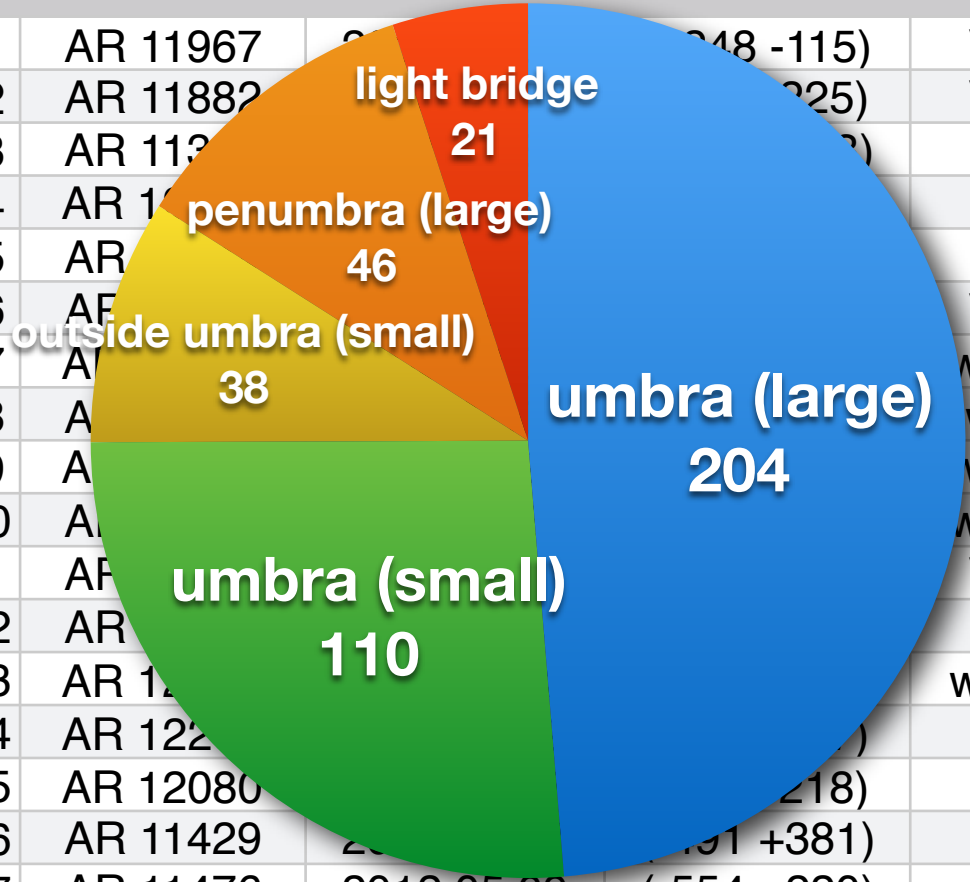


Ranking Top 30

	AR number	date	coordinates	spectral shape	location	redshift			fitting	multi comp	strength	
						PIL	↓	flow	↓		MERLIN	MEKSY
1	AR 11967	2014.02.04	(+248 -115)	VVV	light br	o	o	o	O	-mul	6251 G	
2	AR 11882	2013.10.28	(-464 -225)	VVV	light br	o	o	o	O		5046 G	
3	AR 11302	2011.09.30	(+331 + 93)	_/	light br	o	o	o	X		4991 G	--> 4055 G
4	AR 12297	2015.03.12	(- 77 -168)	_/	light br	o	o	o	X		4985 G	--> 4049 G
5	AR 11944	2014.01.05	(-509 -111)	V	lb/p (s)	o	o	o	X	-mul	4915 G	--> 3306 G
6	AR 11974	2014.02.14	(+356 -112)	VVV	light br	o	o	o	X		4855 G	--> 4225 G
7	AR 10930	2006.12.09	(-410 - 93)	ww-IV	umbra				O		4836 G	
8	AR 11515	2012.07.05	(+437 -350)	ww-I	penumbra	o	o	o	X	-mul	4807 G	--> 3913 G
9	AR 12192	2014.10.25	(+275 -323)	ww-IV	umbra				O		4743 G	
10	AR 11899	2013.11.21	(+574 + 51)	ww-IV	umbra				O		4702 G	
11	AR 11045	2010.02.09	(+362 +461)	VVV	light br	o	o	o	O	-mul	4692 G	
12	AR 11560	2012.09.03	(+368 - 87)	_/	penumbra	o	o	o	X		4691 G	--> 3817 G
13	AR 12546	2016.05.22	(+418 -143)	ww-IV	umbra				N		4684 G	
14	AR 12209	2014.11.19	(-199 -307)	_/	penumbra	o	o	o	O	-mul	4673 G	
15	AR 12080	2014.06.07	(-222 -218)	V	penumbra	o	o	o	X	-mul	4542 G	
16	AR 11429	2012.03.07	(-491 +381)	_/	penumbra		o	o	X	-mul	4503 G	
17	AR 11476	2012.05.09	(-554 +220)	_/	light br	o	o	o	O		4477 G	
18	AR 11890	2013.11.10	(+337 -267)	_/	light br	o	o	o	X		4461 G	--> 3708 G
19	AR 11785	2013.07.07	(-114 -256)	_/	penumbra	o	o	o	X		4365 G	--> 3601 G
20	AR 11339	2011.11.06	(-387 +259)	_/	penumbra	o	o	o	X		4363 G	--> 3679 G
21	AR 12497	2016.02.12	(+340 +310)	VVV	light br	o	o	o	O		4349 G	
22	AR 12422	2015.09.27	(+221 -458)	_/	light br	o	o	o	X		4320 G	--> 4700 G
23	AR 11166	2011.03.10	(+339 +257)	_/	penumbra	o	o	o	X	-mul	4271 G	--> 3249 G
24	AR 12529	2016.04.12	(-283 +245)	ww-IV	umbra				N		4262 G	
25	AR 11748	2013.05.17	(-455 +193)	_/	light br	o	o	o	X	-mul	4241 G	--> 3629 G
26	AR 12222	2014.11.30	(-224 -350)	ww-IV	umbra				O		4178 G	
27	AR 10956	2007.05.19	(+ 10 + 61)	_/	lb/p (s)	o	o	o	O		4160 G	
28	AR 10923	2006.11.12	(-305 -114)	ww-IV	umbra				O		4137 G	
29	AR 11161	2011.02.19	(+271 +415)	_/	light br	o	o	o	O		4135 G	
30	AR 11263	2011.08.02	(-197 +171)	ww-IV	umbra				O		4099 G	

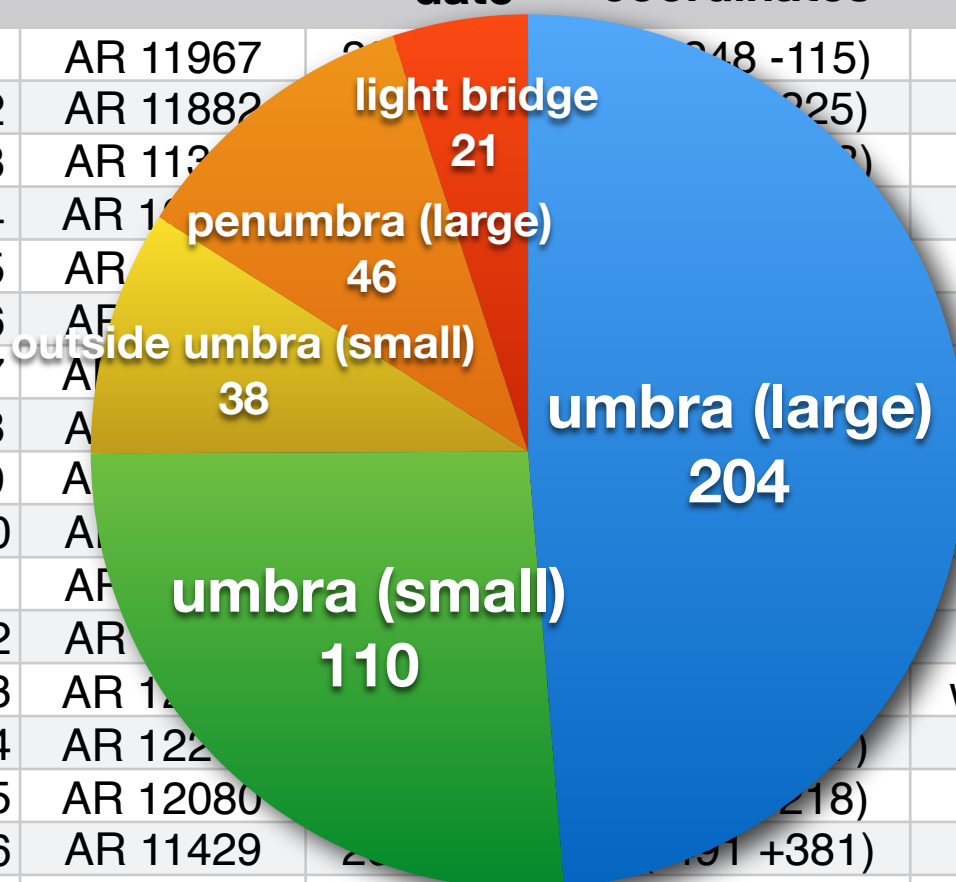
Ranking Top 30

	AR number	date	coordinates	spectral shape	location	redshift			fitting	multi comp	strength	
						PIL	↓ flow	↓	↓		MERLIN	MEKSY
1	AR 11967	2012.05.09	(-548 -115)	VVV	light br	o	o	o	O	-mul	6251 G	
2	AR 11882	2012.05.09	(-225)	VVV	light br	o	o	o	O		5046 G	
3	AR 11339	2011.11.06	(-387 +259)	_/	light br	o	o	o	X		4991 G	--> 4055 G
4	AR 11339	2011.11.06	(-387 +259)	_/	light br	o	o	o	X		4985 G	--> 4049 G
5	AR 11748	2013.05.17	(-455 +193)	V	lb/p (s)	o	o	o	X	-mul	4915 G	--> 3306 G
6	AR 11967	2012.05.09	(-548 -115)	VVV	light br	o	o	o	X		4855 G	--> 4225 G
7	AR 11967	2012.05.09	(-548 -115)	ww-IV	umbra				O		4836 G	
8	AR 11967	2012.05.09	(-548 -115)	ww-I	penumbra	o	o	o	X	-mul	4807 G	--> 3913 G
9	AR 11967	2012.05.09	(-548 -115)	ww-IV	umbra				O		4743 G	
10	AR 11967	2012.05.09	(-548 -115)	ww-IV	umbra				O		4702 G	
11	AR 11967	2012.05.09	(-548 -115)	VVV	light br	o	o	o	O	-mul	4692 G	
12	AR 11967	2012.05.09	(-548 -115)	_/	penumbra	o	o	o	X		4691 G	--> 3817 G
13	AR 11967	2012.05.09	(-548 -115)	ww-IV	umbra				N		4684 G	
14	AR 12222	2014.11.30	(-224 -350)	_/	penumbra	o	o	o	O	-mul	4673 G	
15	AR 12080	2015.09.27	(+221 -458)	V	penumbra	o	o	o	X	-mul	4542 G	
16	AR 11429	2012.05.09	(-548 -115)	_/	penumbra		o	o	X	-mul	4503 G	
17	AR 11476	2012.05.09	(-554 +220)	_/	light br	o	o	o	O		4477 G	
18	AR 11890	2013.11.10	(+337 -267)	_/	light br	o	o	o	X		4461 G	--> 3708 G
19	AR 11785	2013.07.07	(-114 -256)	_/	penumbra	o	o	o	X		4365 G	--> 3601 G
20	AR 11339	2011.11.06	(-387 +259)	_/	penumbra	o	o	o	X		4363 G	--> 3679 G
21	AR 12497	2016.02.12	(+340 +310)	VVV	light br	o	o	o	O		4349 G	
22	AR 12422	2015.09.27	(+221 -458)	_/	light br	o	o	o	X		4320 G	--> 4700 G
23	AR 11166	2011.03.10	(+339 +257)	_/	penumbra	o	o	o	X	-mul	4271 G	--> 3249 G
24	AR 12529	2016.04.12	(-283 +245)	ww-IV	umbra				N		4262 G	
25	AR 11748	2013.05.17	(-455 +193)	_/	light br	o	o	o	X	-mul	4241 G	--> 3629 G
26	AR 12222	2014.11.30	(-224 -350)	ww-IV	umbra				O		4178 G	
27	AR 10956	2007.05.19	(+ 10 + 61)	_/	lb/p (s)	o	o	o	O		4160 G	
28	AR 10923	2006.11.12	(-305 -114)	ww-IV	umbra				O		4137 G	
29	AR 11161	2011.02.19	(+271 +415)	_/	light br	o	o	o	O		4135 G	
30	AR 11263	2011.08.02	(-197 +171)	ww-IV	umbra				O		4099 G	



Ranking Top 30

	AR number	date	coordinates	spectral shape	location	redshift			fitting	multi comp	strength	
						PIL	↓ flow	↓	↓		MERLIN	MEKSY
1	AR 11967	2011.08.02	(-248 -115)	VVV	light br	0	0	0	O	-mul	6251 G	
2	AR 11882	2011.08.02	(-225)	VVV	light br	0	0	0	O		5046 G	
3	AR 11339	2011.11.06	(-387 +259)	_/	light br	0	0	0	X		4991 G	--> 4055 G
4	AR 11339	2011.11.06	(-387 +259)	_/	light br	0	0	0	X		4985 G	--> 4049 G
5	AR 11748	2013.05.17	(-455 +193)	V	lb/p (s)	0	0	0	X	-mul	4915 G	--> 3306 G
6	AR 11967	2011.08.02	(-248 -115)	VVV	light br	0	0	0	X		4855 G	--> 4225 G
7	AR 11748	2013.05.17	(-455 +193)	ww-IV	umbra				O		4836 G	
8	AR 11748	2013.05.17	(-455 +193)	ww-I	penumbra	0	0	0	X	-mul	4807 G	--> 3913 G
9	AR 11748	2013.05.17	(-455 +193)	ww-IV	umbra				O		4743 G	
10	AR 11748	2013.05.17	(-455 +193)	ww-IV	umbra				O		4702 G	
11	AR 11967	2011.08.02	(-248 -115)	VVV	light br	0	0	0	O	-mul	4692 G	
12	AR 11748	2013.05.17	(-455 +193)	_/	penumbra	0	0	0	X		4691 G	--> 3817 G
13	AR 11748	2013.05.17	(-455 +193)	ww-IV	umbra				N		4684 G	
14	AR 12222	2014.11.30	(-224 -350)	_/	penumbra	0	0	0	O	-mul	4673 G	
15	AR 12080	2015.09.27	(+221 -458)	V	penumbra	0	0	0	X	-mul	4542 G	
16	AR 11429	2012.05.09	(-554 +220)	_/	penumbra		0	0	X	-mul	4503 G	
17	AR 11476	2012.05.09	(-554 +220)	_/	light br	0	0	0	O		4477 G	
18	AR 11890	2013.11.10	(+337 -267)	_/	light br	0	0	0	X		4461 G	--> 3708 G
19	AR 11785	2013.07.07	(-114 -256)	_/	penumbra	0	0	0	X		4365 G	--> 3601 G
20	AR 11339	2011.11.06	(-387 +259)	_/	penumbra	0	0	0	X		4363 G	--> 3679 G
21	AR 12497	2016.02.12	(+340 +310)	VVV	light br	0	0	0	O		4349 G	
22	AR 12422	2015.09.27	(+221 -458)	_/	light br	0	0	0	X		4320 G	--> 4700 G
23	AR 11166	2011.03.10	(+339 +257)	_/	penumbra	0	0	0	X	-mul	4271 G	--> 3249 G
24	AR 12529	2016.04.12	(-283 +245)	ww-IV	umbra				N		4262 G	
25	AR 11748	2013.05.17	(-455 +193)	_/	light br	0	0	0	X	-mul	4241 G	--> 3629 G
26	AR 12222	2014.11.30	(-224 -350)	ww-IV	umbra				O		4178 G	
27	AR 10956	2007.05.19	(+ 10 + 61)	_/	lb/p (s)	0	0	0	O		4160 G	
28	AR 10923	2006.11.12	(-305 -114)	ww-IV	umbra				O		4137 G	
29	AR 11161	2011.02.19	(+271 +415)	_/	light br	0	0	0	O		4135 G	
30	AR 11263	2011.08.02	(-197 +171)	ww-IV	umbra				O		4099 G	



Extracting Information (example)

(97) AR 11271

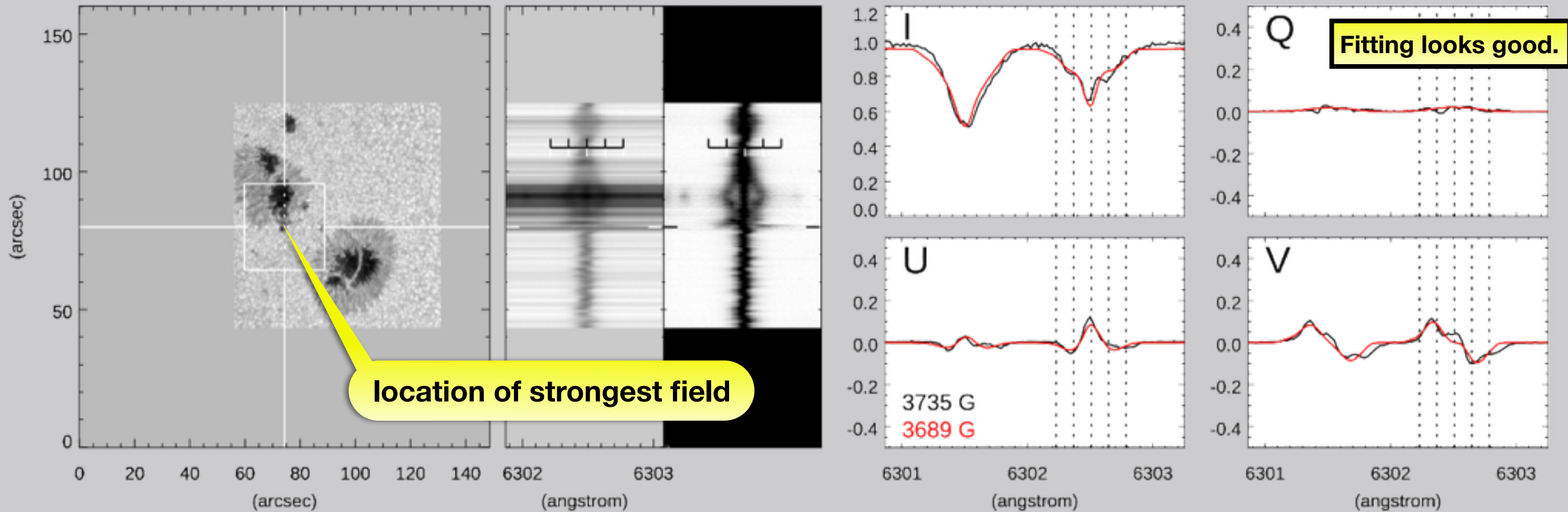
[20110819_100506]

Loc P Spec V PIL O Red O Flow O

Continuum

Stokes I (emphasized)

Full Stokes profiles at the location of the strongest field



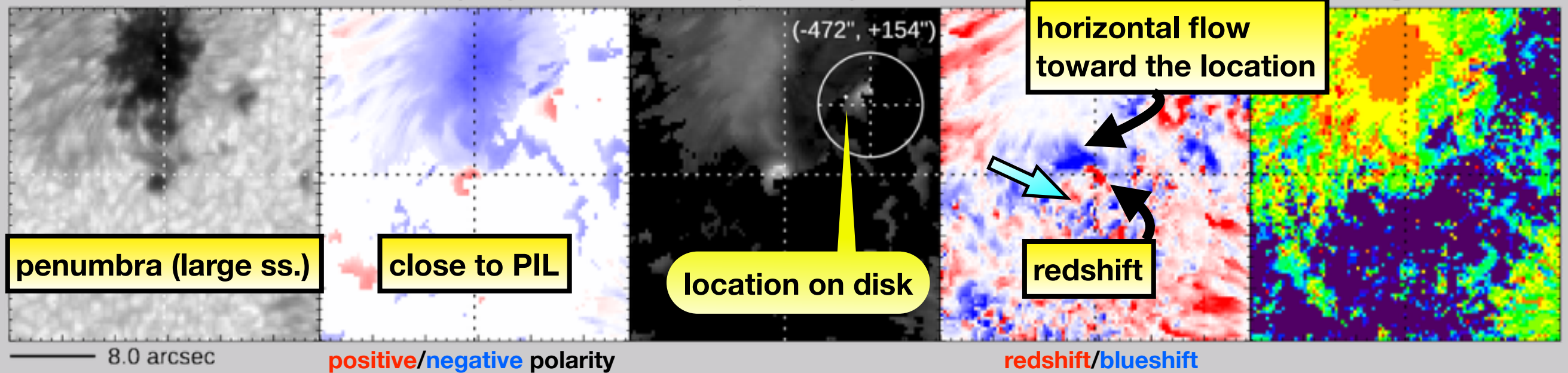
Continuum

B (LOS)

B (transverse)

Doppler velocity

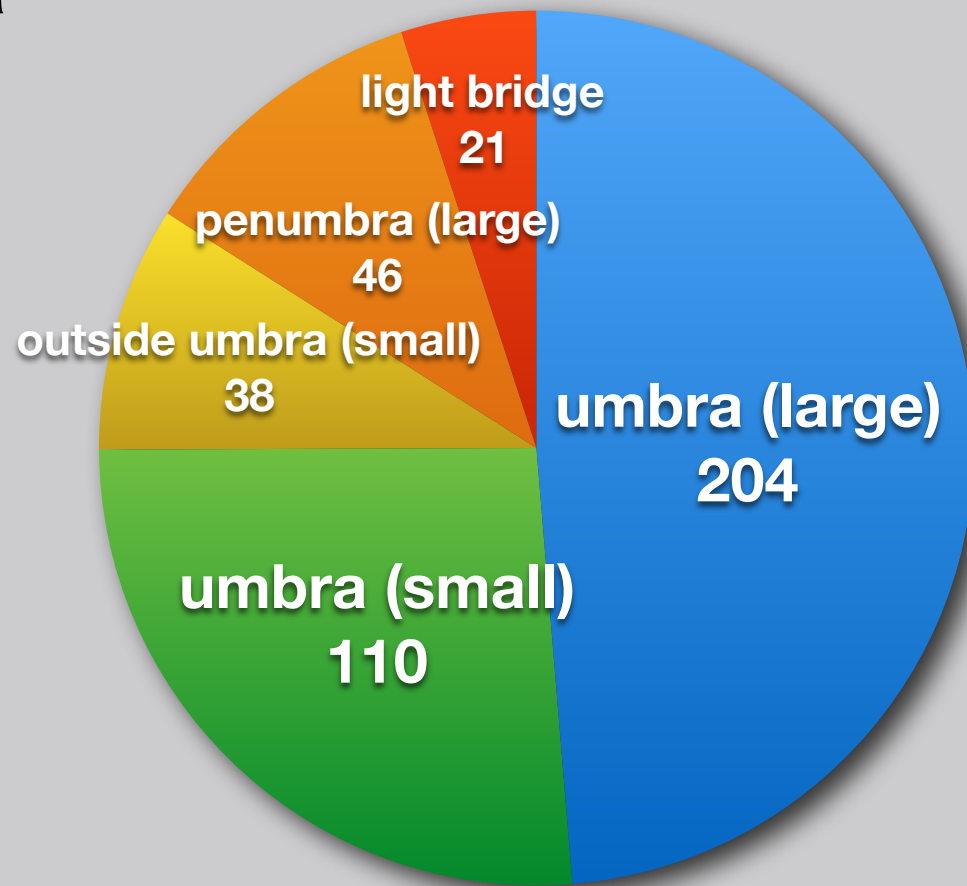
Filling factor



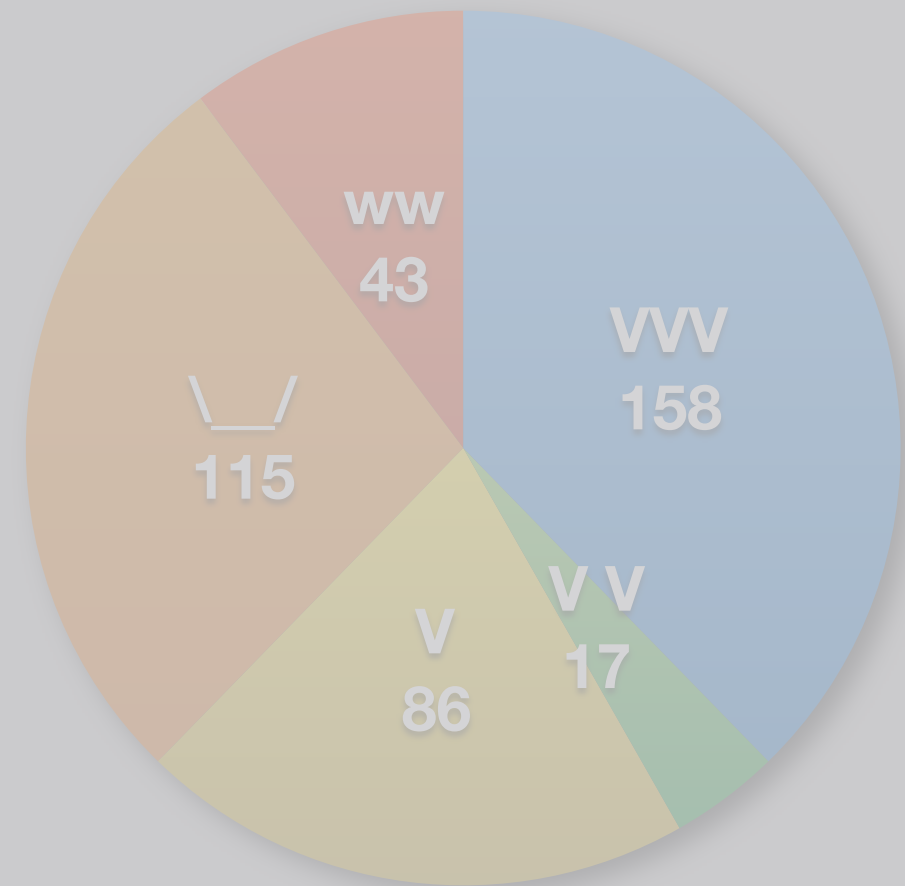
Extracting Information

419 AR

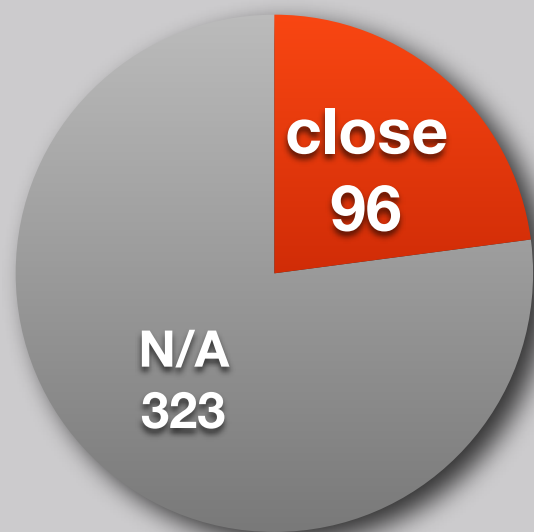
Location



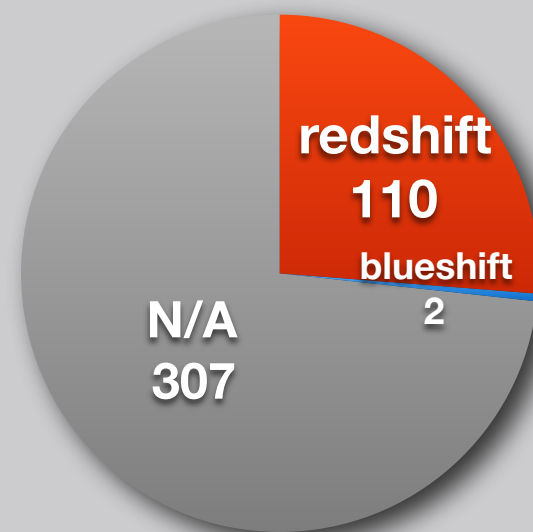
Spectral shape



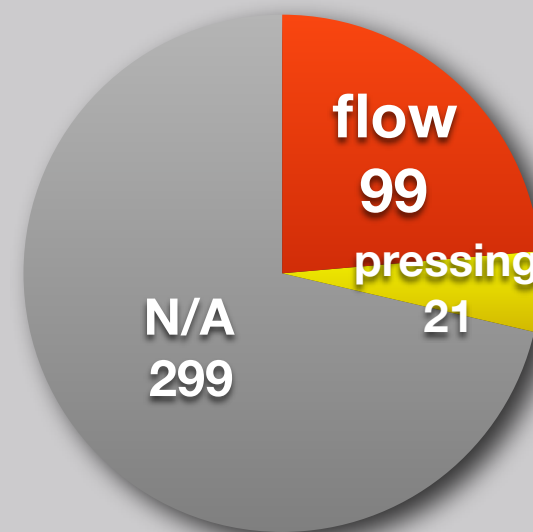
Close to PIL



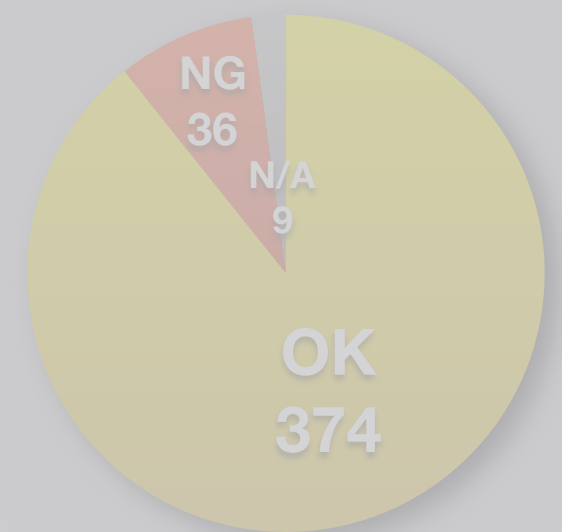
Redshift



Horizontal flow

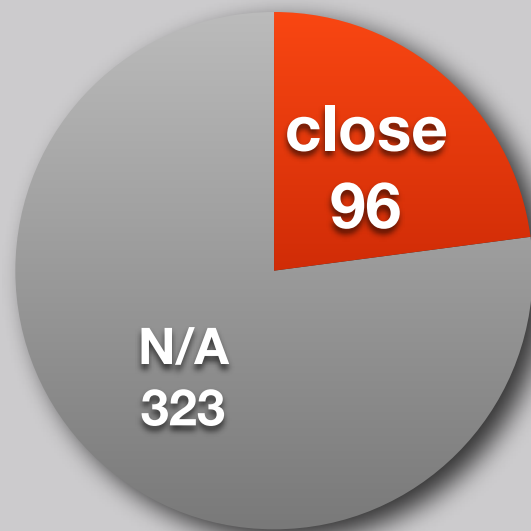


Fitting result

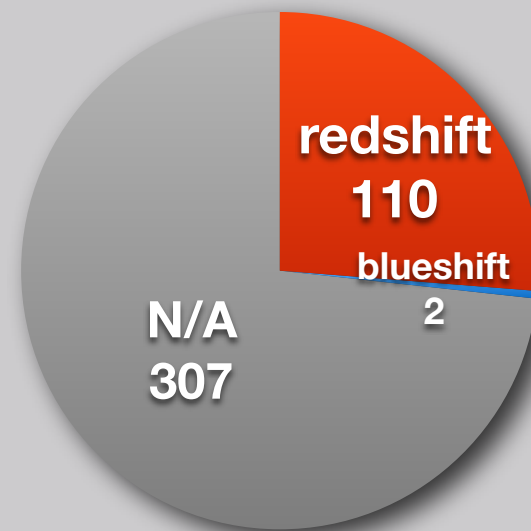


Field Strength and Surrounding Environment

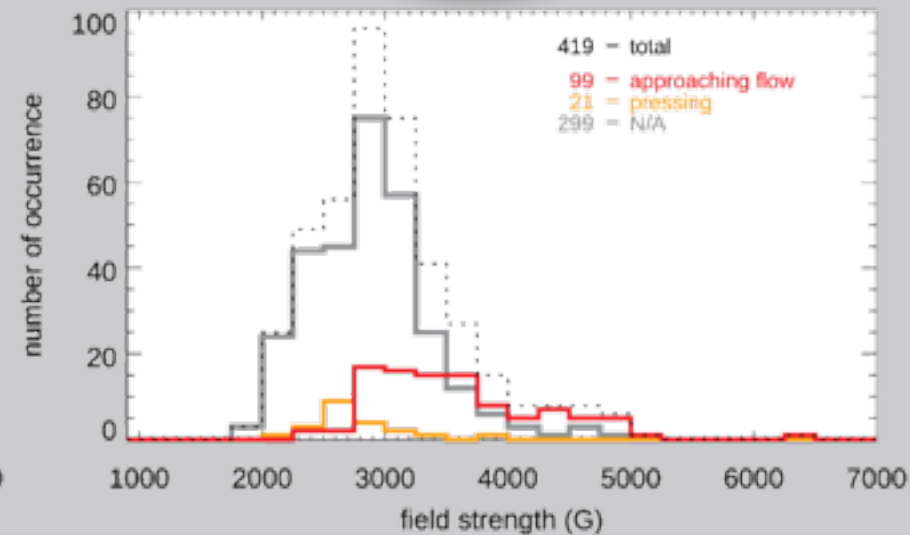
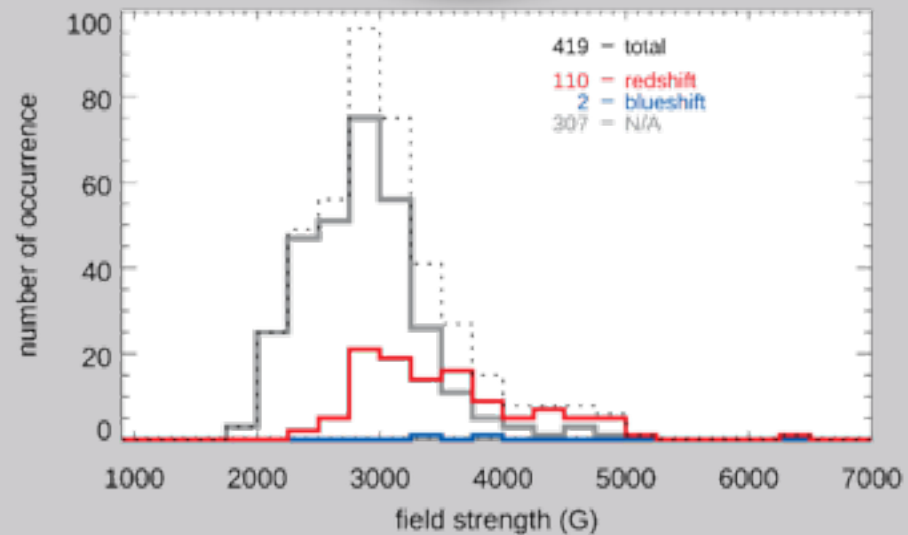
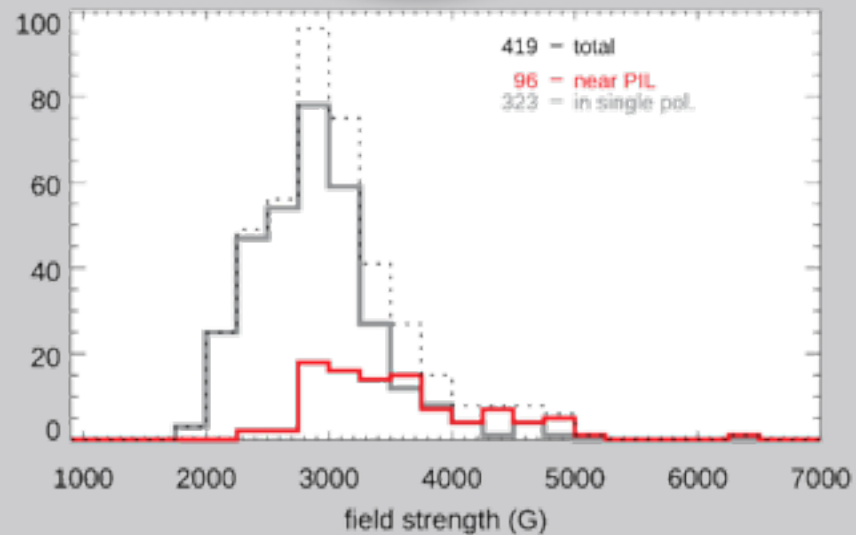
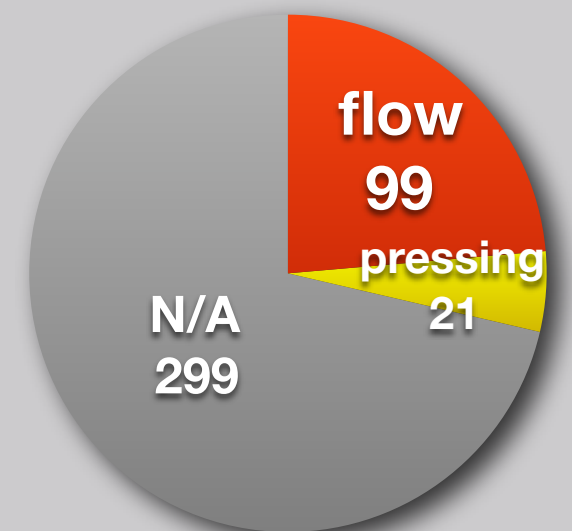
Close to PIL



Redshift



Horizontal flow



89 ARs have all of these 3 features, and they have stronger fields

- close to PIL
- redshift at the strong field region
- horizontal flow toward the strong field region

Location and Surrounding Environment

		total	PIL	redshift	flow (press)	overlap
non-umbra	outside umbra (small)	38	37	34	34 (1)	33
	penumbra (large)	46	36	44	43 (1)	35
	light bridge	21	21	20	20 (0)	20
umbra	umbra (large)	204	2	3	2 (0)	1
	umbra (small)	110	0	8	0 (19)	0
total		419	96	109	99 (21)	89

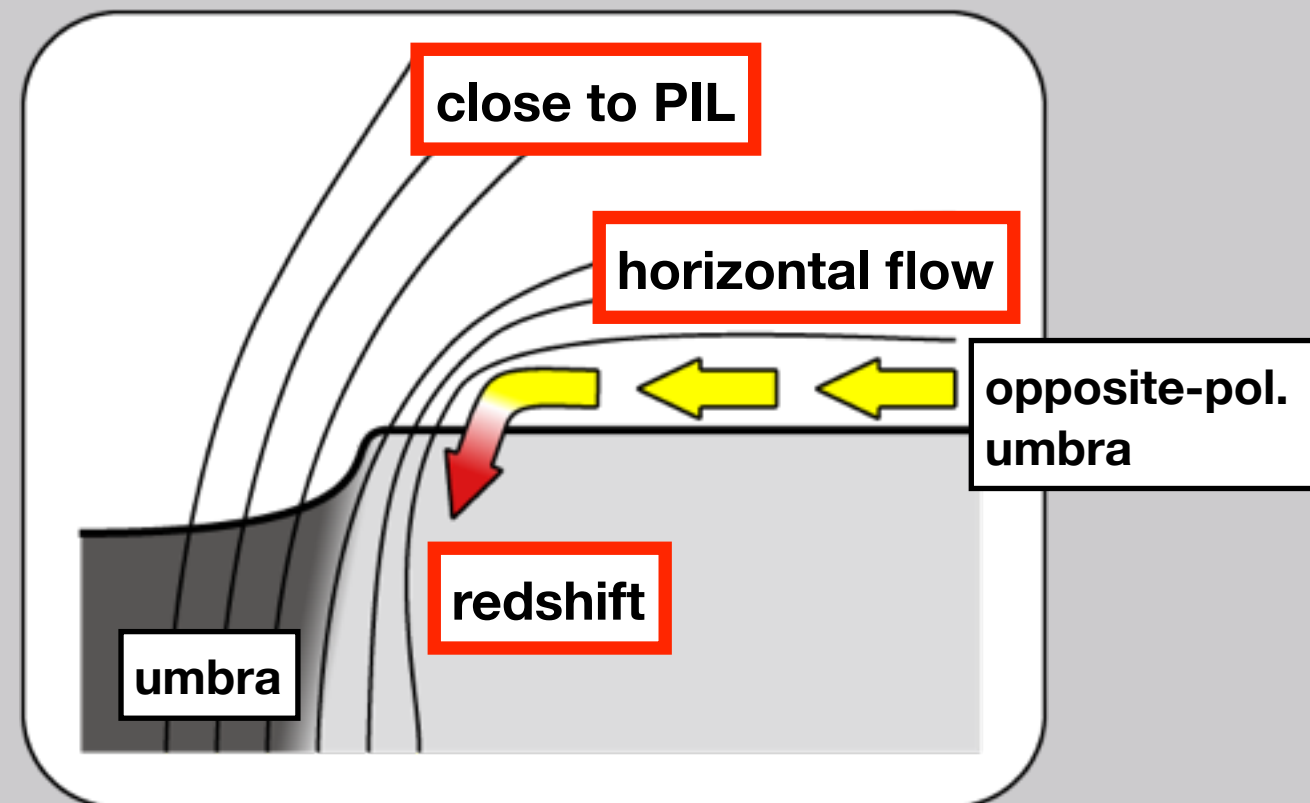
88

84% (88/105) of strongest fields outside umbrae have these 3 features.

Penumbral flows compress umbral fields and enhance magnetic fields.

Okamoto & Sakurai 2018

3 important features



Example of Enhanced Field by Horizontal Flow

(356) AR 12403

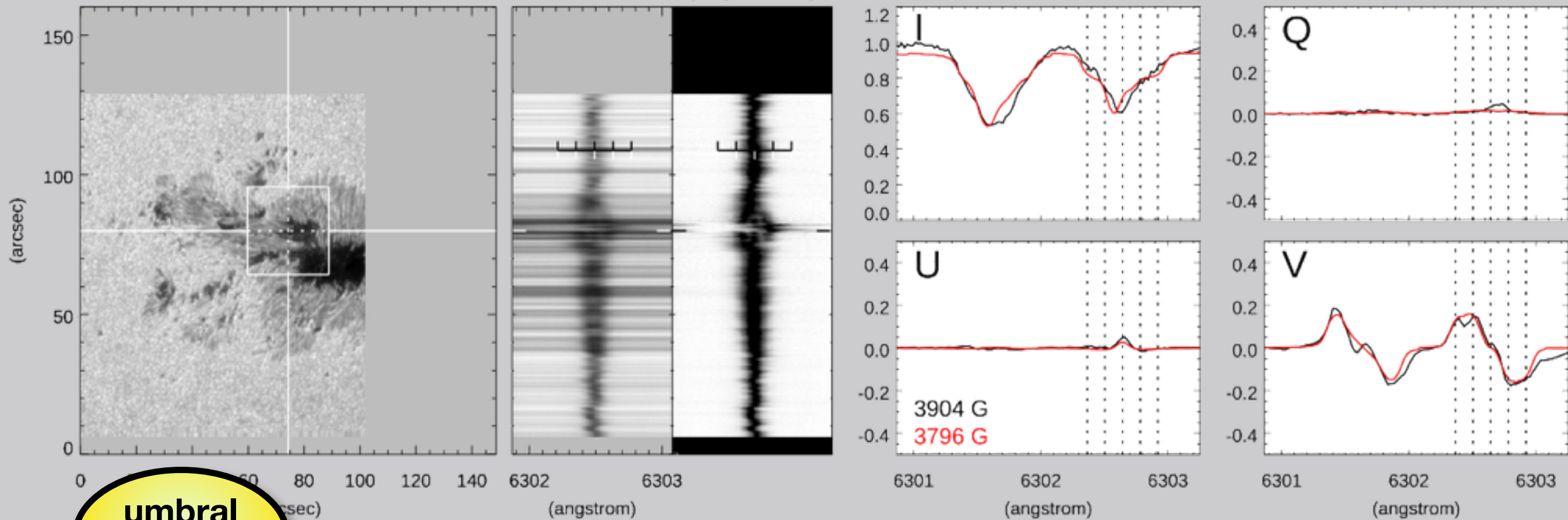
[20150826_053005]

Loc P Spec _/ PIL - Red O Flow O

Continuum

Stokes I (emphasized)

Full Stokes profiles at the location of the strongest field



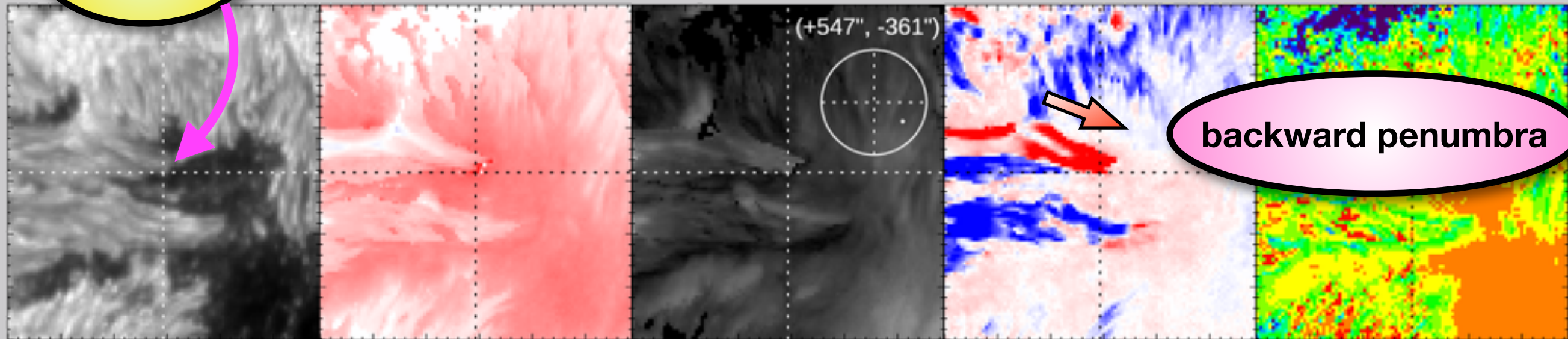
umbral boundary

B (LOS)

B (transverse)

Doppler velocity

Filling factor



backward penumbra

8.0 arcsec

positive/negative polarity

redshift/blueshift

Pressing Pores

19 examples

(76) AR 11190

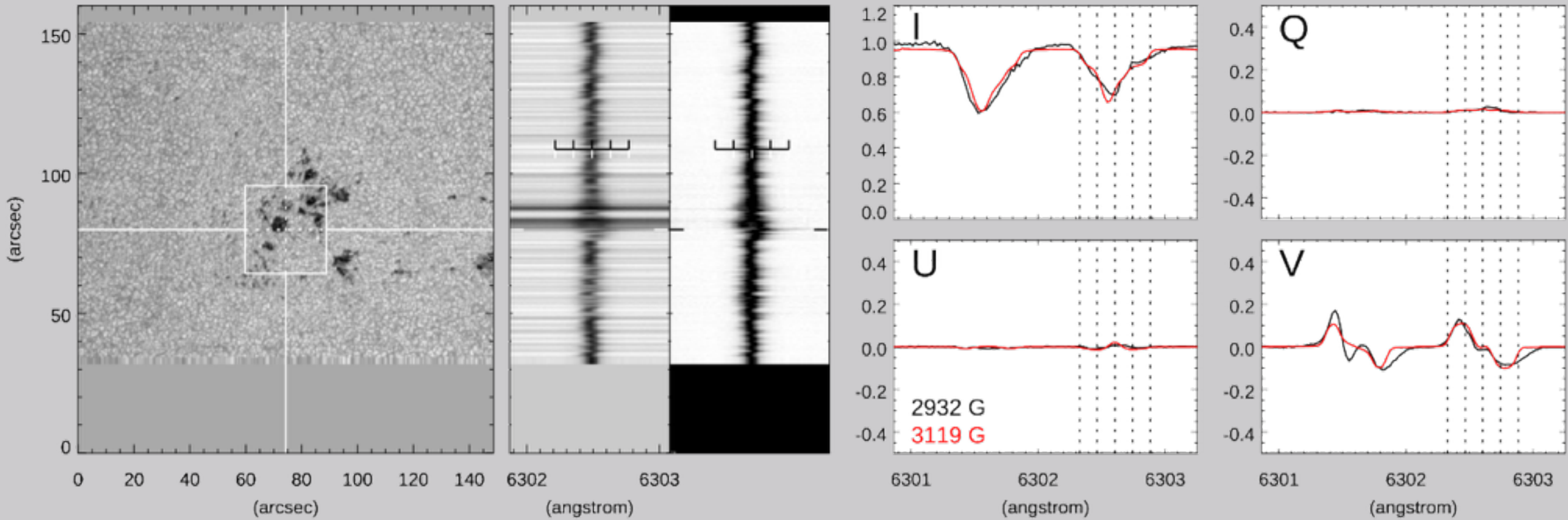
[20110412_161433]

Loc u Spec _/ - O O Flow

Continuum

Stokes I (emphasized)

Full Stokes profiles at the location of the strongest field



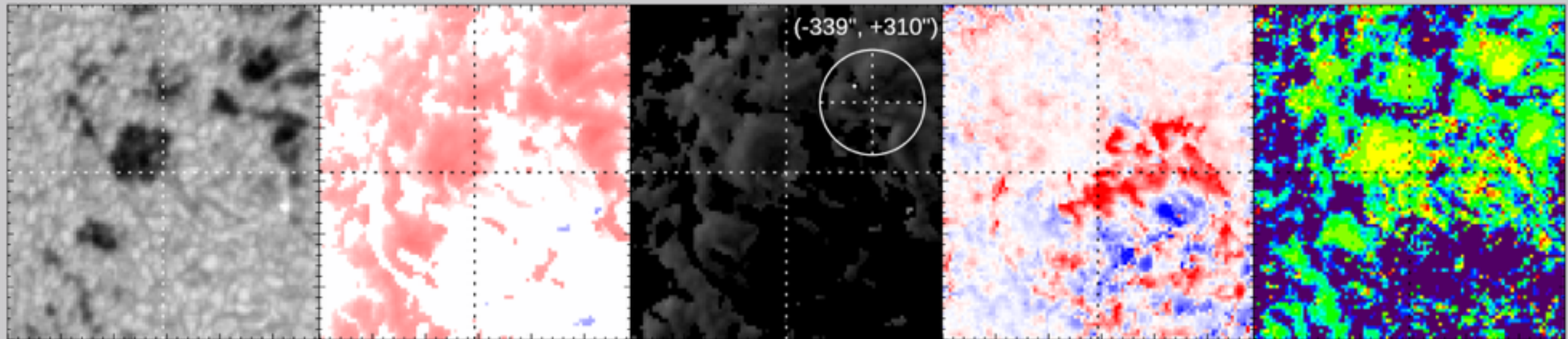
Continuum

B (LOS)

B (transverse)

Doppler velocity

Filling factor



8.0 arcsec

positive/negative polarity

redshift/blueshift

Not Caused by Flux Emergence

only redshift observed in **79** ARs

(11) AR 10956

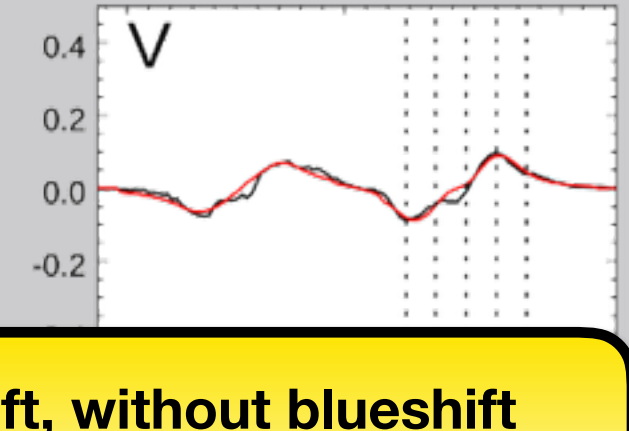
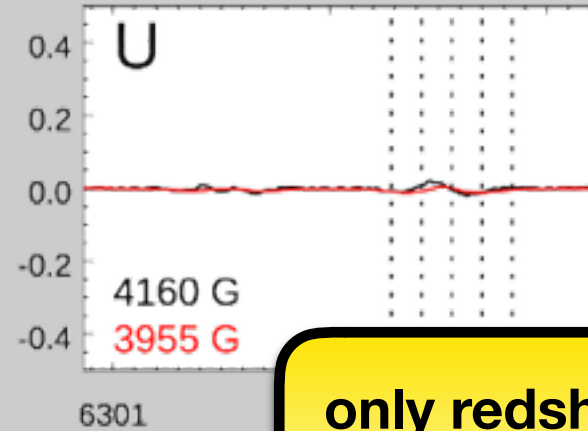
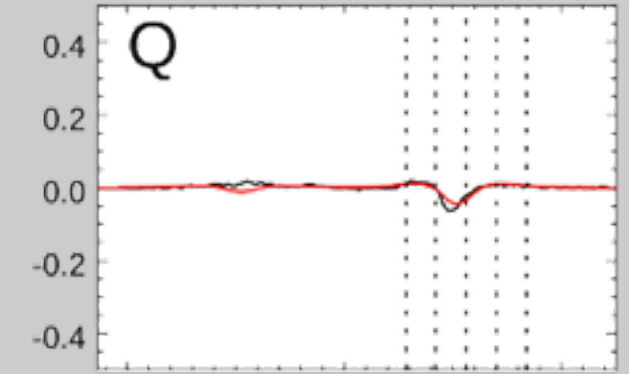
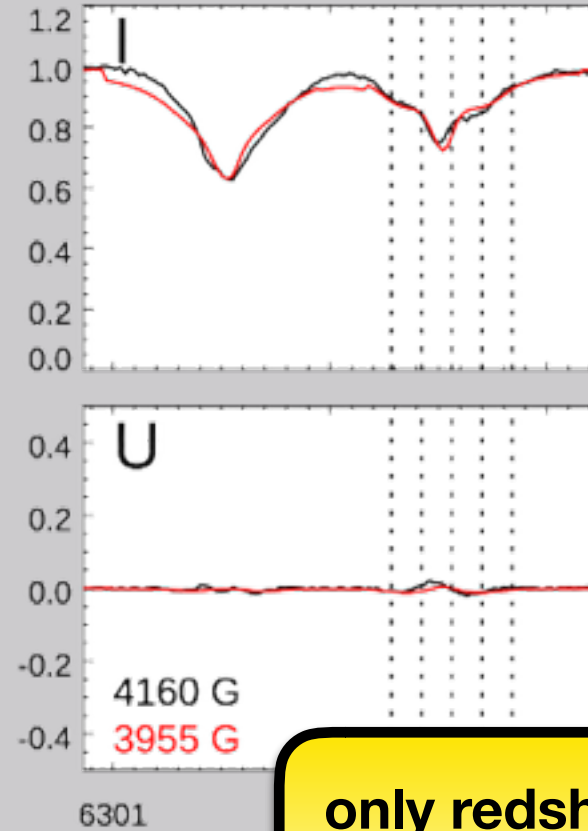
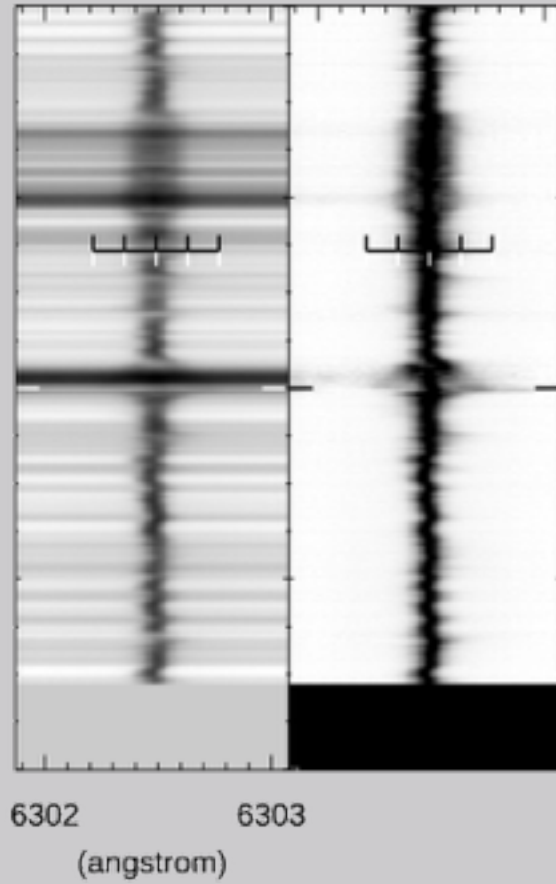
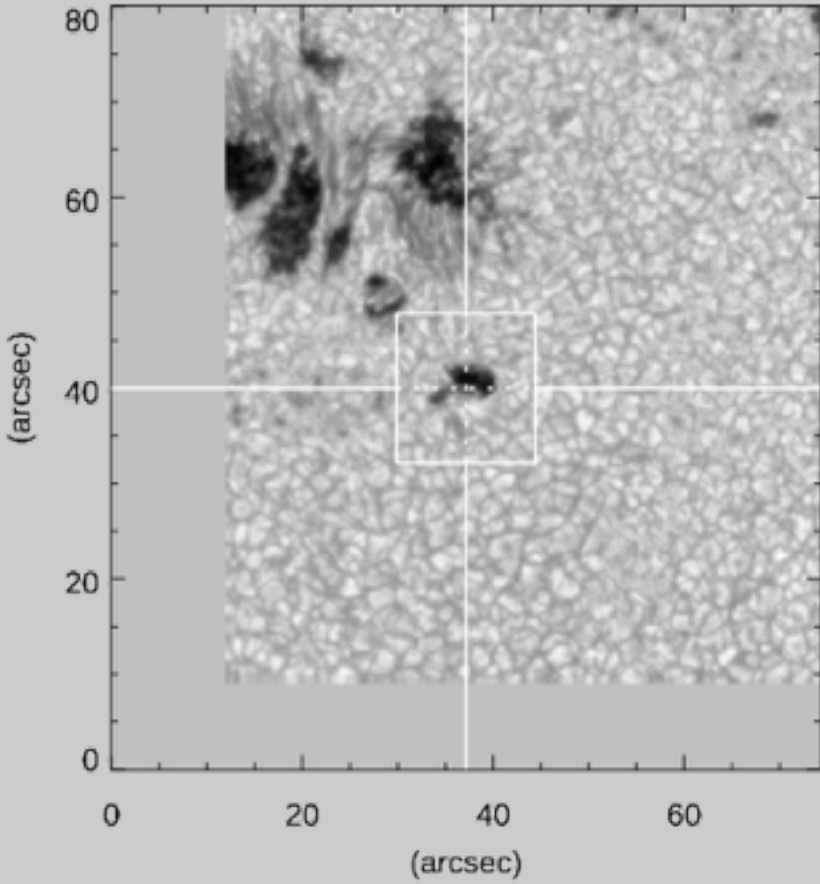
[20070519_123821]

Loc
p

Continuum

Stokes I (emphasized)

Full Stokes profiles at the location of the strongest field

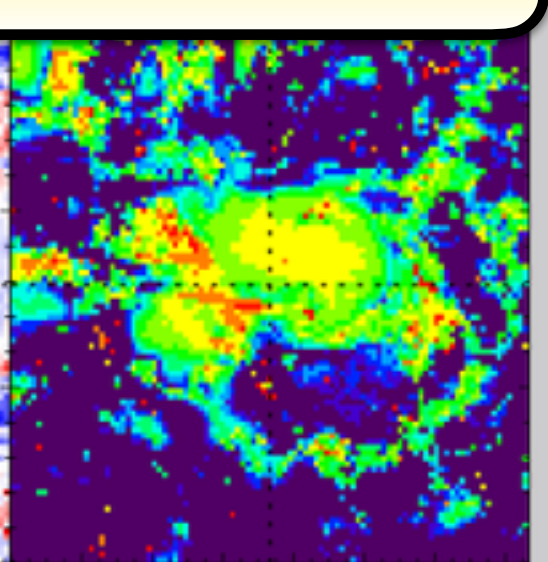
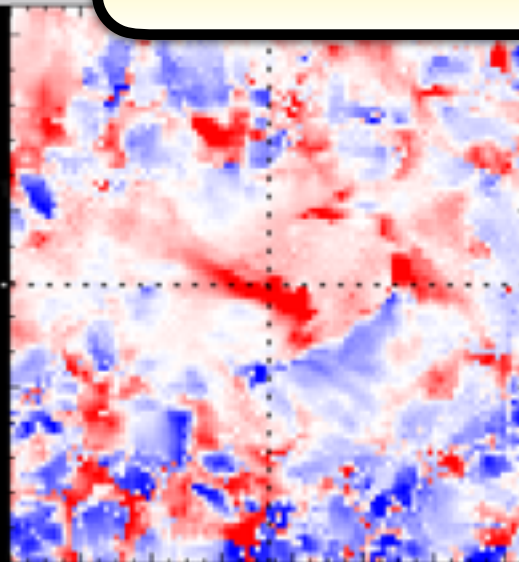
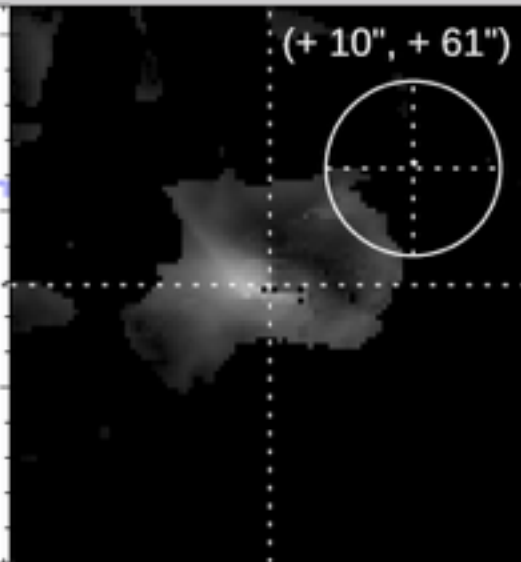
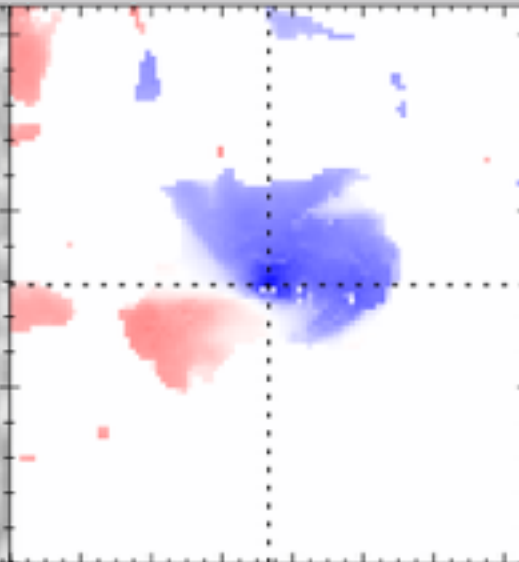
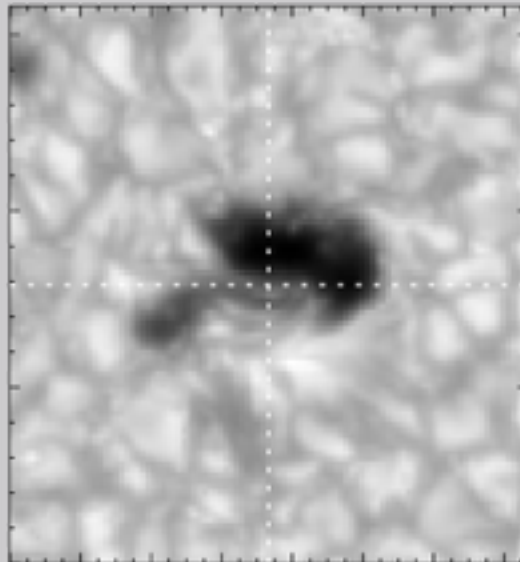


only redshift, without blueshift even at DC
→ not caused by flux emergence

Continuum

B (LOS)

B (transverse)



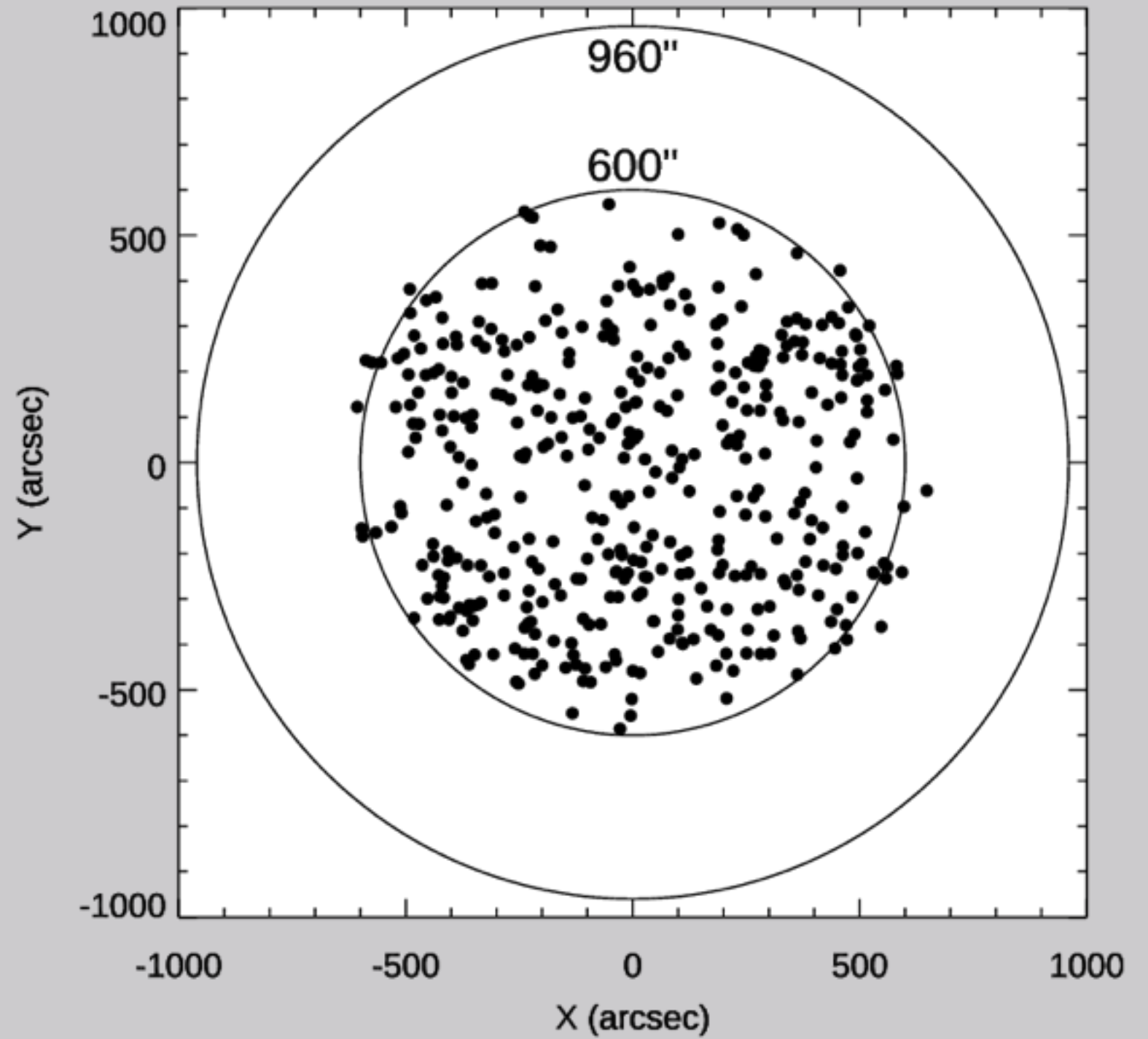
4.0 arcsec

positive/negative polarity

redshift/blueshift

Distribution of Strongest Fields

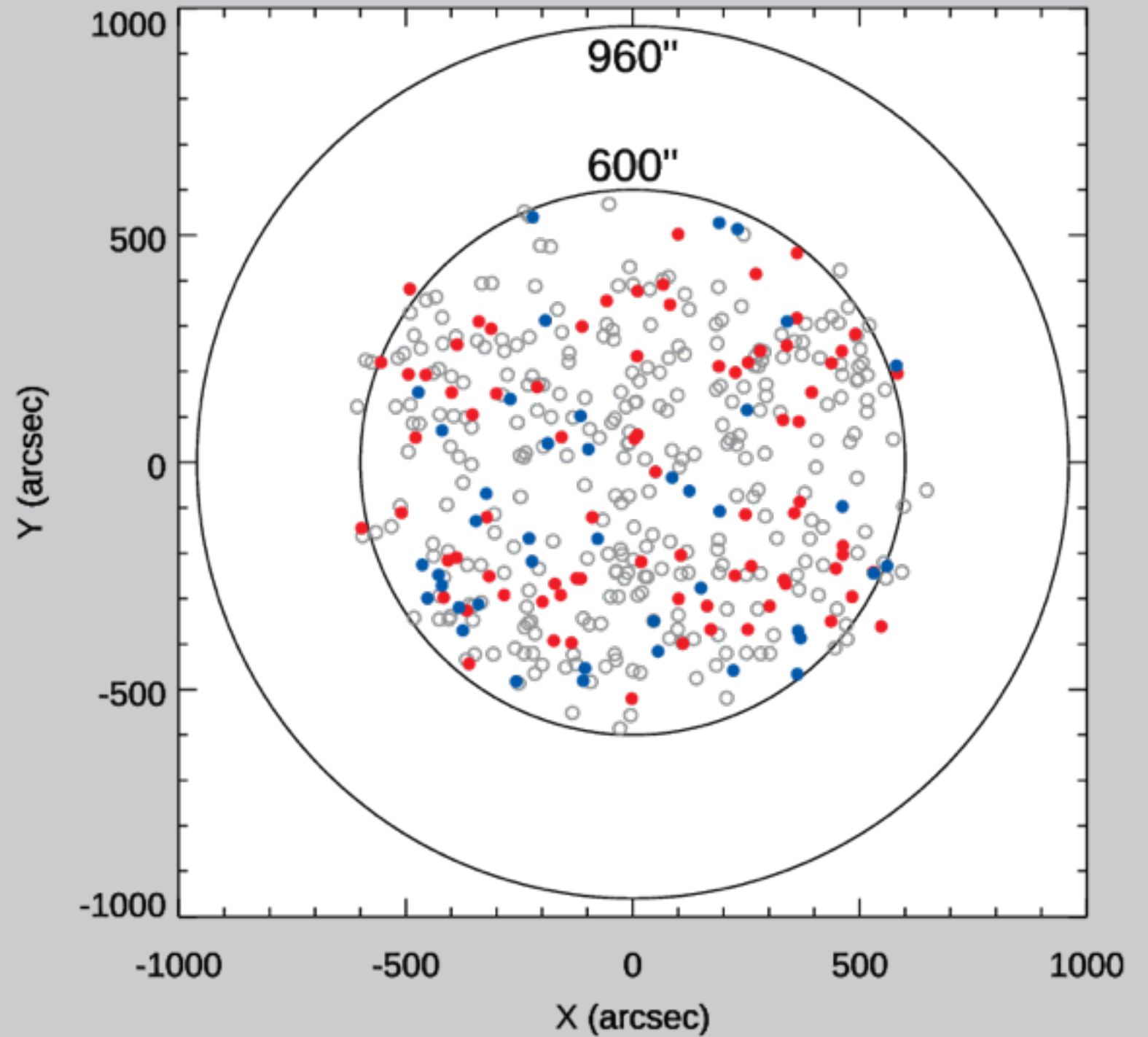
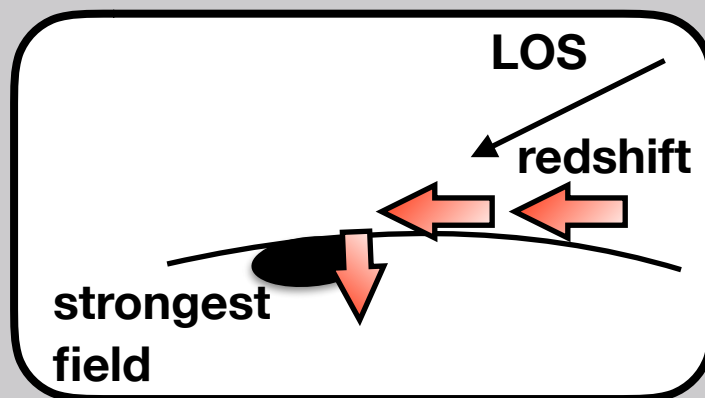
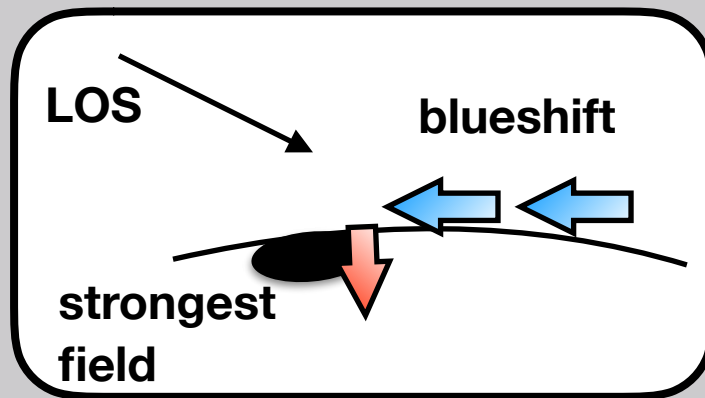
all 419 ARs



Distribution of Strongest Fields

all 419 ARs

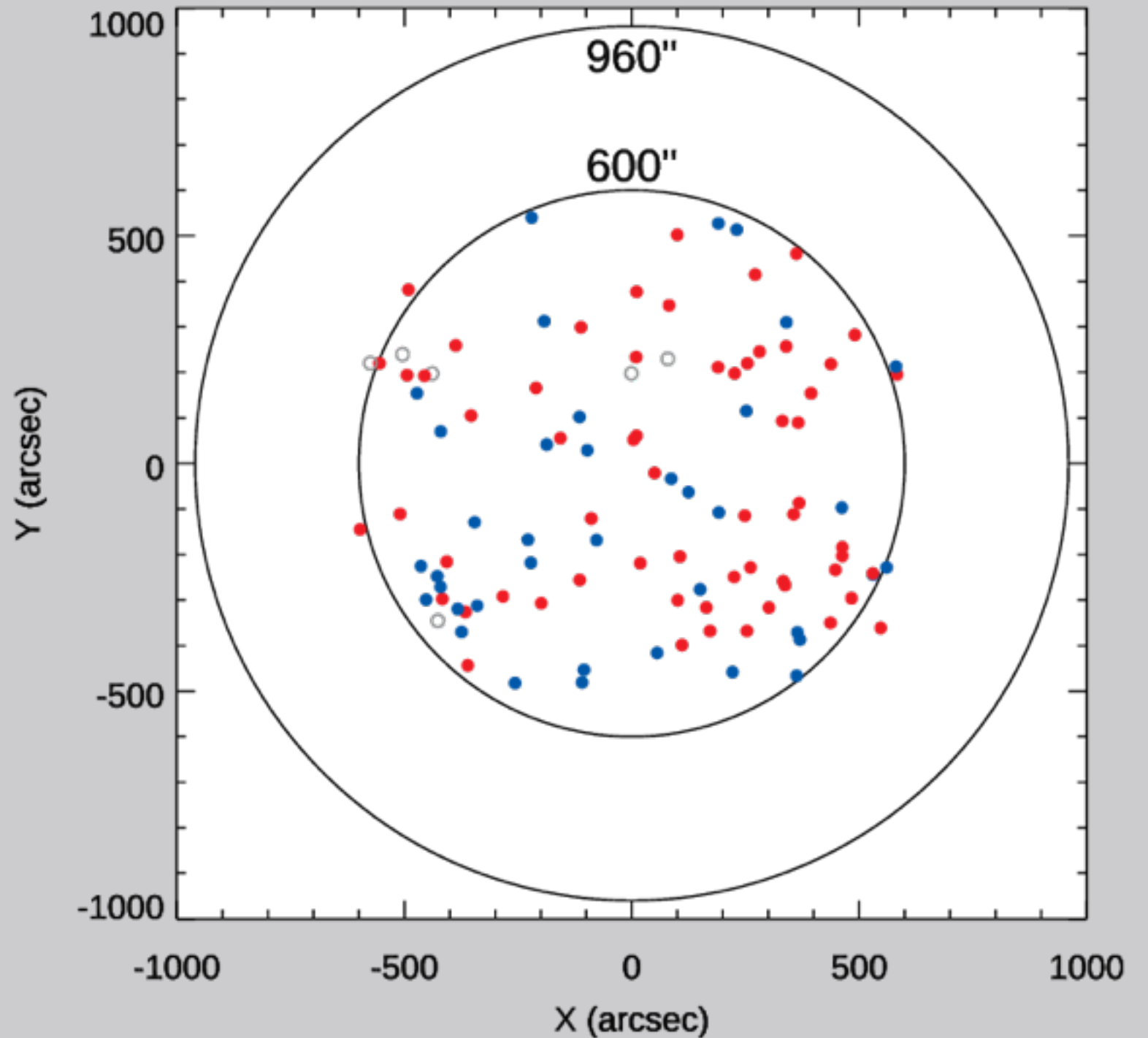
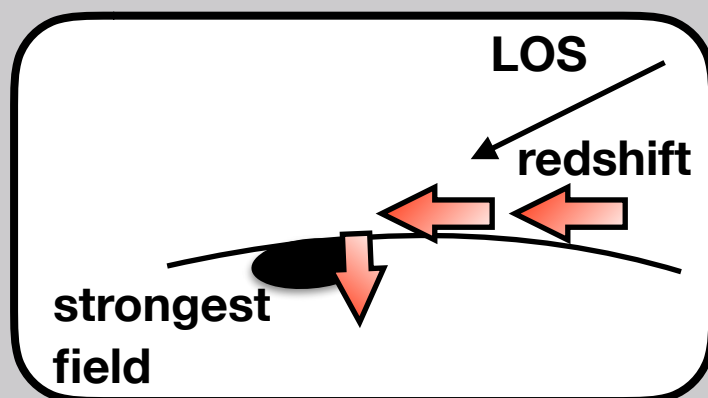
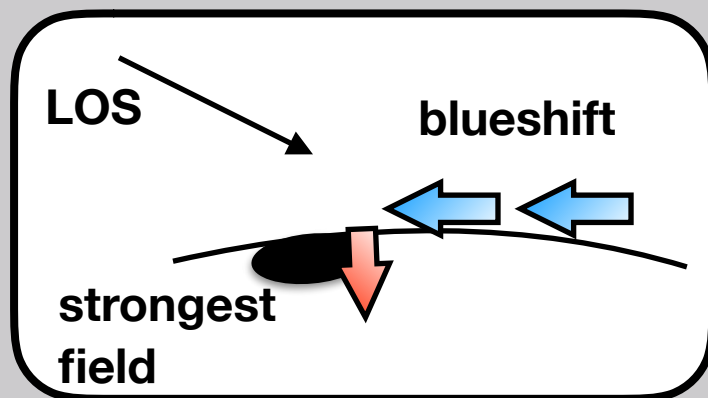
red/blue coloring —
Flow direction derived from
Dopplershift is consistent
with horizontal flows toward
the strong field region



Distribution of Strongest Fields

non-umbra (105)

red/blue coloring —
Flow direction derived from
Dopplershift is consistent
with horizontal flows toward
the strong field region



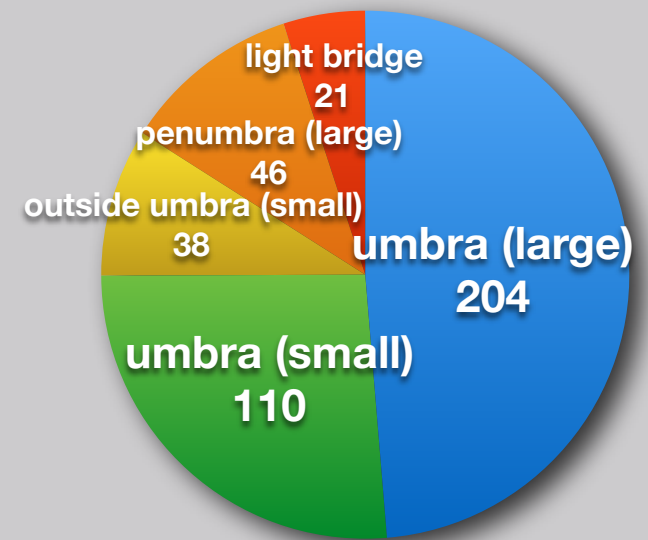
In 94% of ARs with the strongest field in non-umbrae, the Doppler velocity can be interpreted as horizontal flows toward the strong field region.

Conclusion

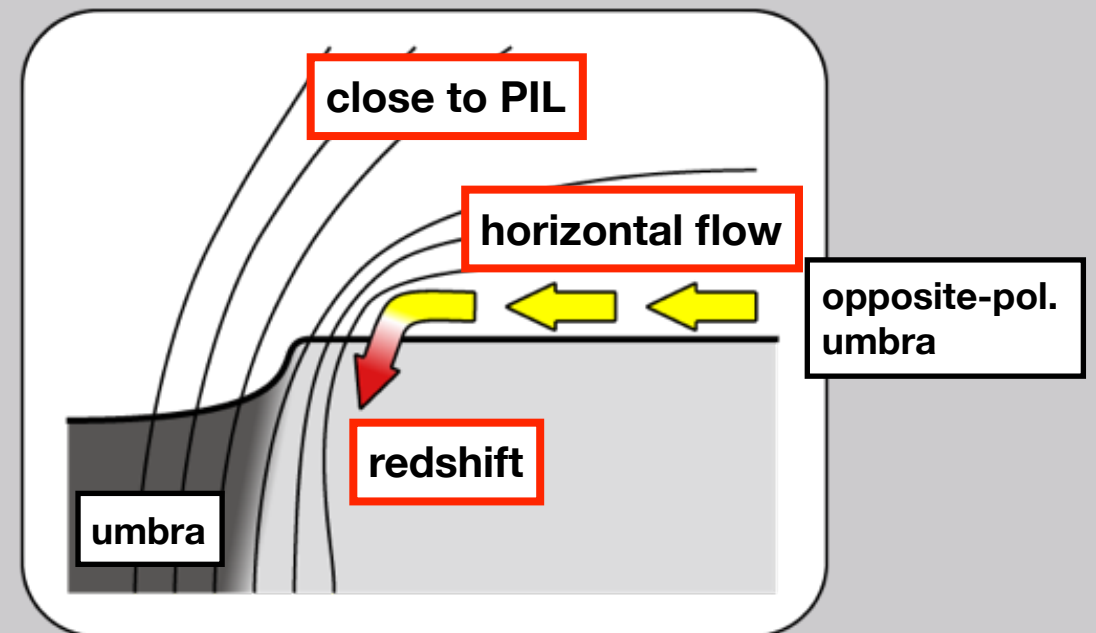
Where is the strongest field in each AR ?

75% in umbrae

25% outside umbrae



The latter 25% of ARs get high in rankings of field strength. 84% of them have the 3 features.



The result statistically supports the mechanism that the strongest fields are generated by the kinematics on the photosphere, not directly attributed to internal origins.

Other statistics and Appendix

Long-term Variation of Field Strength

Location Dependence on Field Strength

Spectral Shape

Fitting Result

Rank 4th – 10th

Pressing Pores

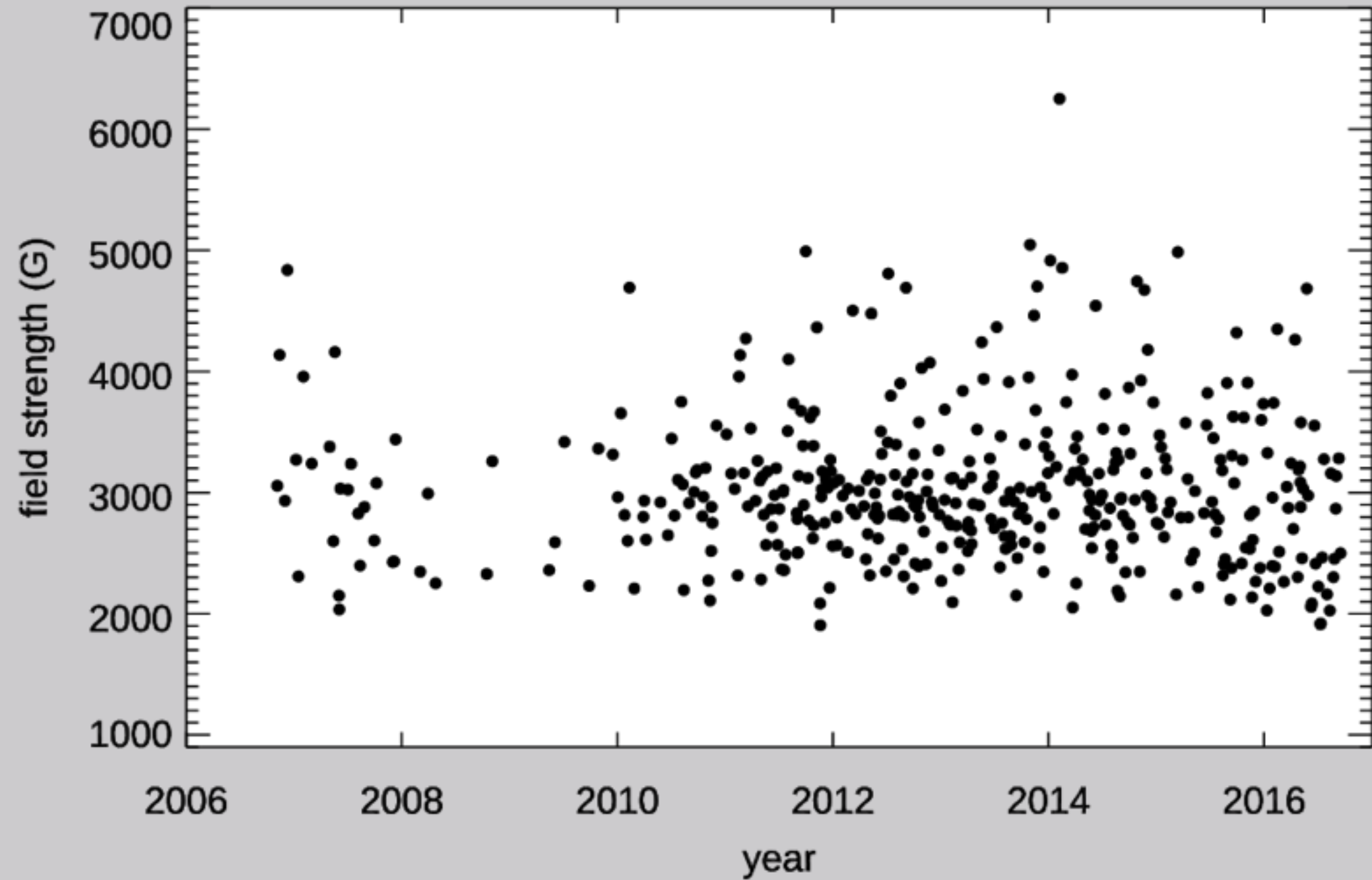
Other Examples

Miscellaneous

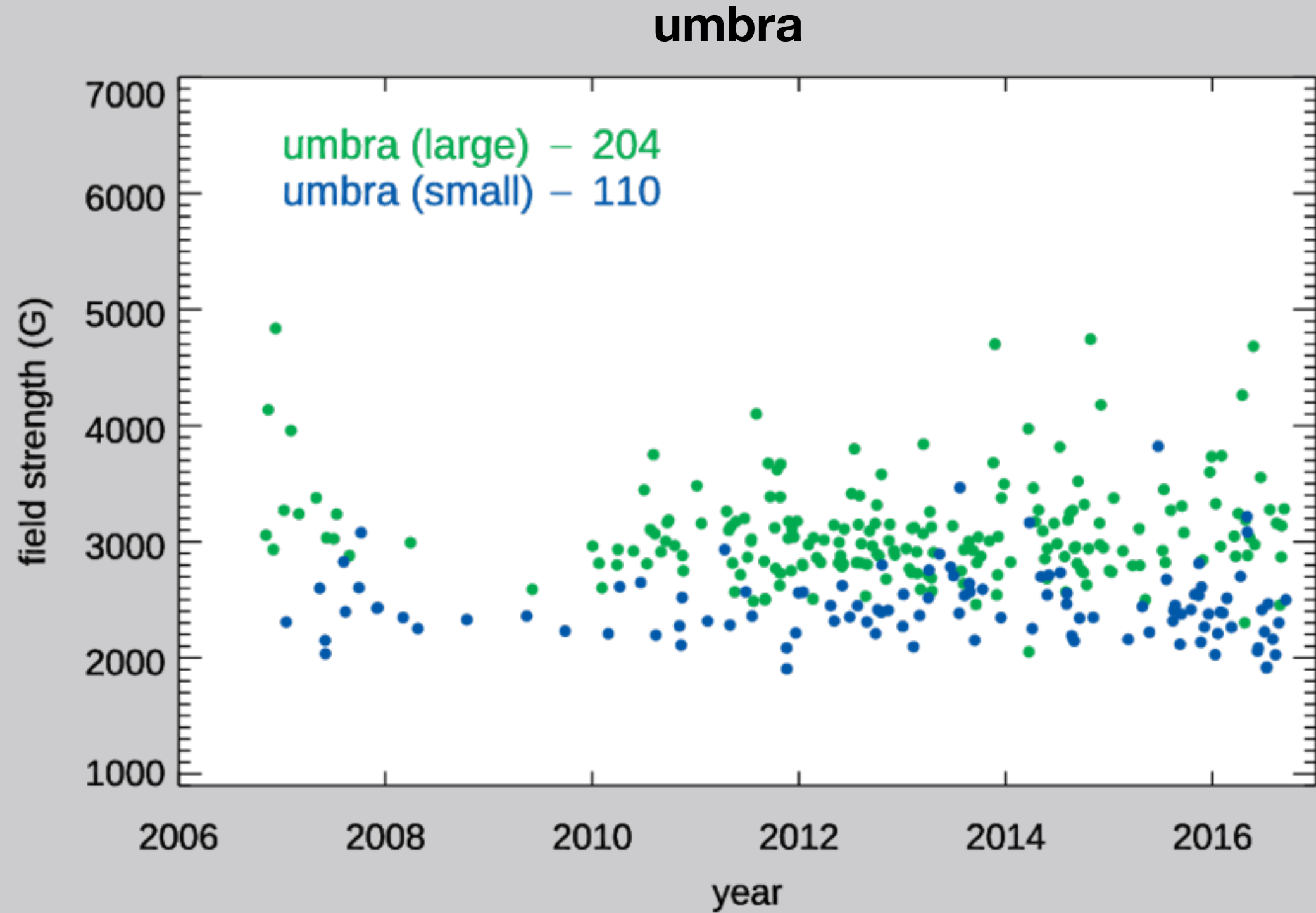
Long-term Variation of Field Strength

Long-term Variation of Strongest Fields

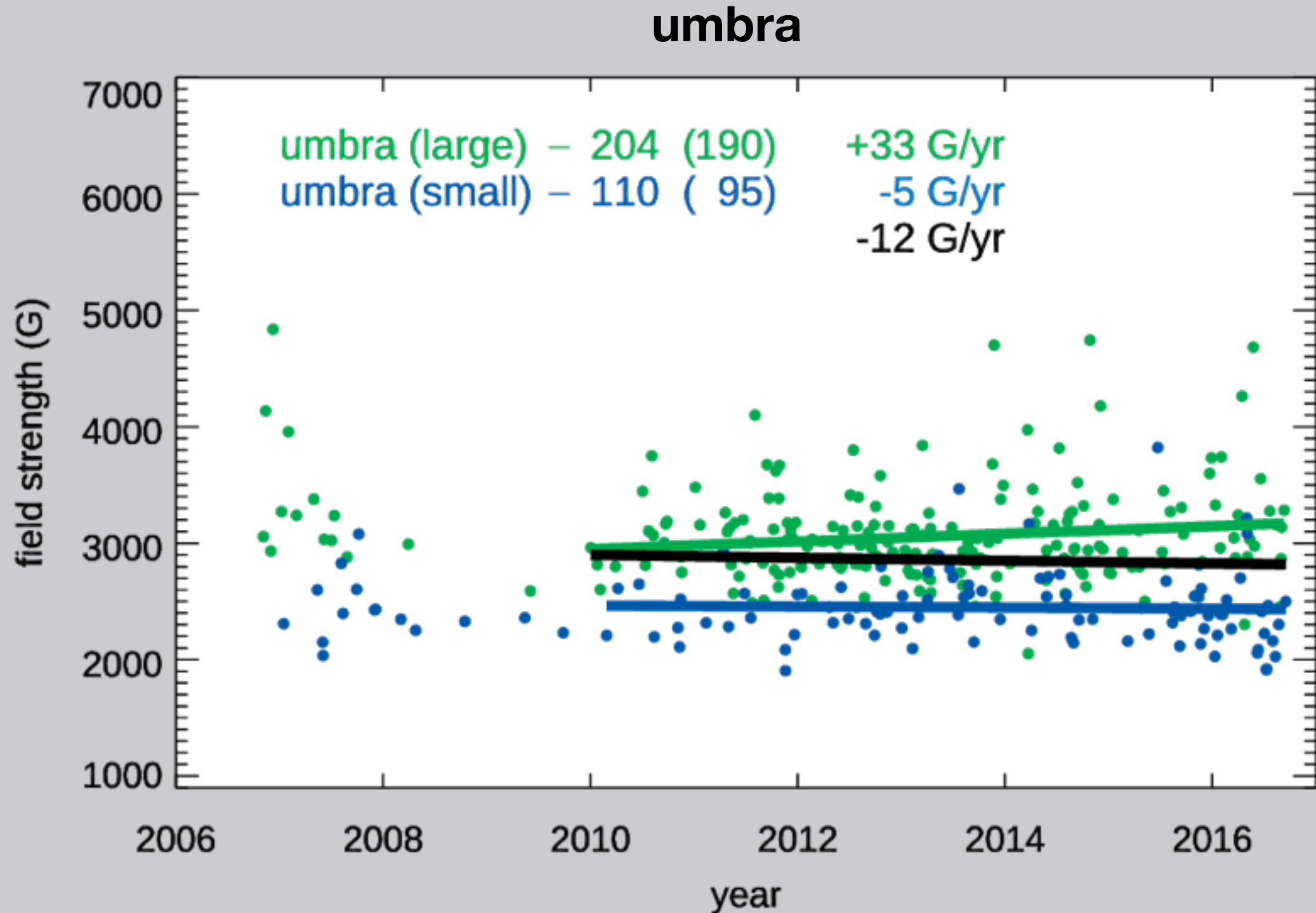
all 419 ARs



Long-term Variation of Strongest Fields



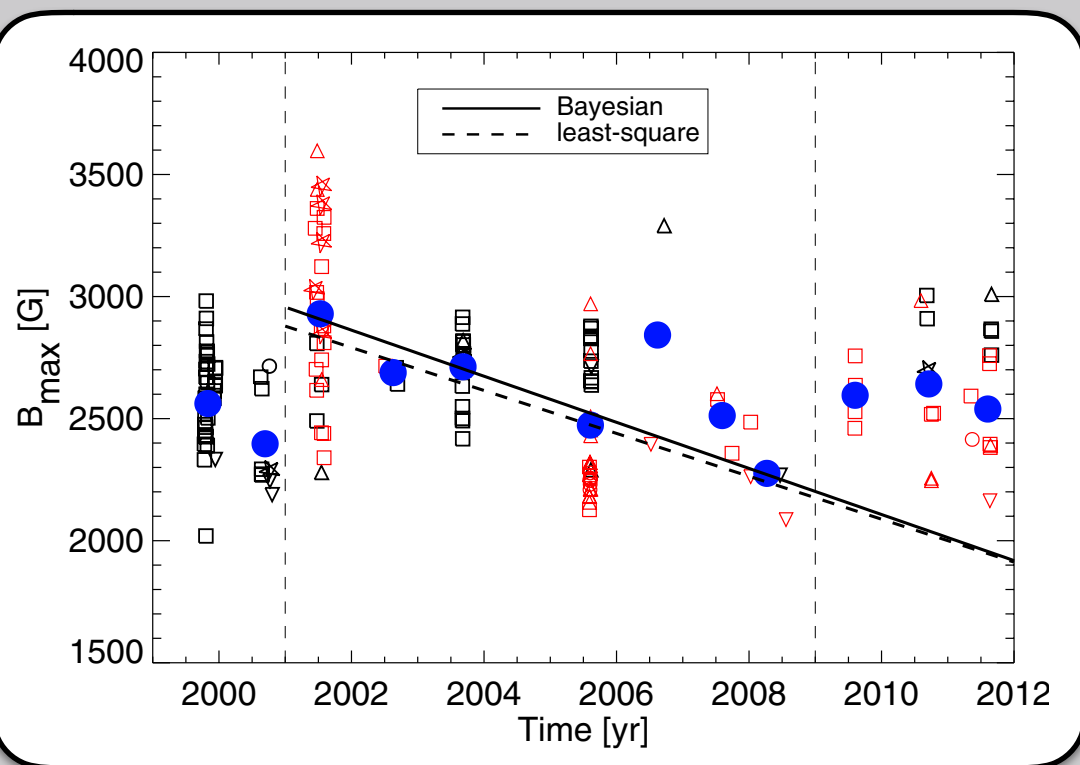
Long-term Variation of Strongest Fields



No clear trend. Note that removal of one-quarters of ARs with their strongest fields outside umbrae is not suitable for this discussion.

Previous Researches on Long-term Variation

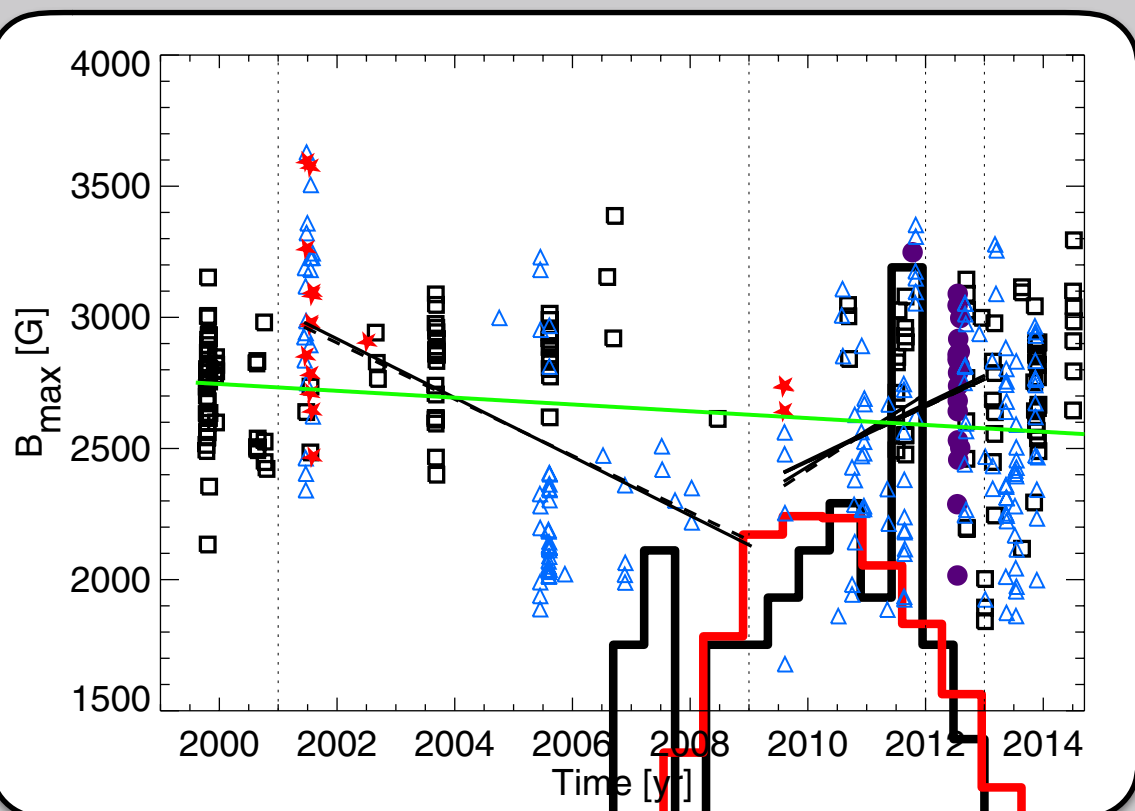
Rezaei+2012



VTT/TIP
infrared, Stokes-V

-94 G / yr

Rezaei+2015



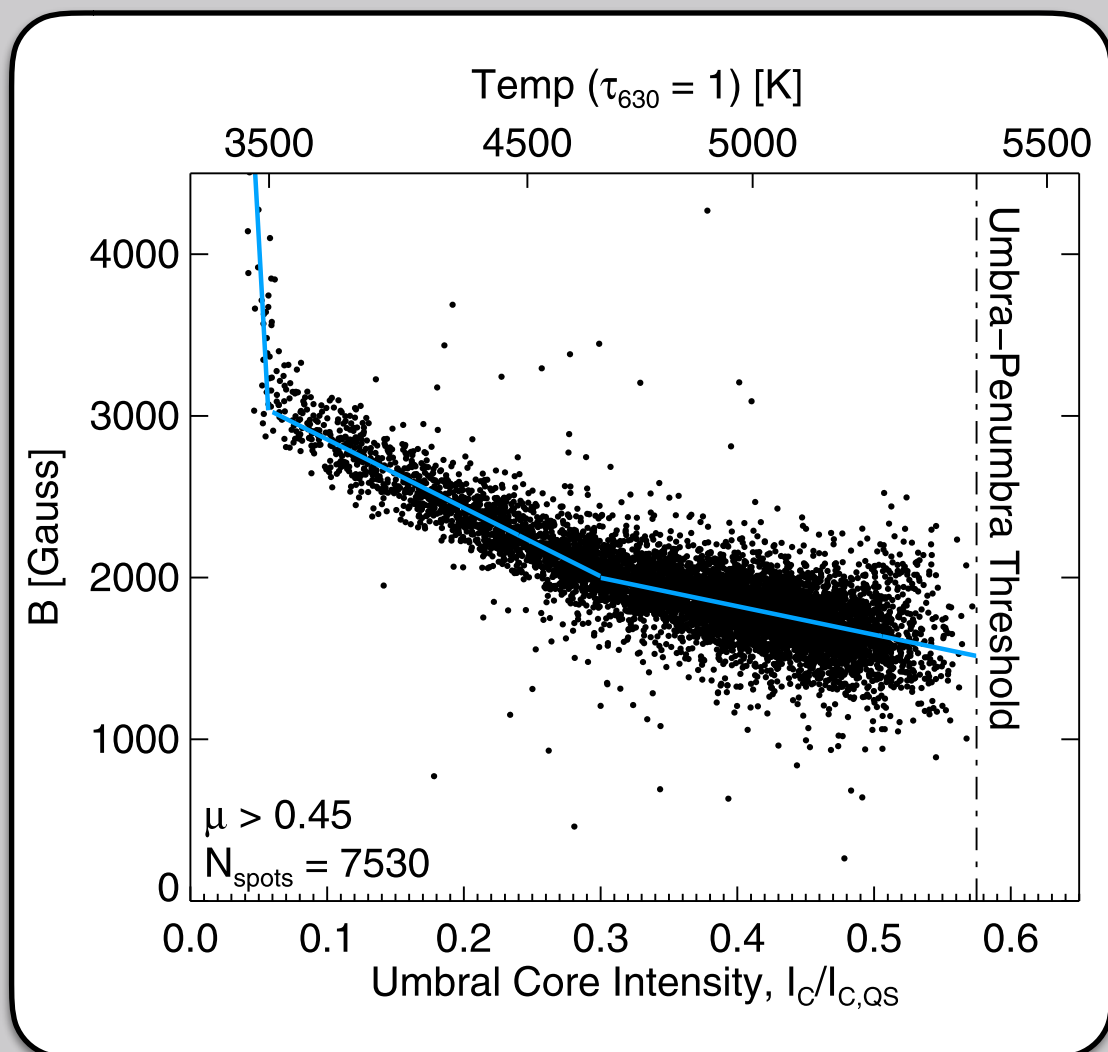
VTT/TIP, DST/FIRS
infrared, Stokes-V

-112 G / yr in Cycle 23

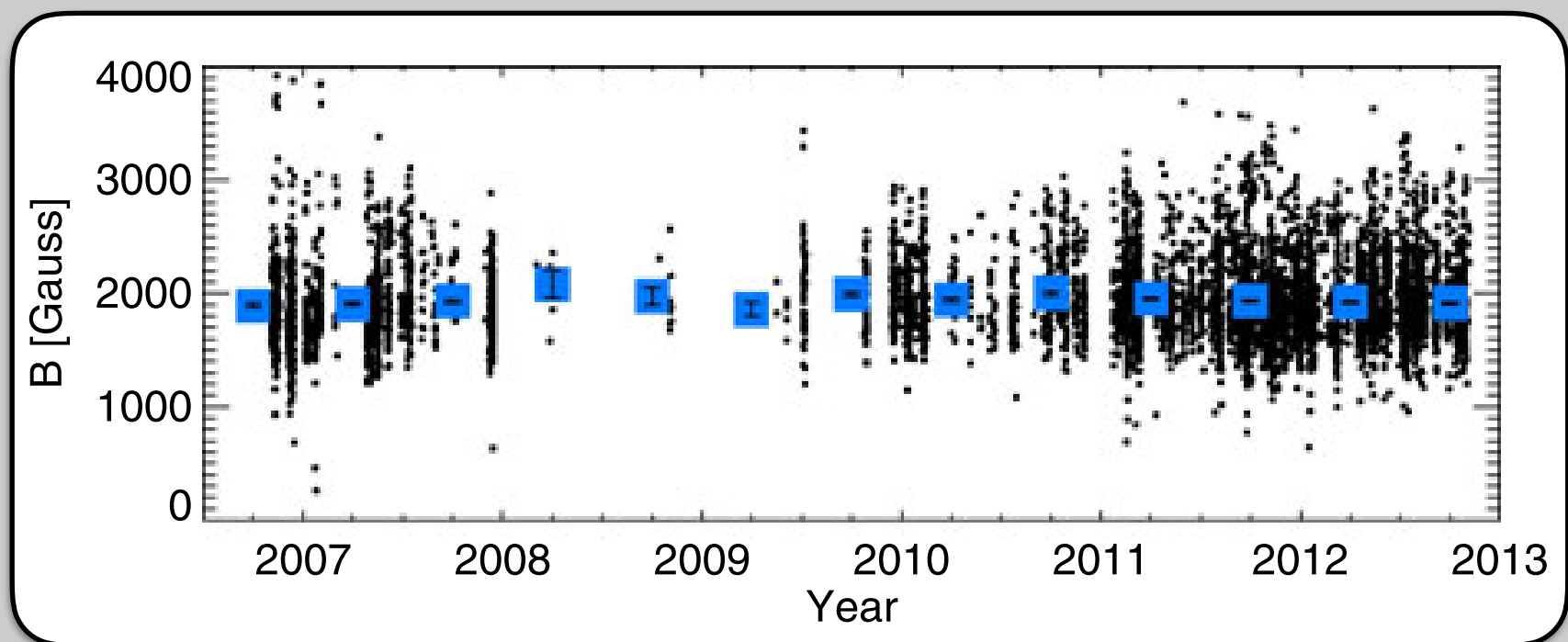
+138 G / yr in Cycle 24 (early phase)

Previous Researches on Long-term Variation

Schad 2014



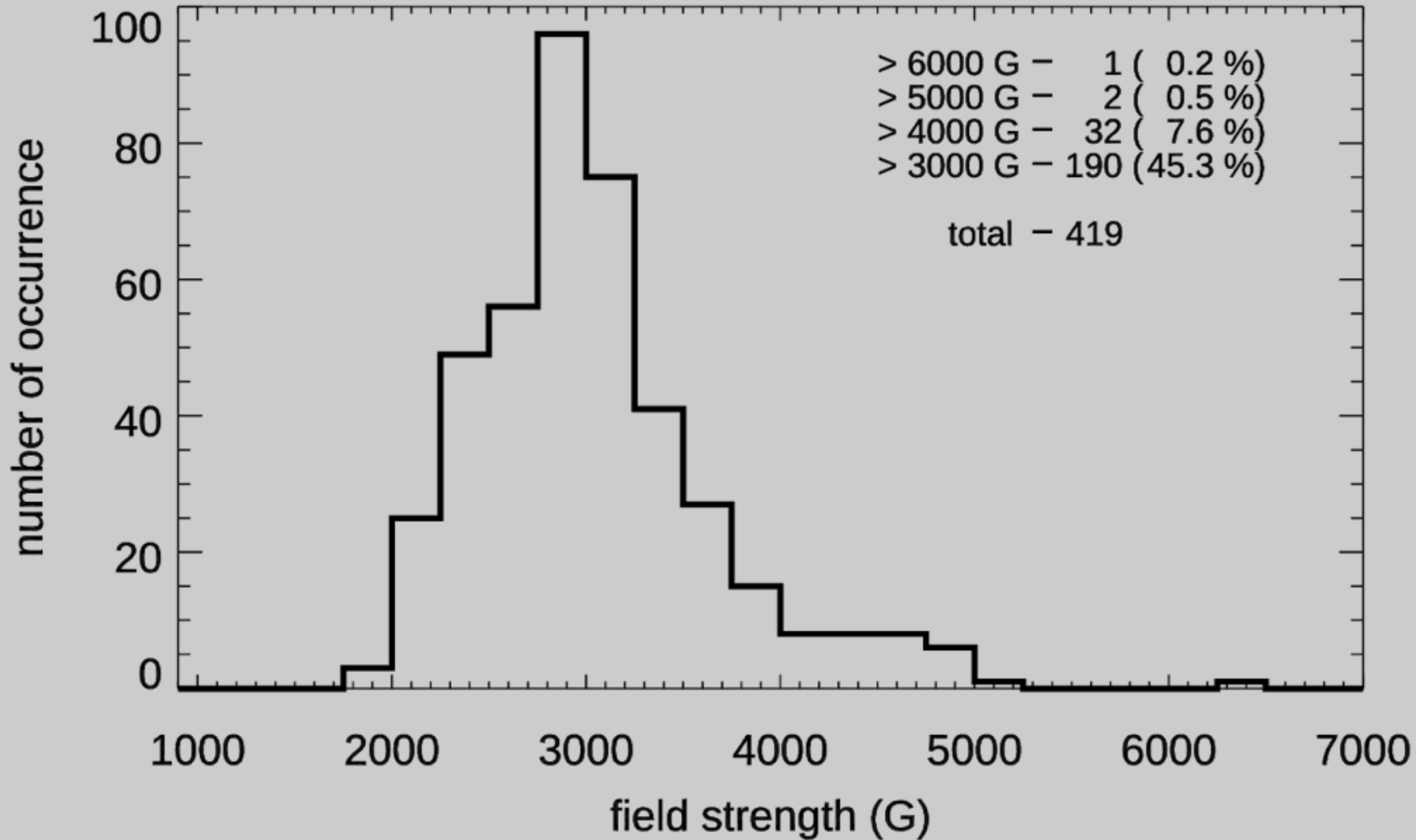
Hinode/SOT/SP
ME inversion
7,530 umbrae and pores
2006-2012



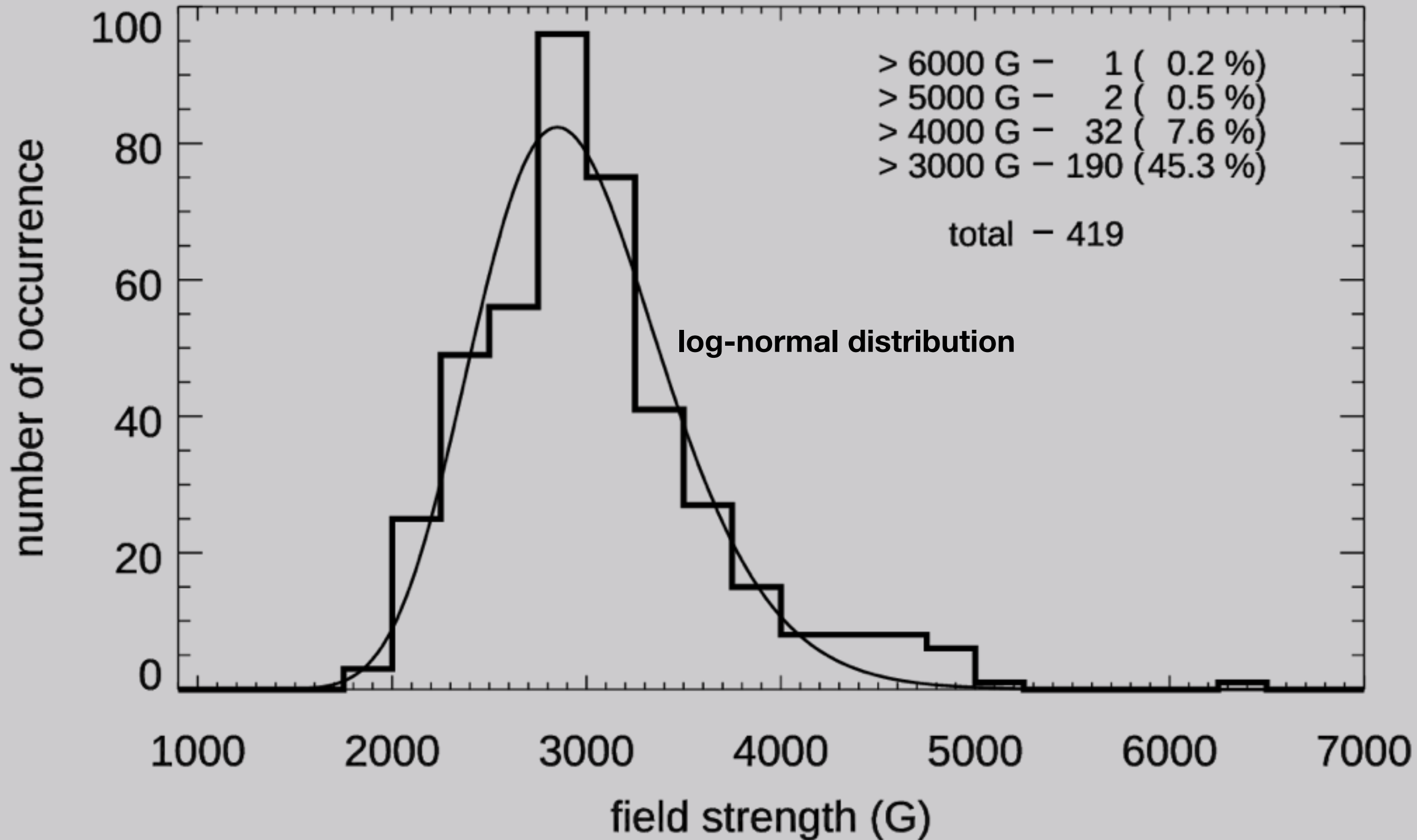
-25 G / yr

Location Dependence on Field Strength

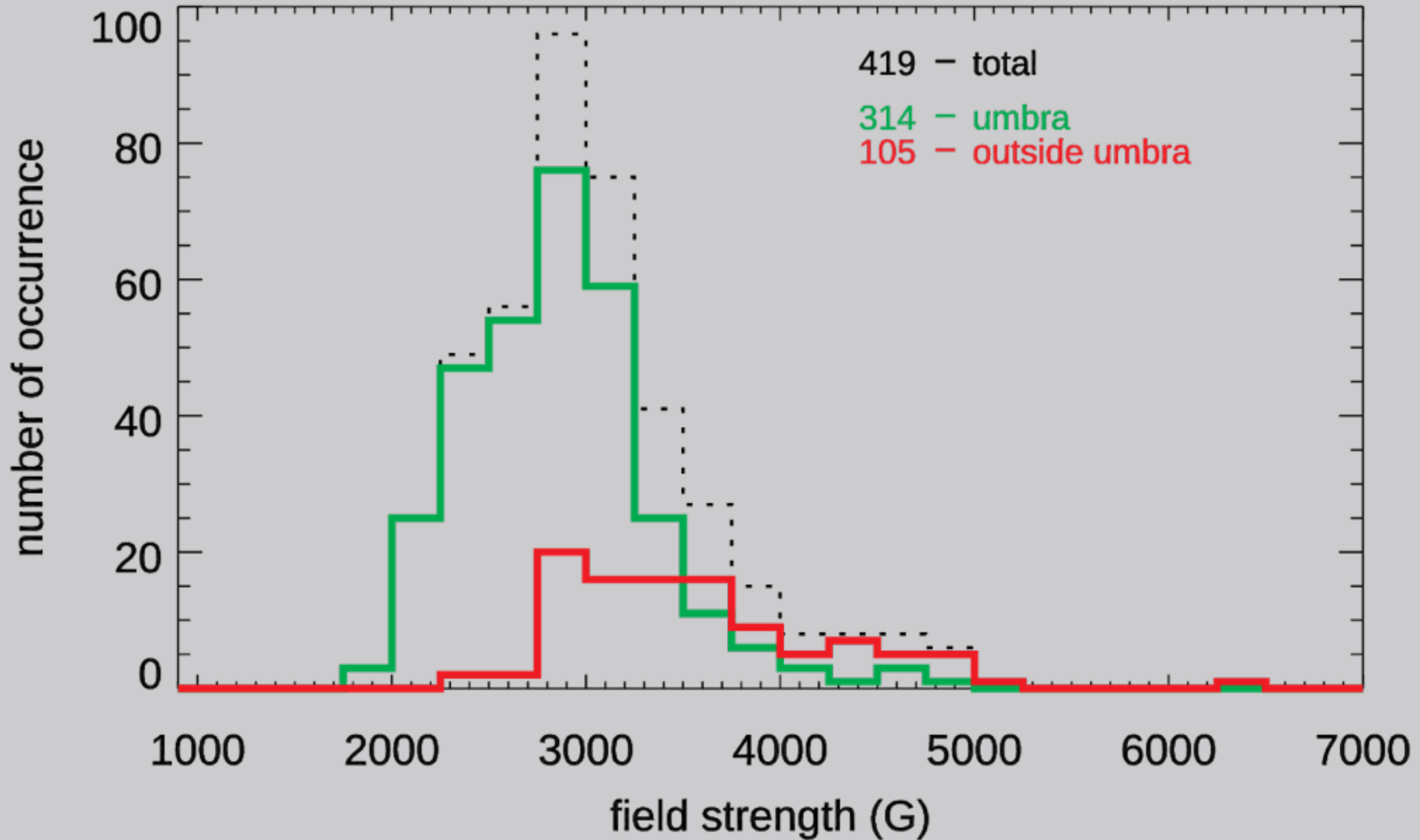
Number Distribution of Field Strength



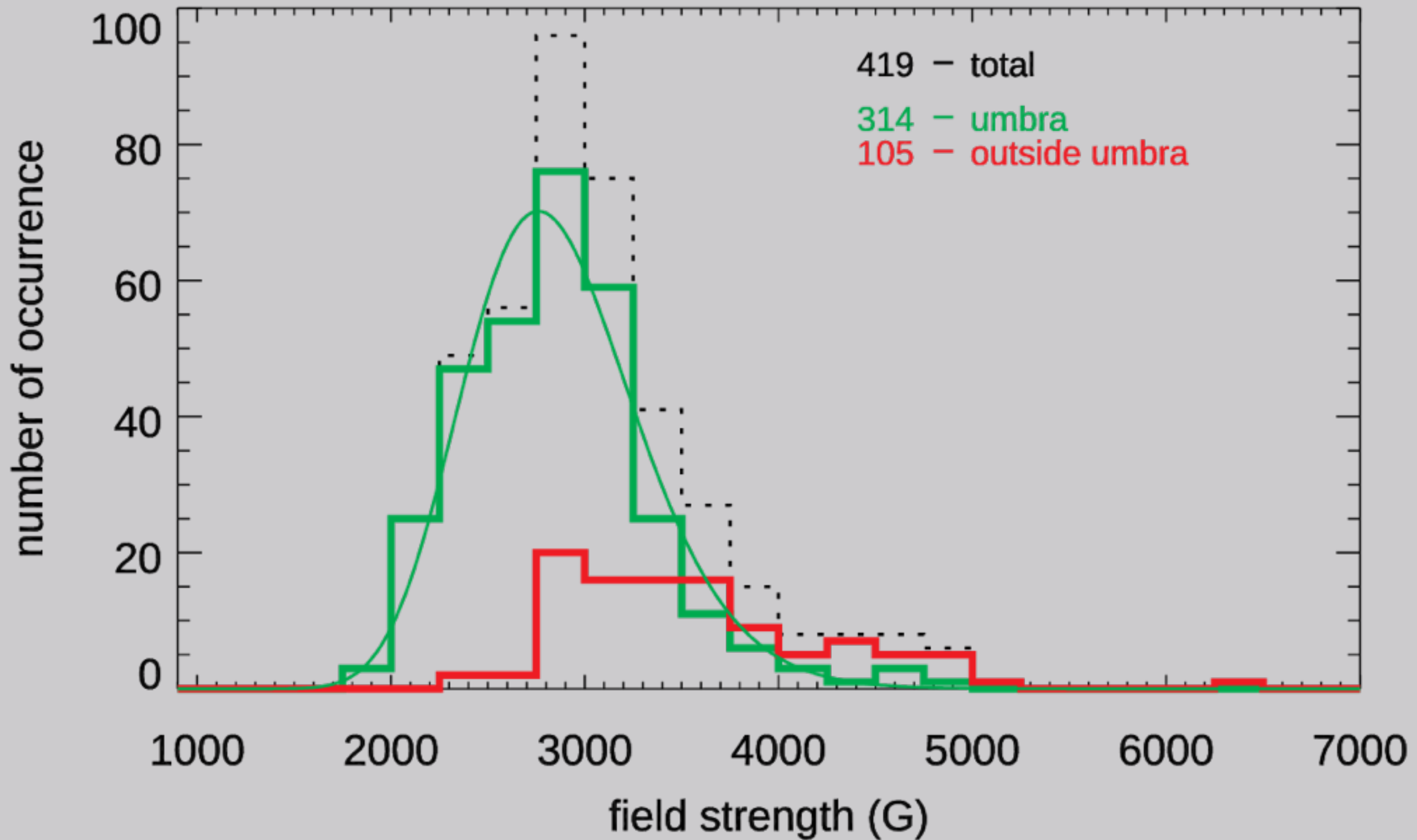
Number Distribution of Field Strength



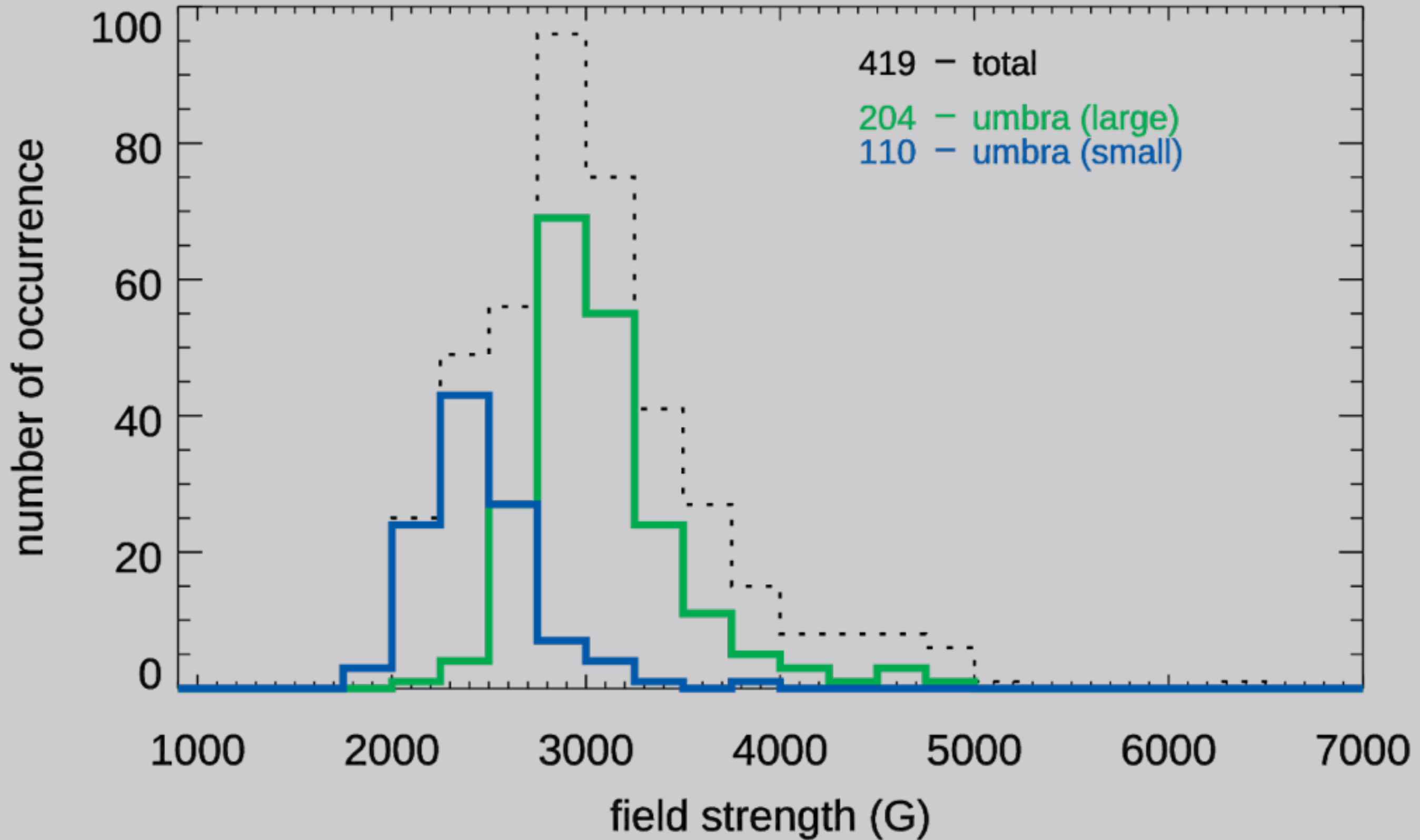
Number Distribution of Field Strength on Location



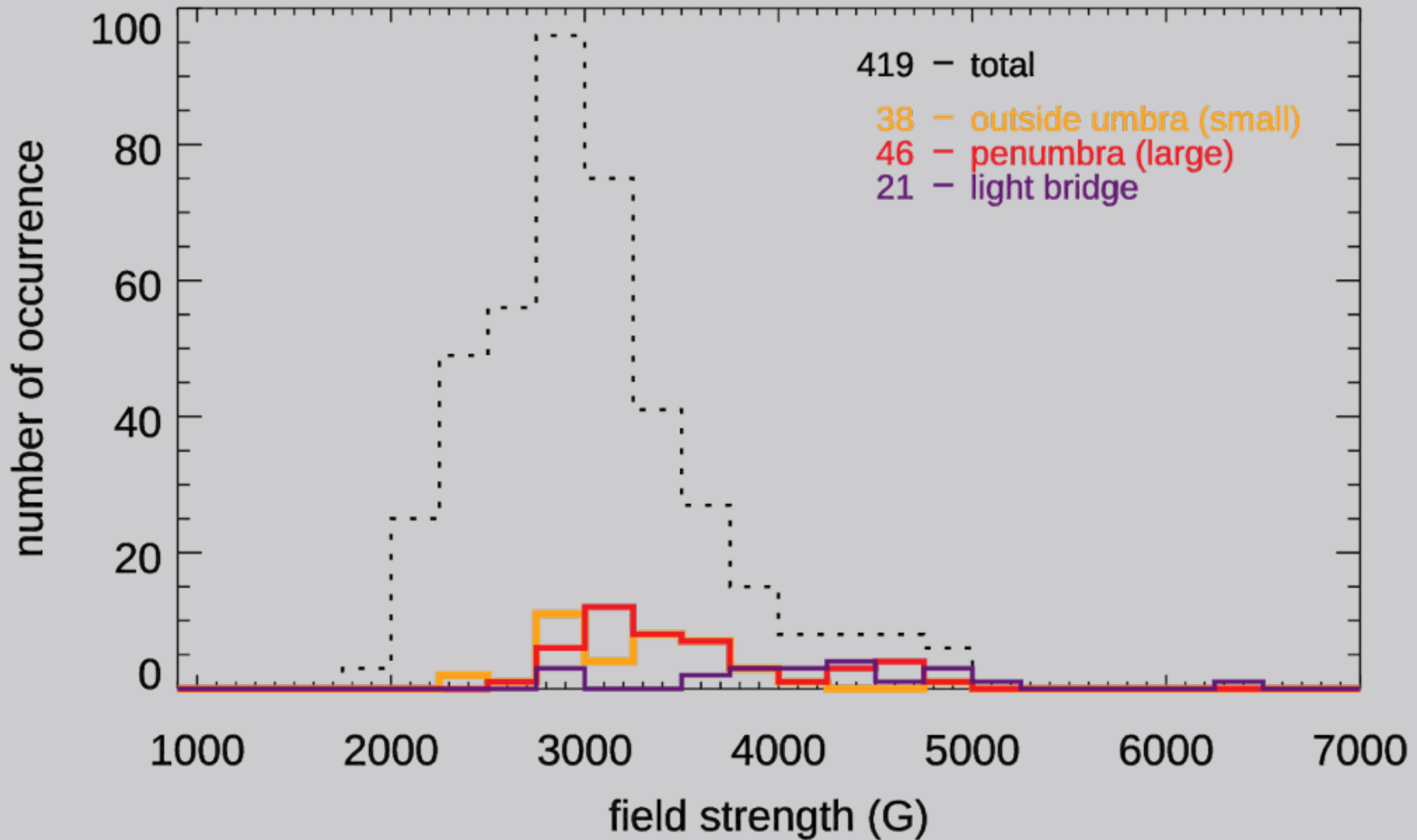
Number Distribution of Field Strength on Location



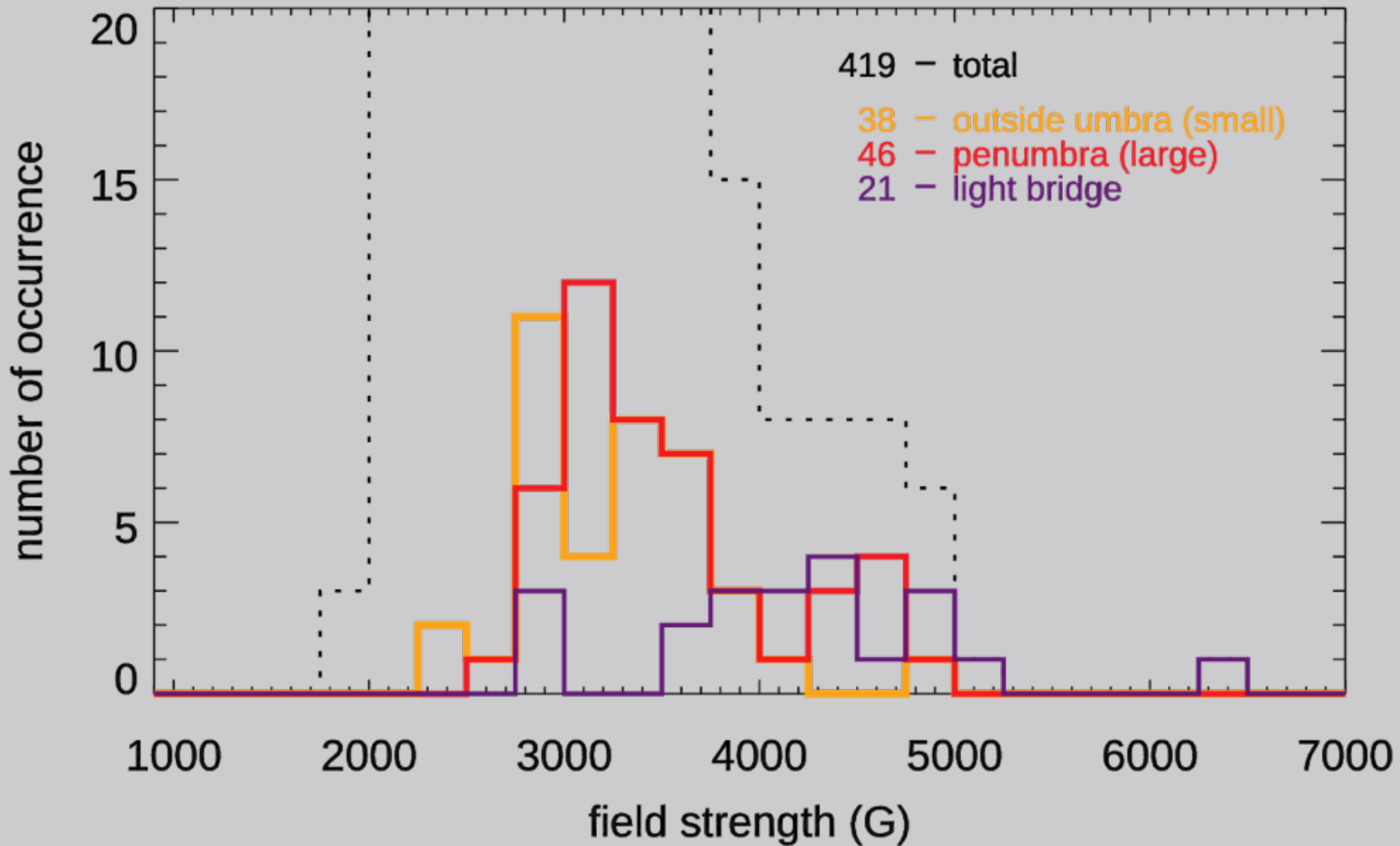
Number Distribution of Field Strength on Location



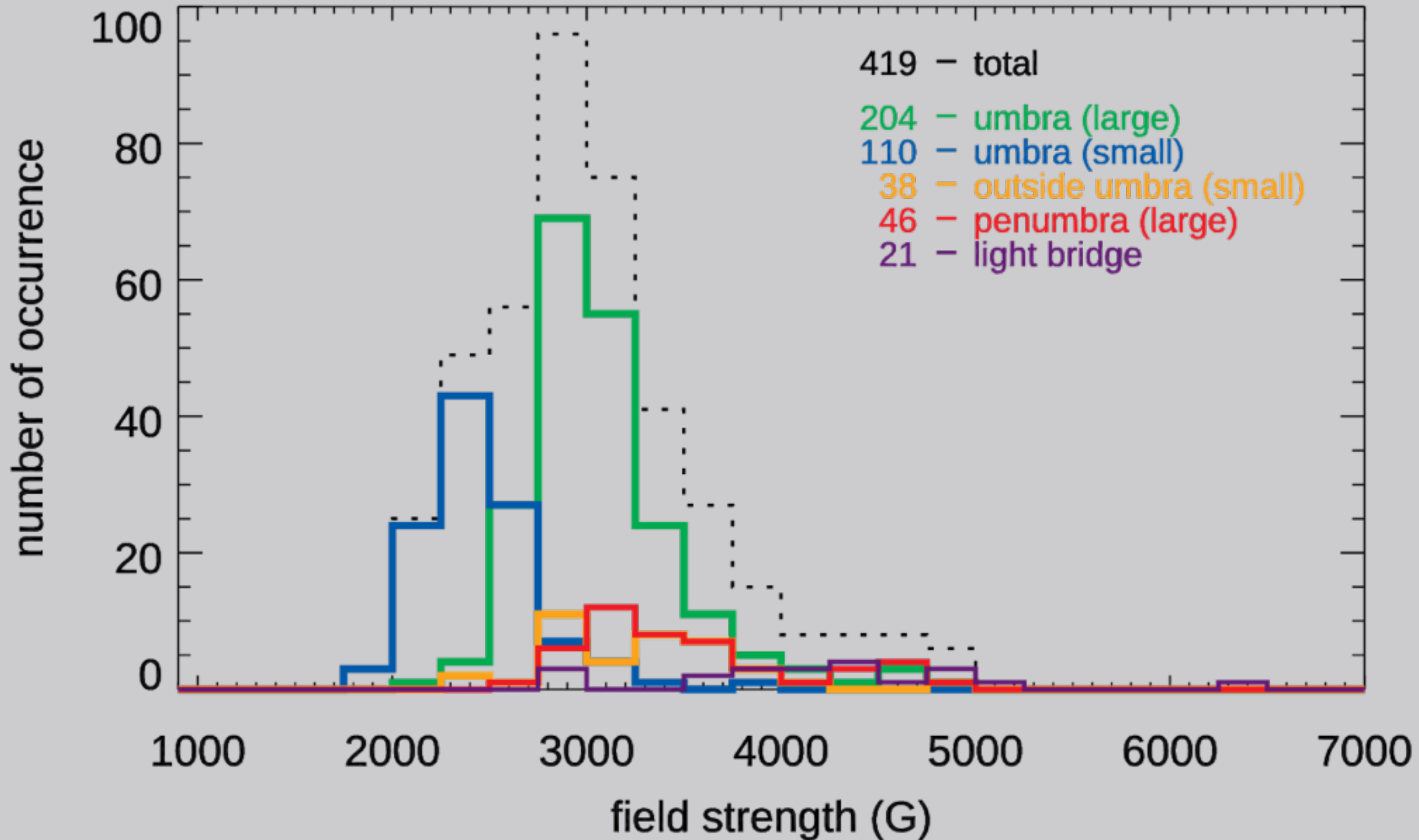
Number Distribution of Field Strength on Location



Number Distribution of Field Strength on Location



Number Distribution of Field Strength on Location

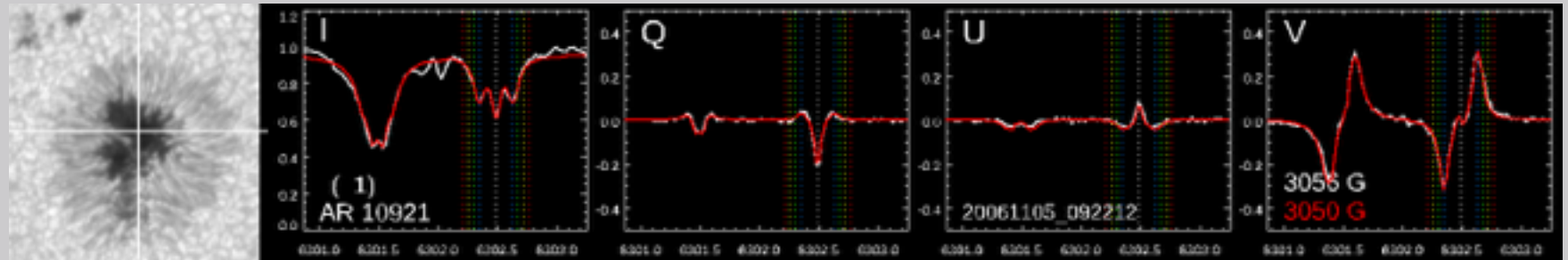


Spectral Shape

Spectral Shape

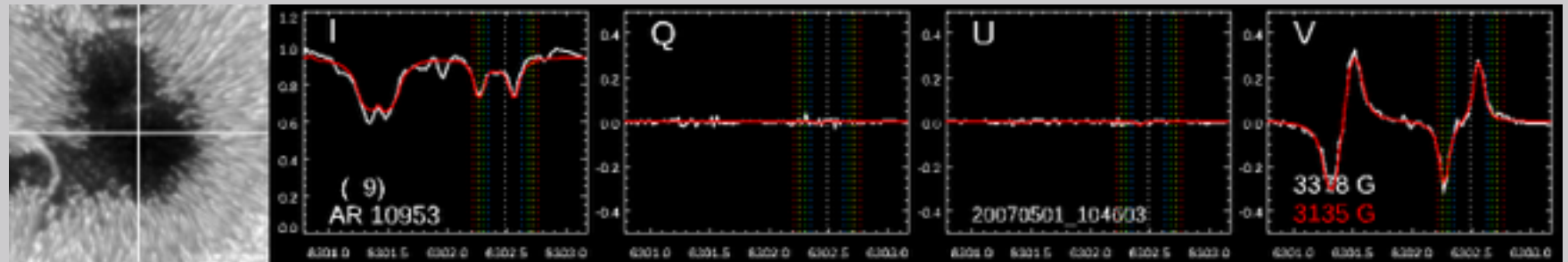
clear 3 splits

VVV



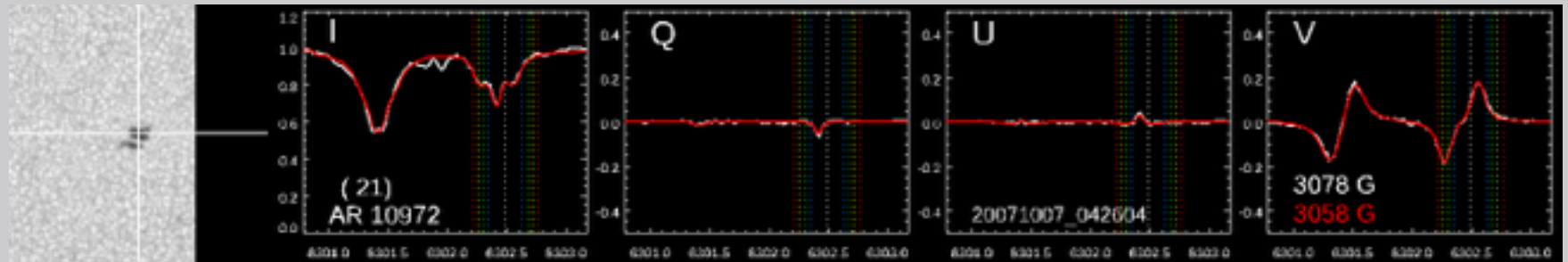
2 splits

V V



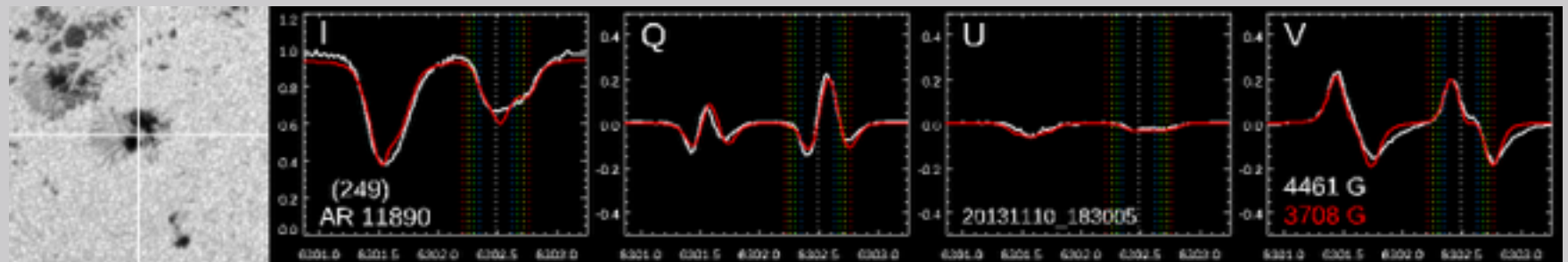
weak split

V



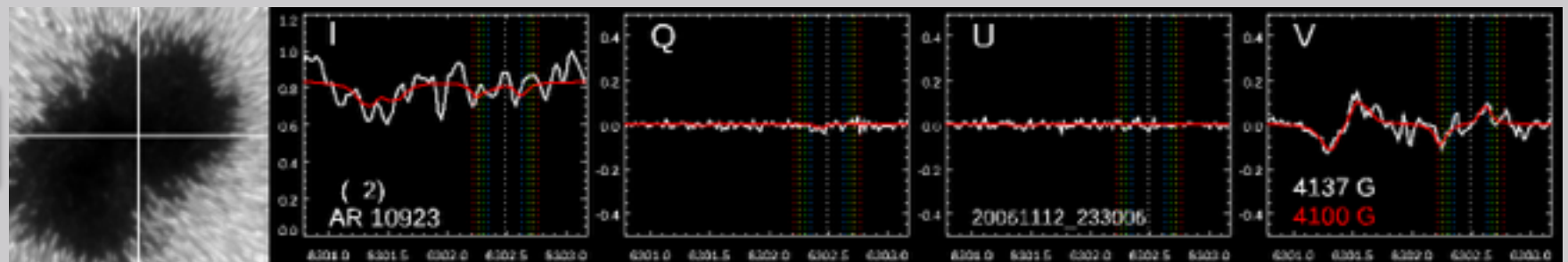
broad

V V



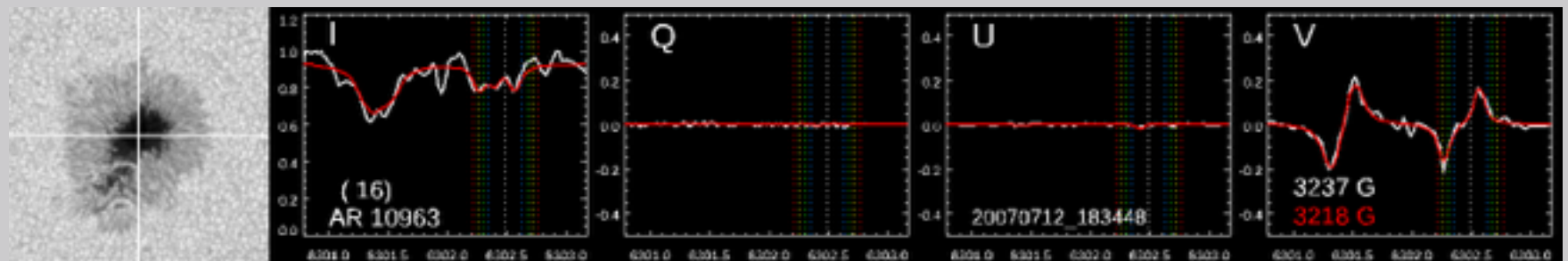
sawtooth
in both IV

ww-IV



sawtooth in I,
but clear V

ww-I



Location Dependence on Spectral Shape

	umbra (large)	umbra (small)	outside umbra (small)	penumbra (large)	light bridge
VVV	130	18	3	1	6 (1)
VV	14	3	0	0	0
V	14	49	11 (1)	10 (1)	2
/	4 (2)	40 (3)	24 (2)	34 (18)	13 (7)
ww-IV	23	0	0	0	0
ww-I	19	0	0	1 (1)	0
total	204 (2)	110 (3)	38 (3)	46 (20)	21 (8)

(red) – NG fitting result

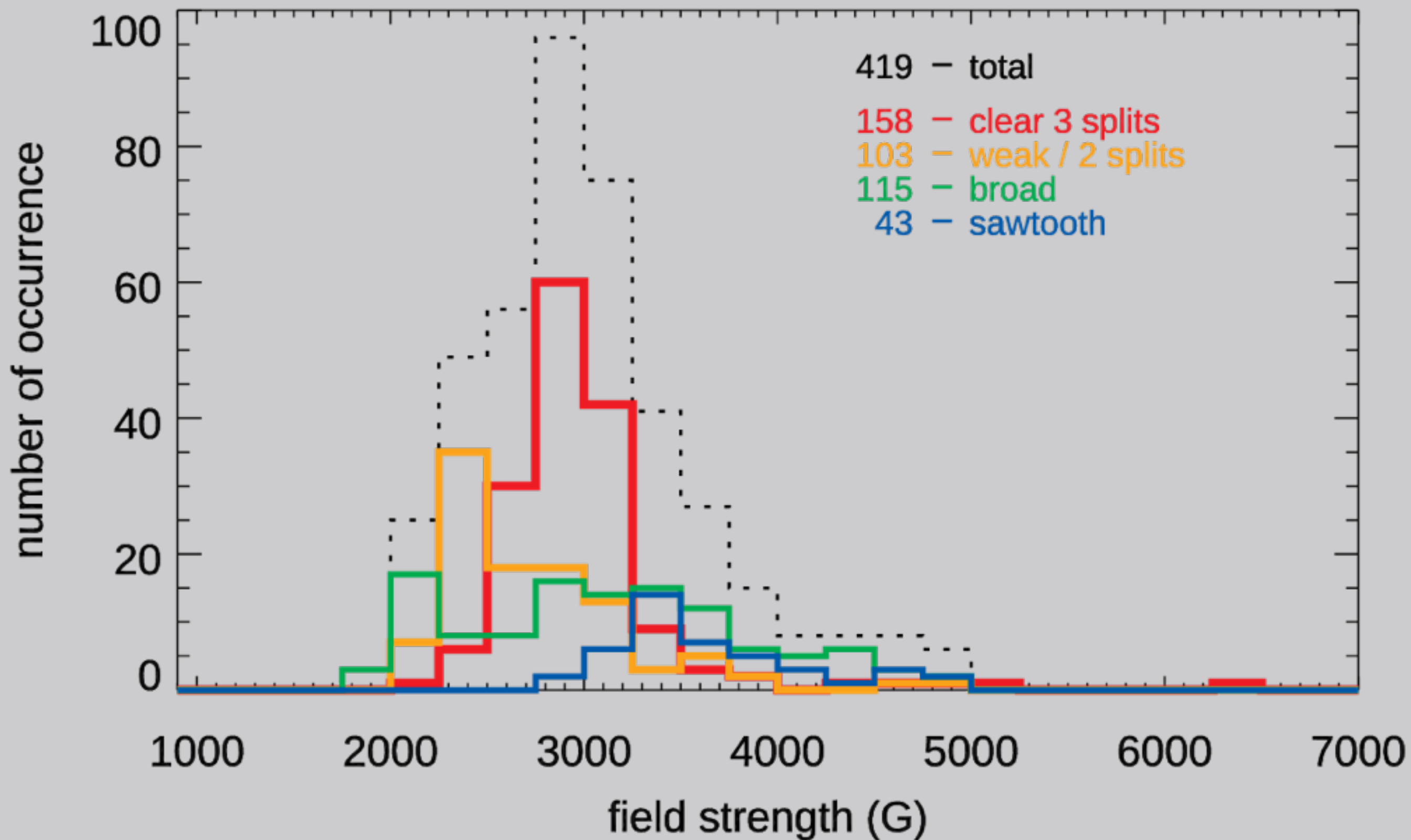
Umbral strong fields have clear 3 splits.

Weak fields in small ss. have weakly-splitting or broad profiles.

Penumbrae seem to have complex structures.

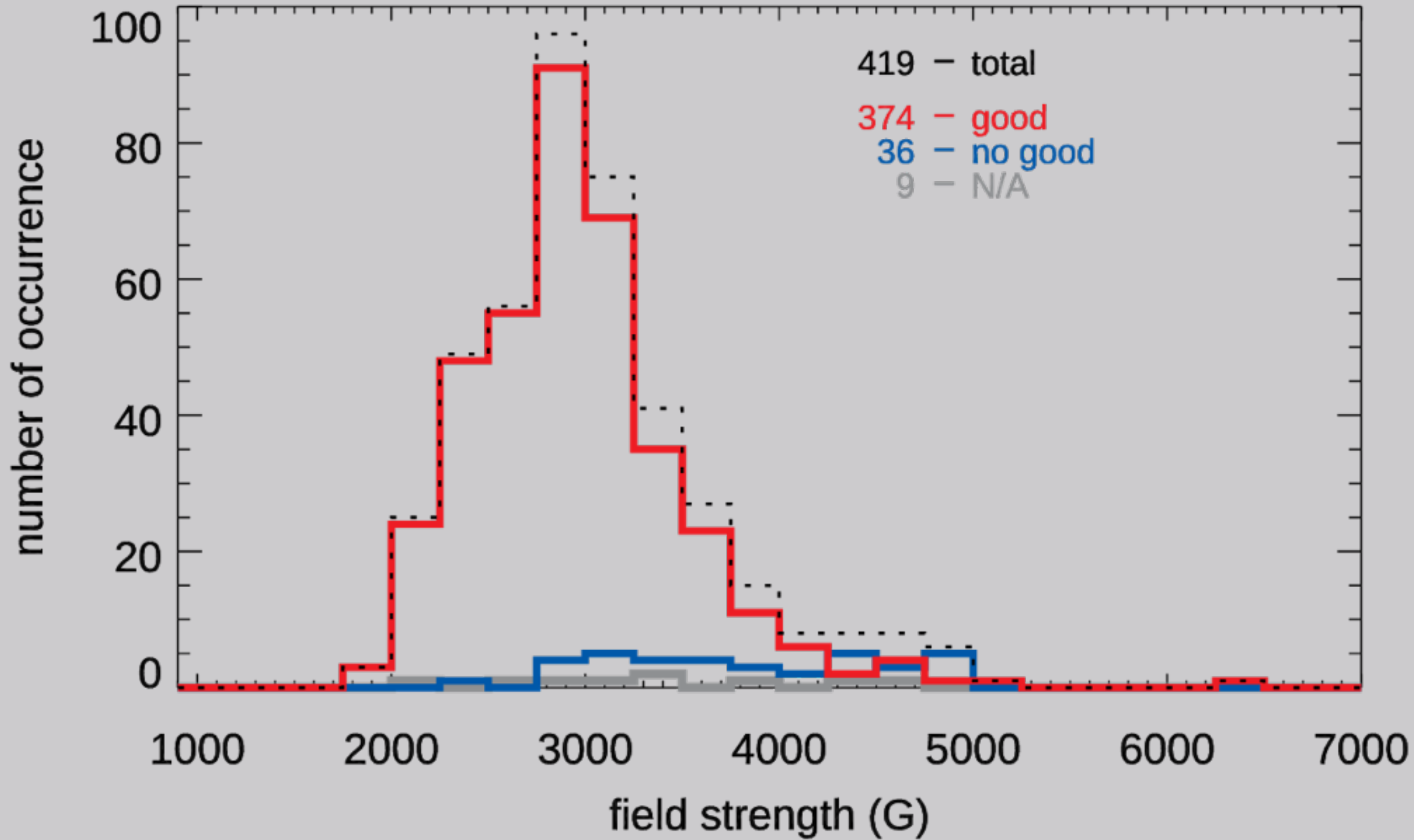
Some fitting results may fail.

Number Dist. of Field Strength on Spectral Shape



Fitting Result

Fitting Result



Rank 4th – 10th

Rank 4th

(334) AR 12297

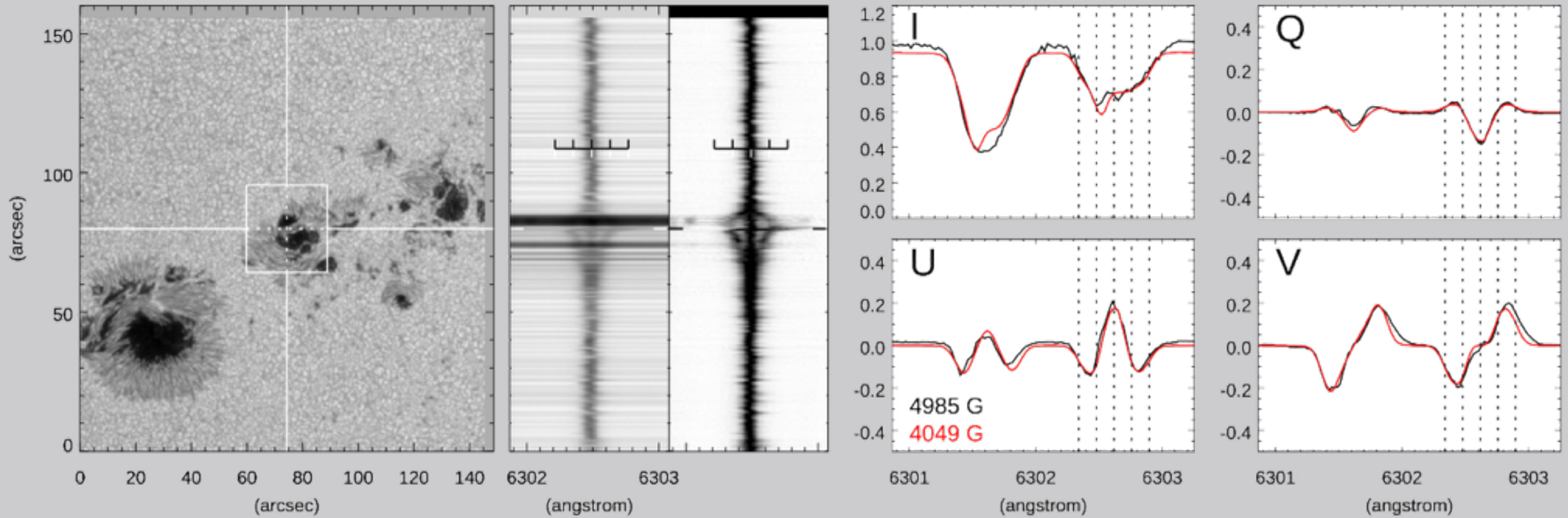
[20150312_210006]

Loc L Spec _/ PIL O Red O Flow O

Continuum

Stokes I (emphasized)

Full Stokes profiles at the location of the strongest field



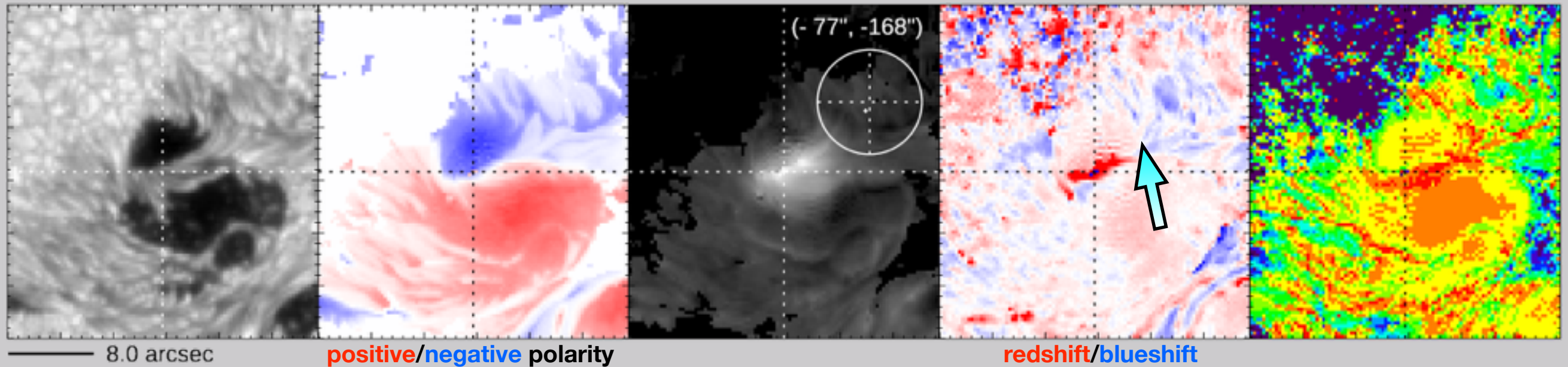
Continuum

B (LOS)

B (transverse)

Doppler velocity

Filling factor



Rank 5th

(261) AR 11944

[20140105_000405]

Loc
p

Spec
V

PIL
O

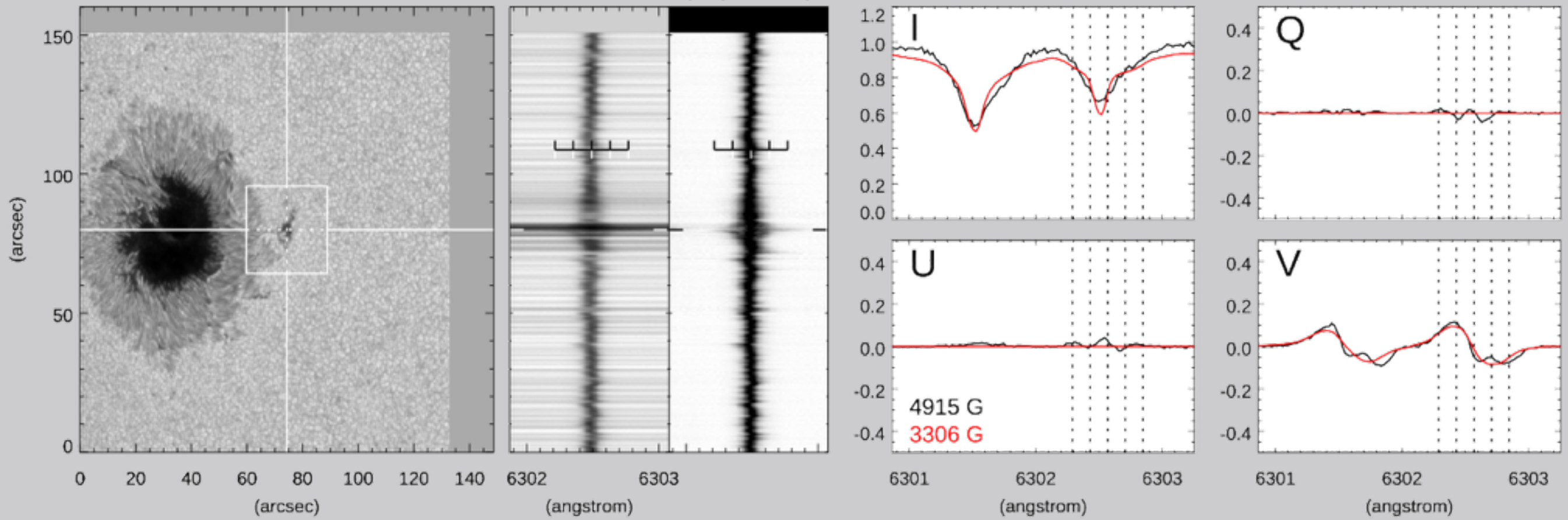
Red
O

Flow
O

Continuum

Stokes I (emphasized)

Full Stokes profiles at the location of the strongest field



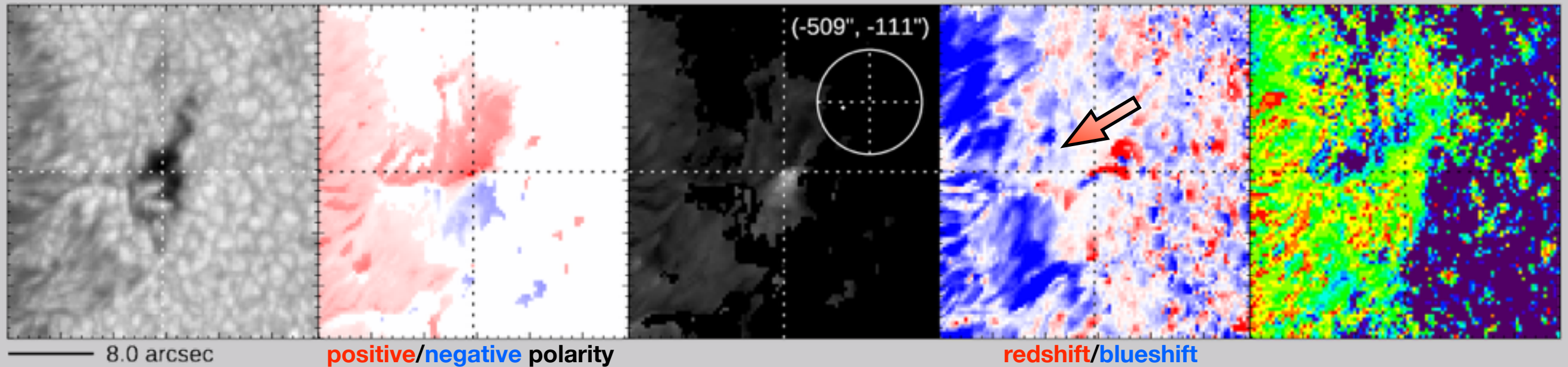
Continuum

B (LOS)

B (transverse)

Doppler velocity

Filling factor



Rank 6th

(265) AR 11974

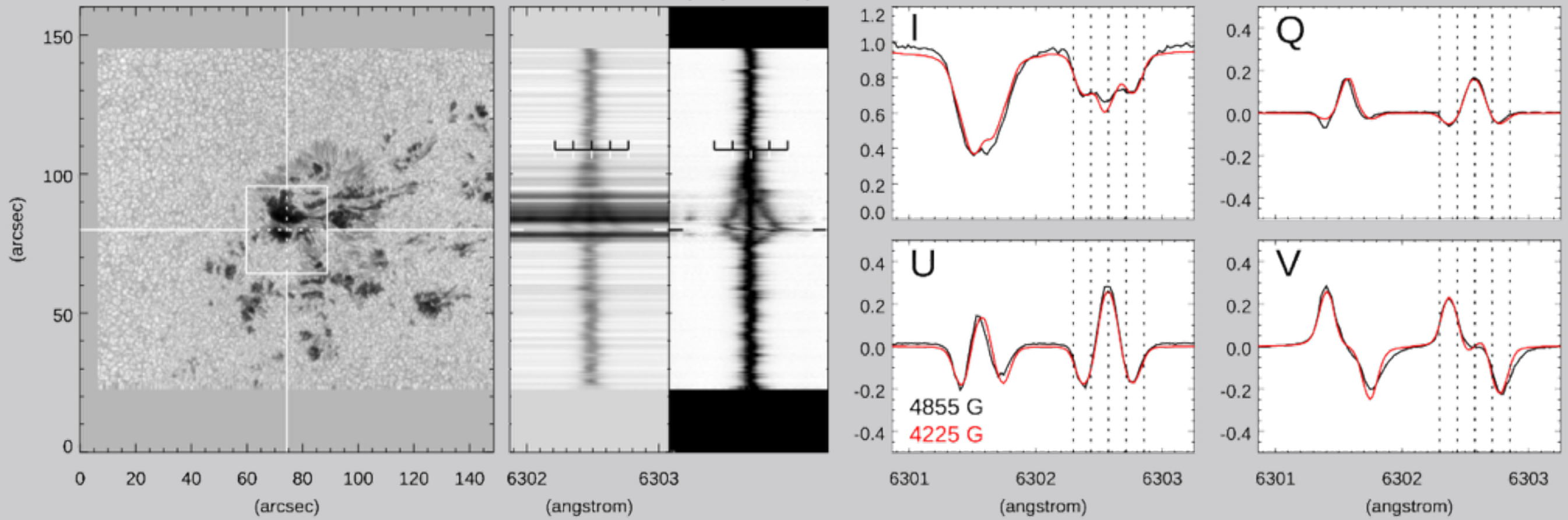
[20140214_063104]

Loc L Spec VVV PIL O Red O Flow O

Continuum

Stokes I (emphasized)

Full Stokes profiles at the location of the strongest field



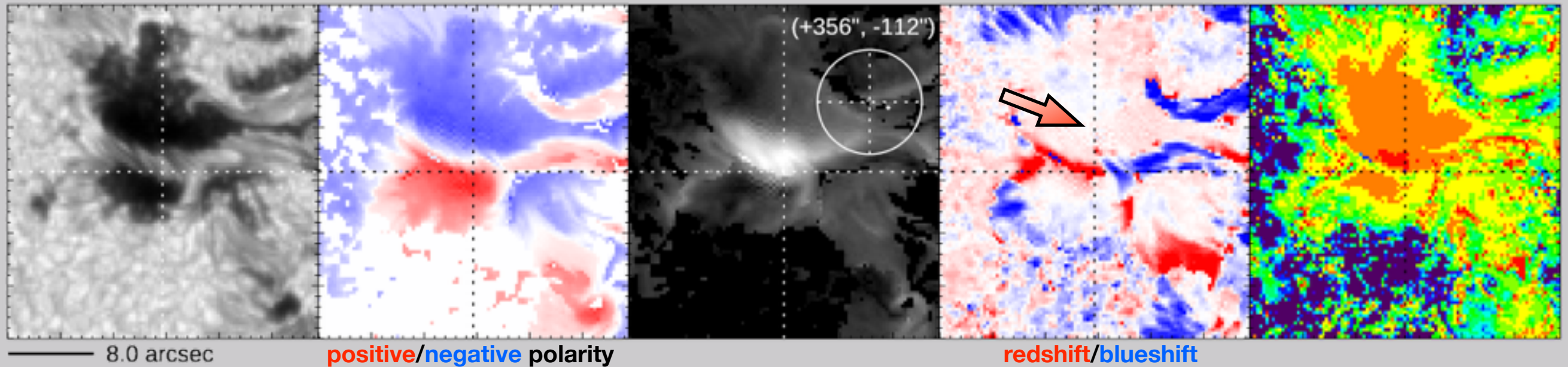
Continuum

B (LOS)

B (transverse)

Doppler velocity

Filling factor



Rank 7th

(4) AR 10930

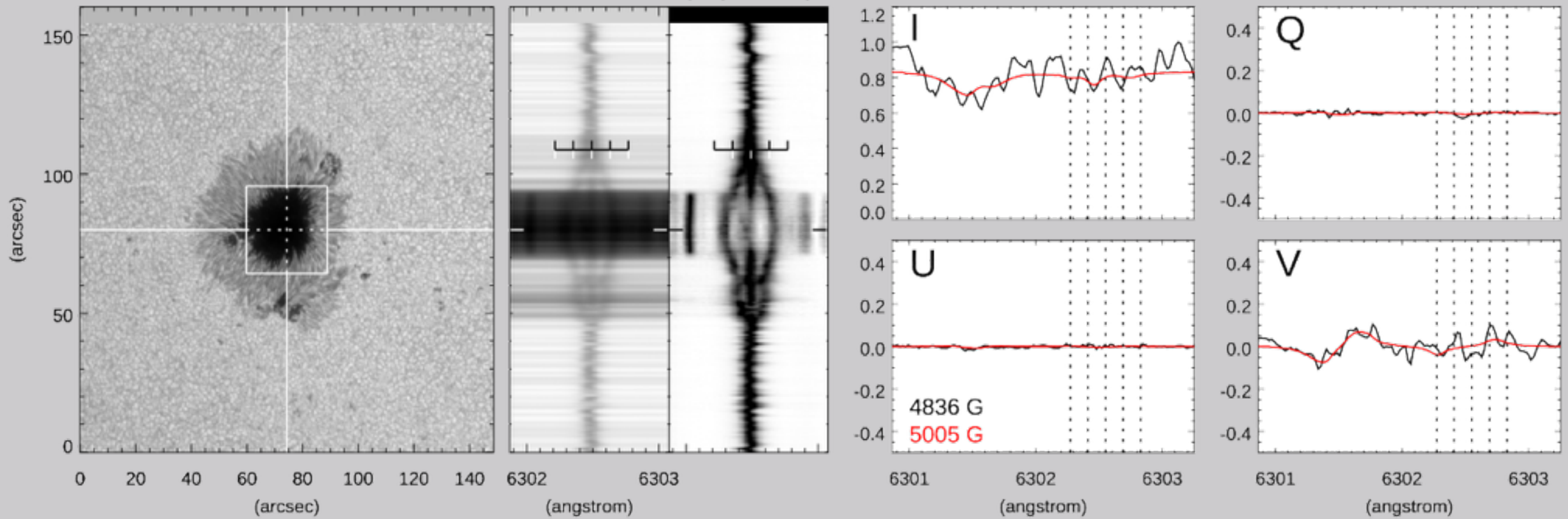
[20061209_140005]

Loc	Spec	PIL	Red	Flow
U	WW	-	-	-

Continuum

Stokes I (emphasized)

Full Stokes profiles at the location of the strongest field



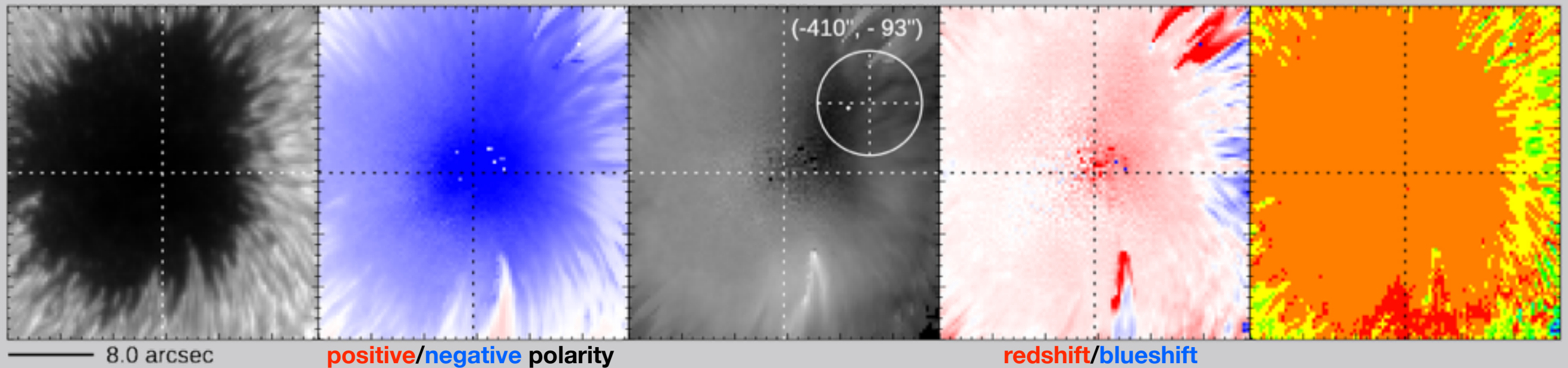
Continuum

B (LOS)

B (transverse)

Doppler velocity

Filling factor



Rank 8th

(157) AR 11515

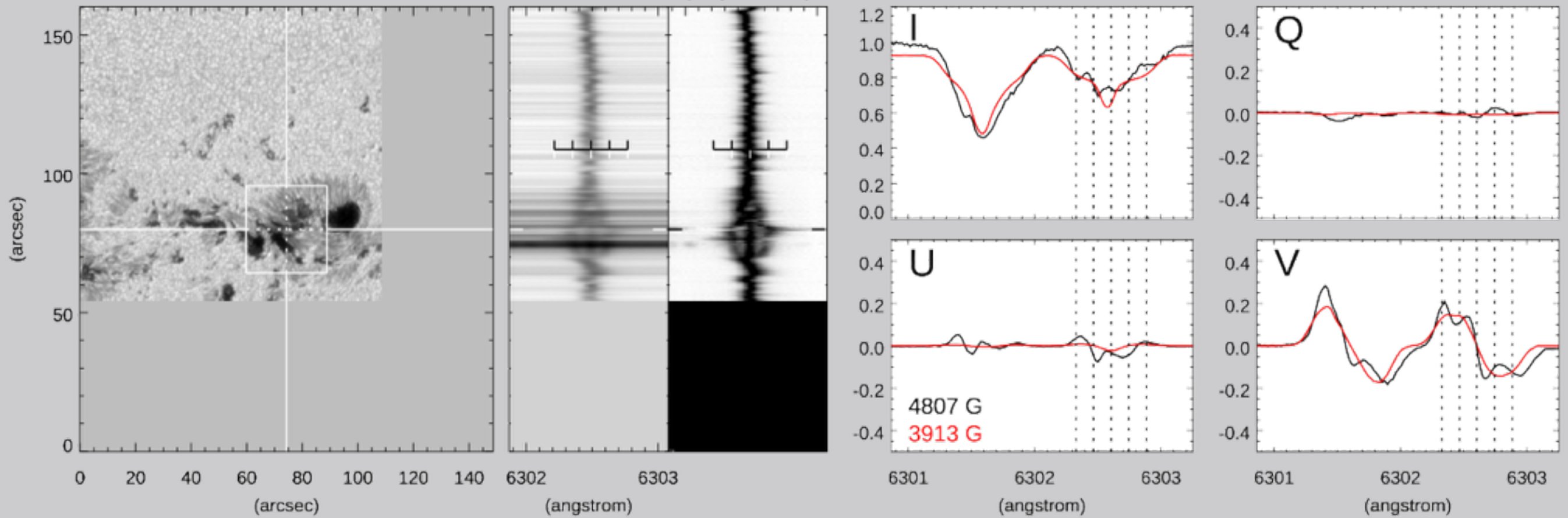
[20120705_065135]

Loc P Spec WW PIL O Red O Flow O

Continuum

Stokes I (emphasized)

Full Stokes profiles at the location of the strongest field



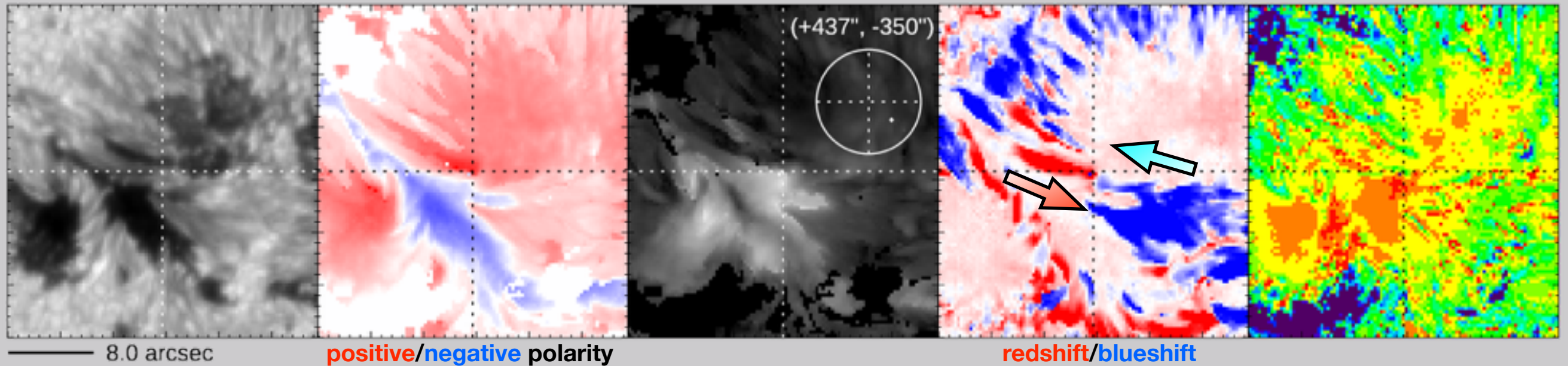
Continuum

B (LOS)

B (transverse)

Doppler velocity

Filling factor



Rank 10th

(251) AR 11899

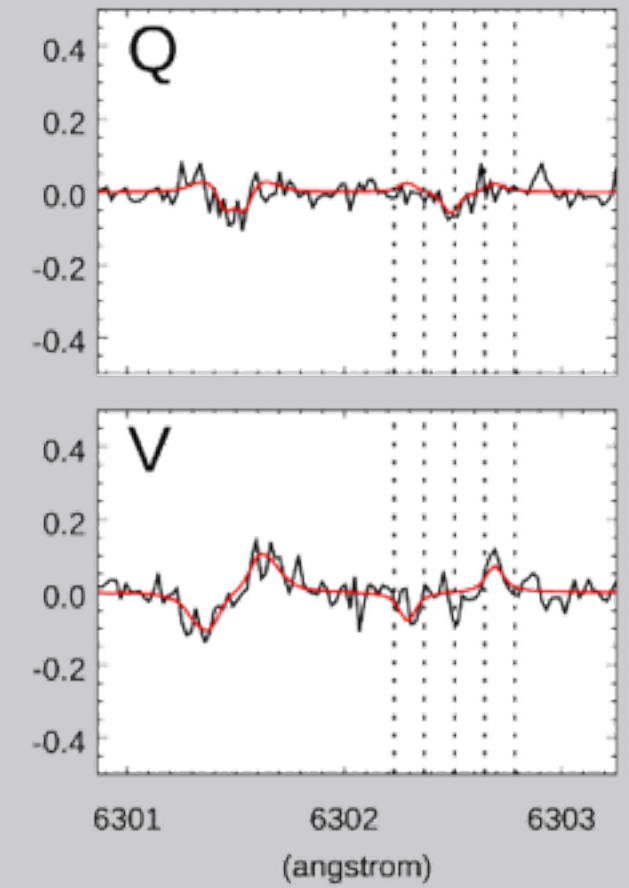
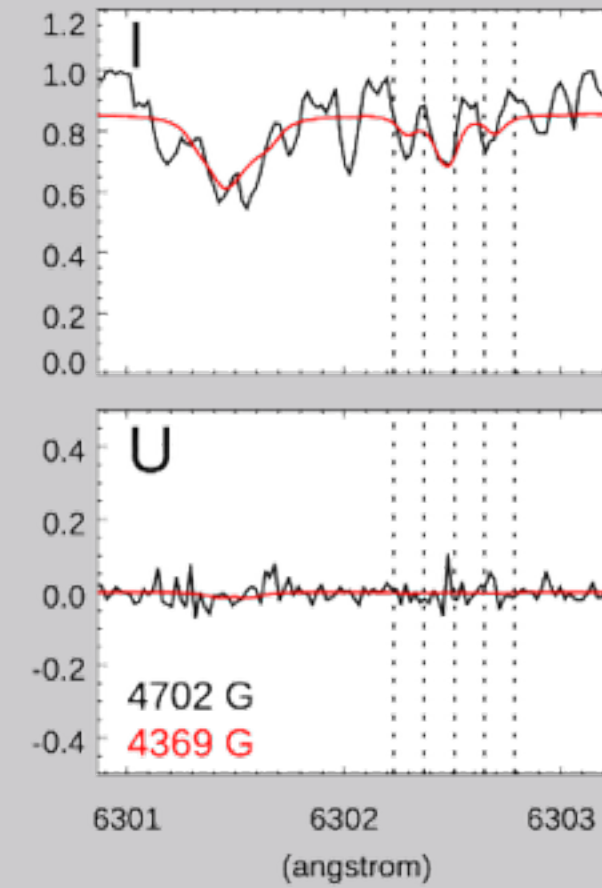
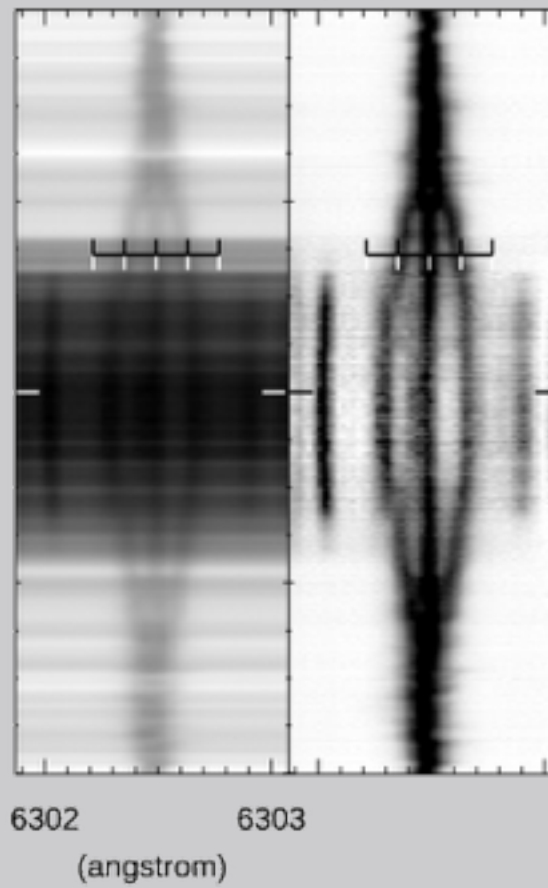
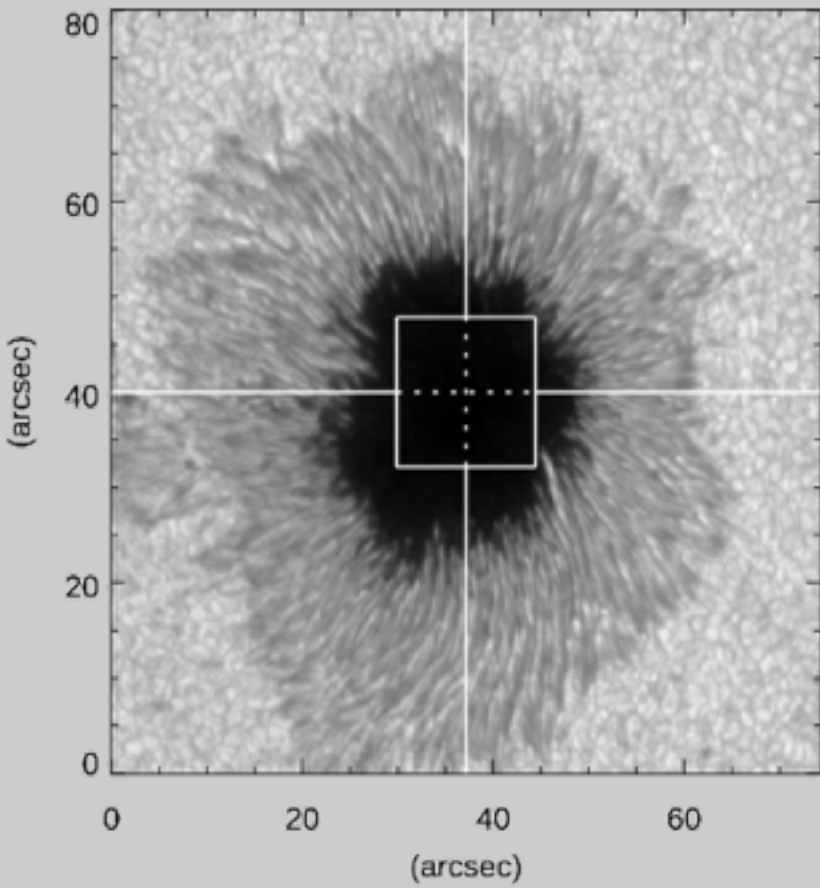
[20131121_101956]

Loc U
Spec WW
PIL -
Red -
Flow -

Continuum

Stokes I (emphasized)

Full Stokes profiles at the location of the strongest field



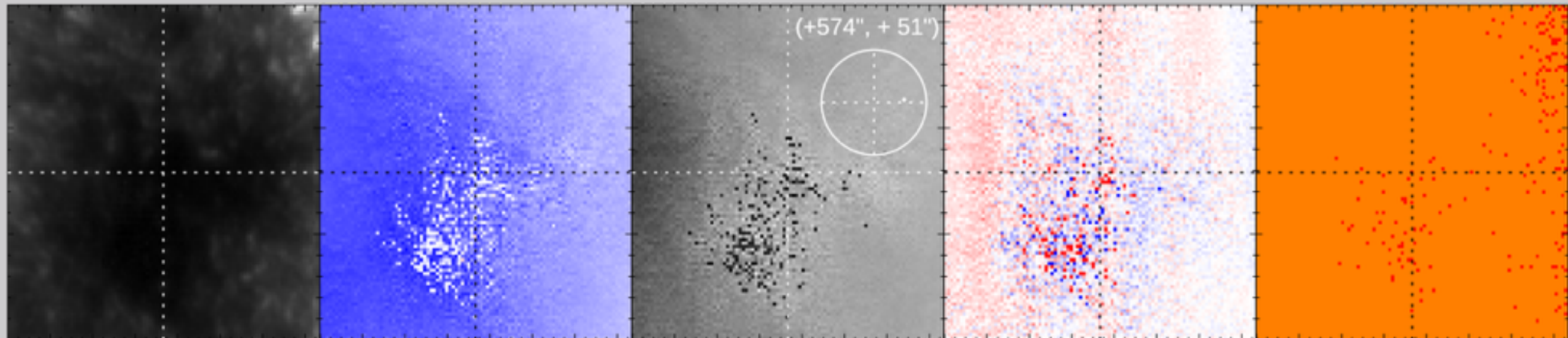
Continuum

B (LOS)

B (transverse)

Doppler velocity

Filling factor



4.0 arcsec

positive/negative polarity

redshift/blueshift

Pressing Pores

Pressing Pores

(28) AR 11005

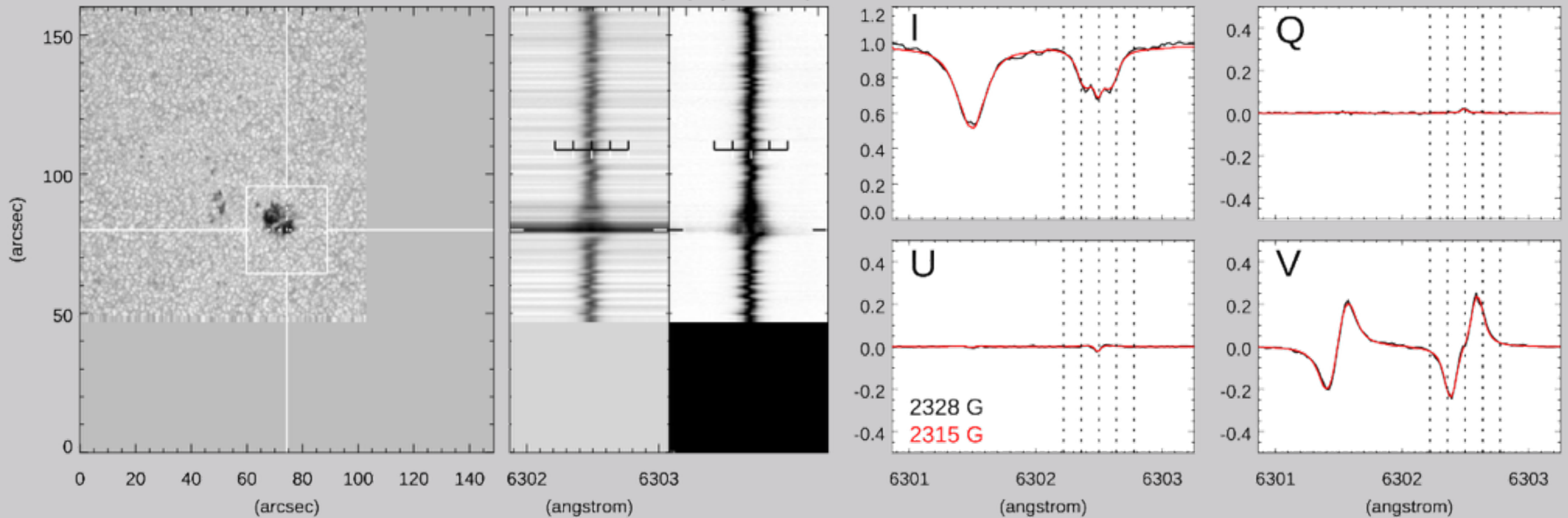
[20081014_124906]

Loc U Spec VVV PIL - Red - Flow O

Continuum

Stokes I (emphasized)

Full Stokes profiles at the location of the strongest field



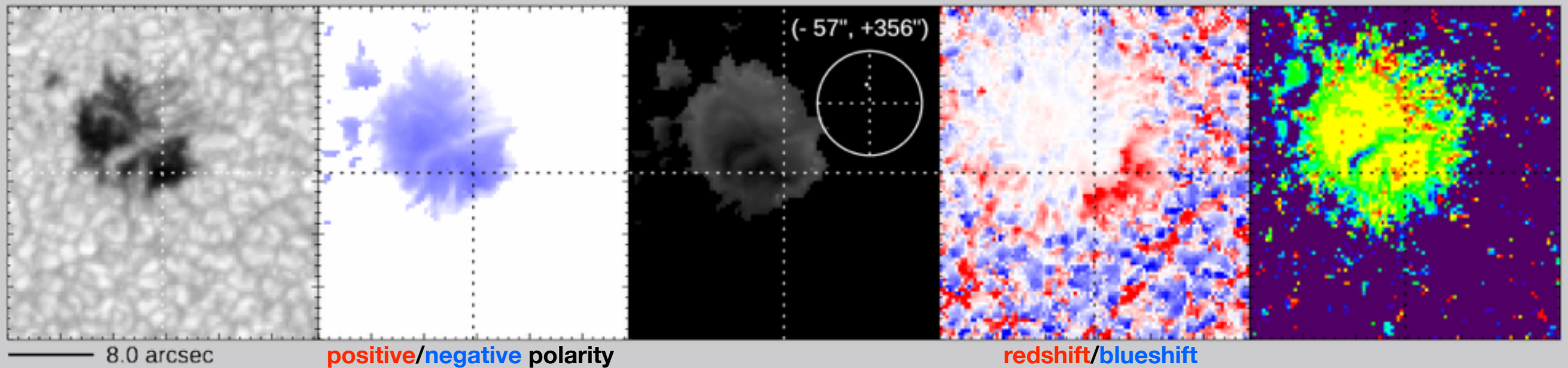
Continuum

B (LOS)

B (transverse)

Doppler velocity

Filling factor



8.0 arcsec

positive/negative polarity

redshift/blueshift

Pressing Pores from Both Sides

(345) AR 12371

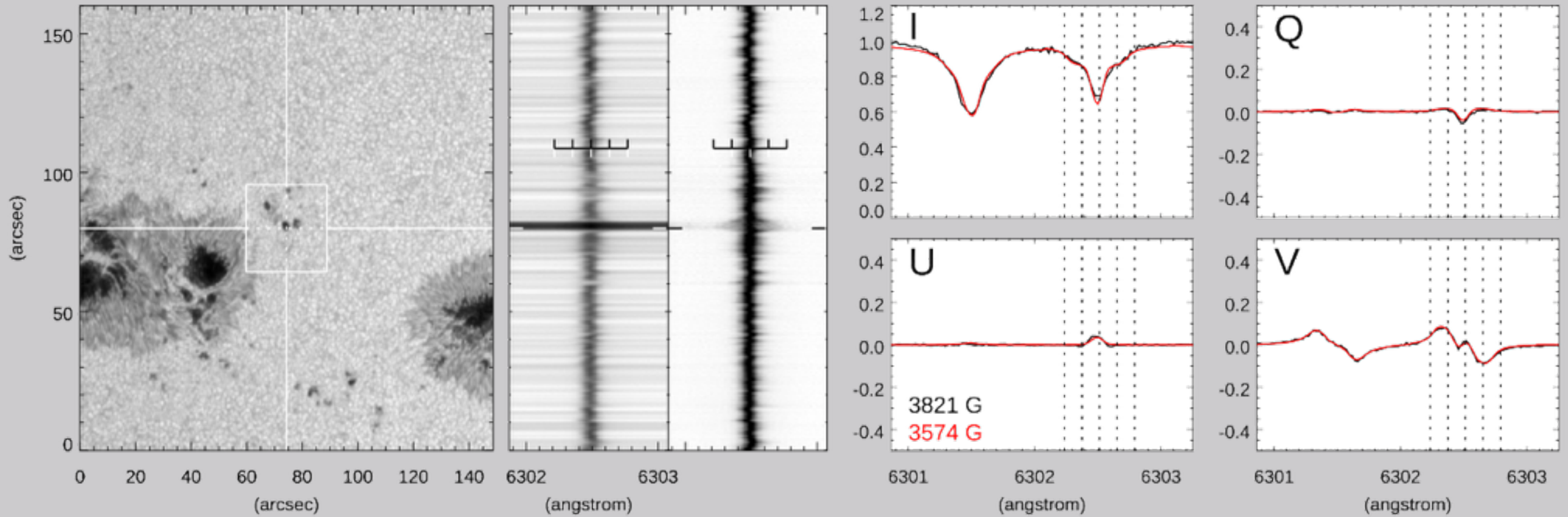
[20150620_194105]

Loc U Spec _/ PIL - Red O Flow O

Continuum

Stokes I (emphasized)

Full Stokes profiles at the location of the strongest field



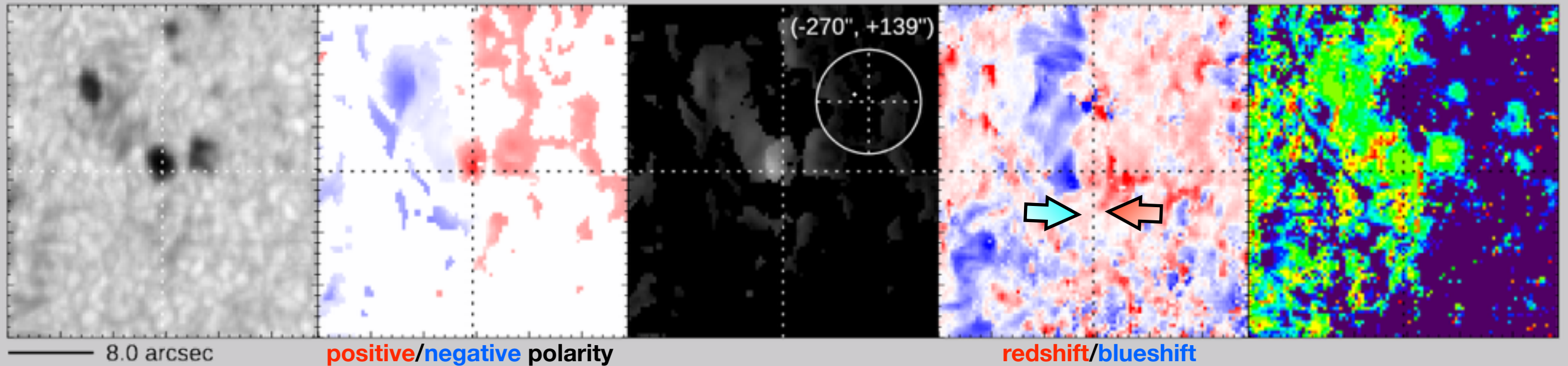
Continuum

B (LOS)

B (transverse)

Doppler velocity

Filling factor



Other Examples

Blueshift at Strongest Field Location (1/2)

(32) AR 11024

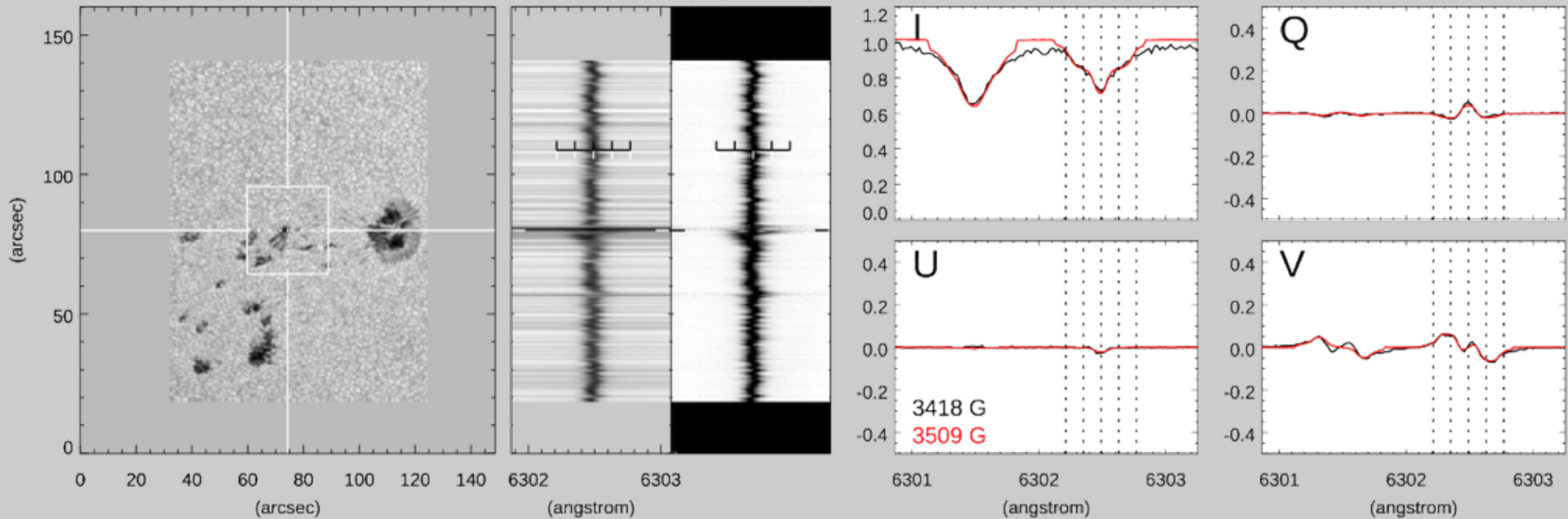
[20090704_115808]

Loc p Spec _/ PIL O Red blue Flow O

Continuum

Stokes I (emphasized)

Full Stokes profiles at the location of the strongest field



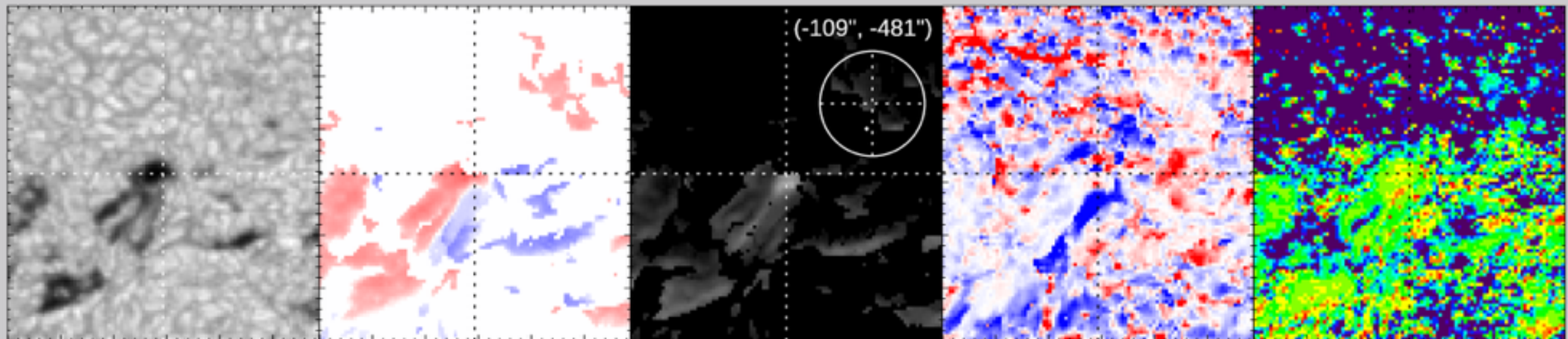
Continuum

B (LOS)

B (transverse)

Doppler velocity

Filling factor



8.0 arcsec

positive/negative polarity

redshift/blueshift

Blueshift at Strongest Field Location (2/2)

(316) AR 12205

[20141107_222544]

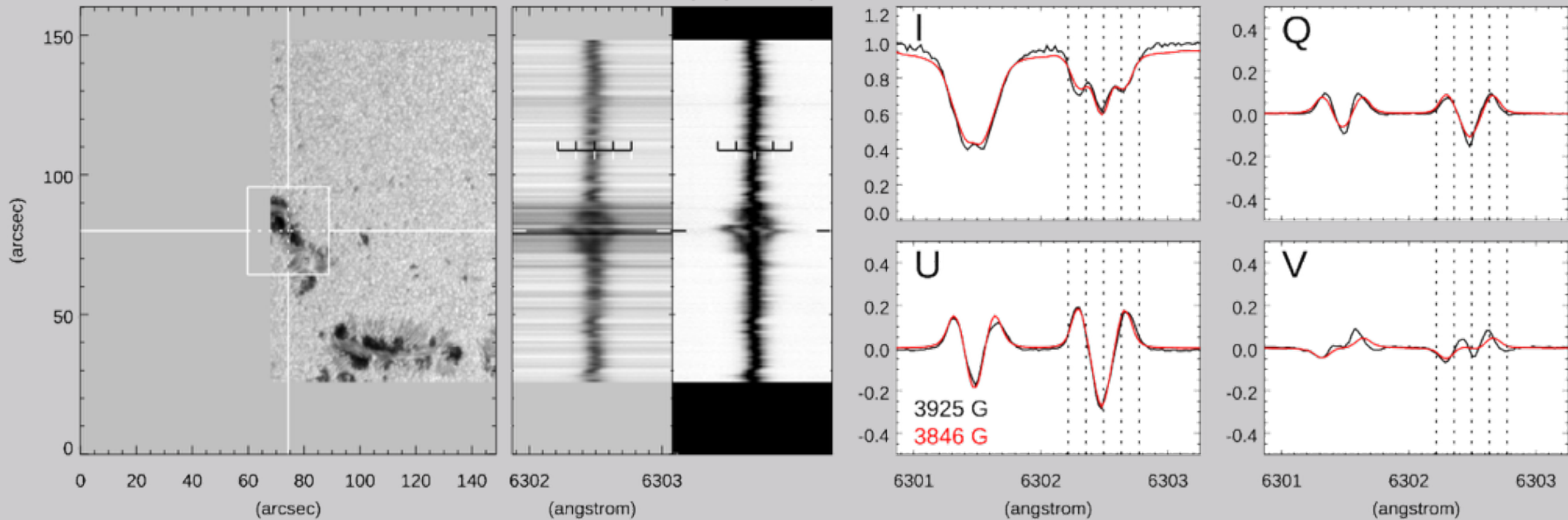
Loc
L

flux emergence ?

Continuum

Stokes I (emphasized)

Full Stokes profiles at the location of the strongest field



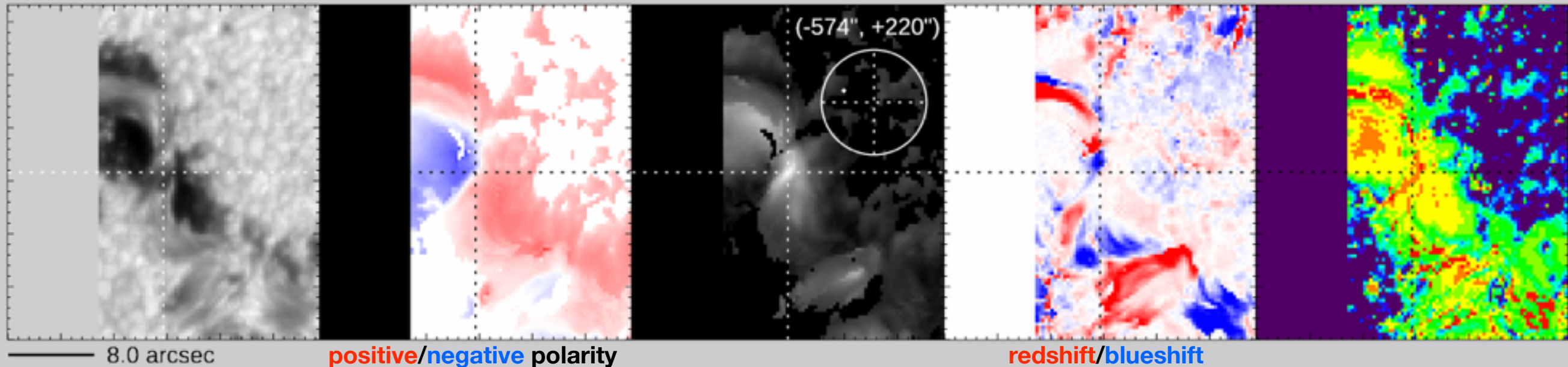
Continuum

B (LOS)

B (transverse)

Doppler velocity

Filling factor



Opposite-polarity Light Bridge in an Umbra (1/2)

(171) AR 11564

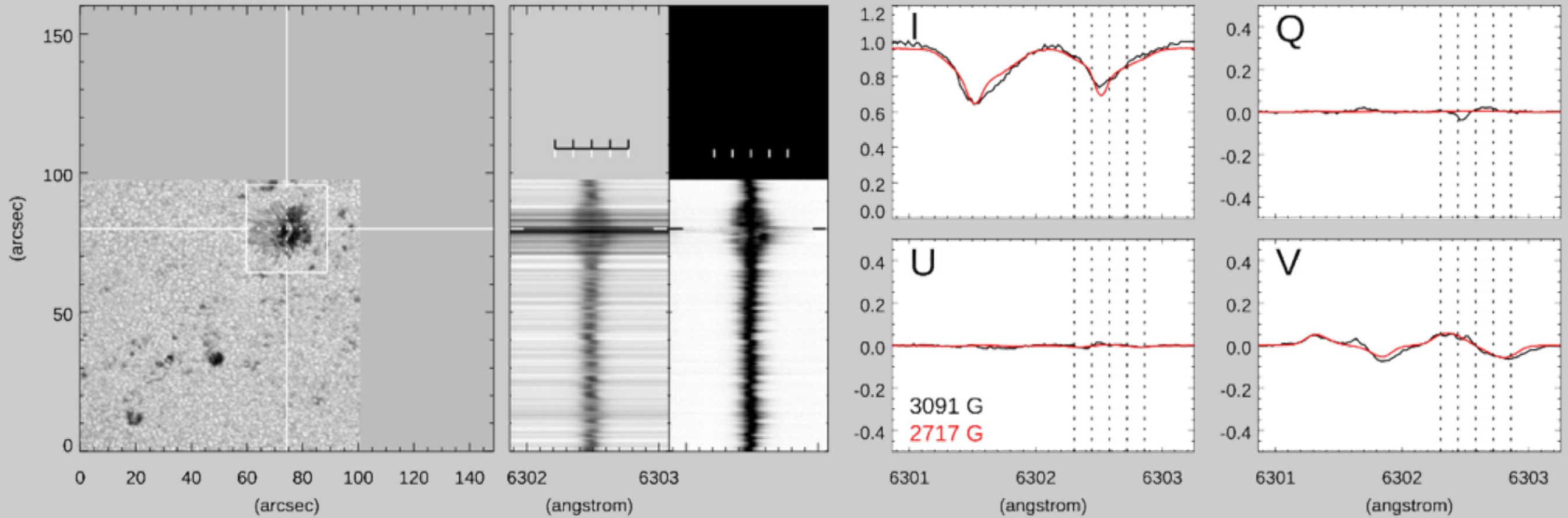
[20120905_073005]

Loc U Spec _/ PIL O Red O Flow O

Continuum

Stokes I (emphasized)

Full Stokes profiles at the location of the strongest field



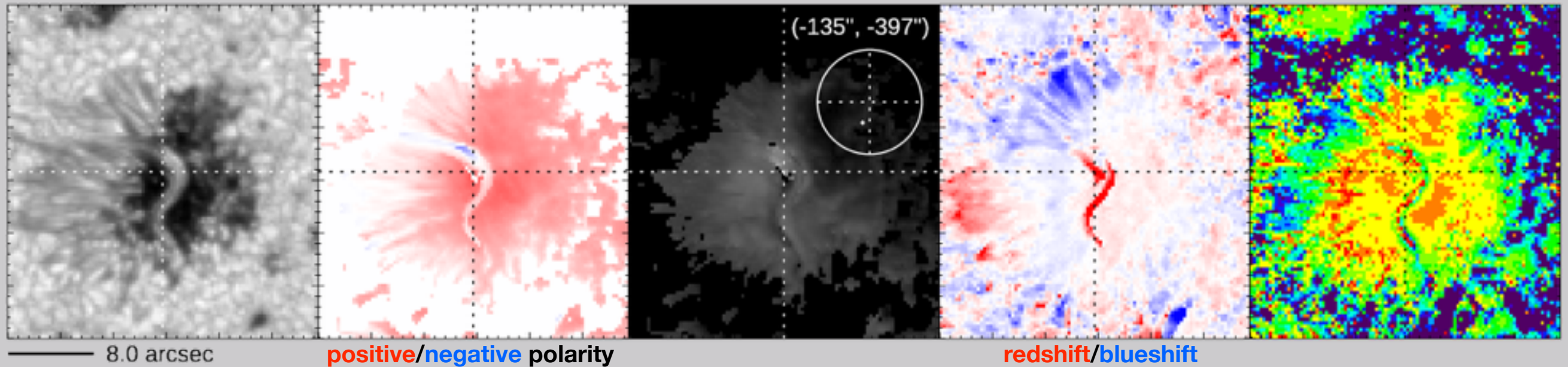
Continuum

B (LOS)

B (transverse)

Doppler velocity

Filling factor



8.0 arcsec

positive/negative polarity

redshift/blueshift

Opposite-polarity Light Bridge in an Umbra (2/2)

(367) AR 12443

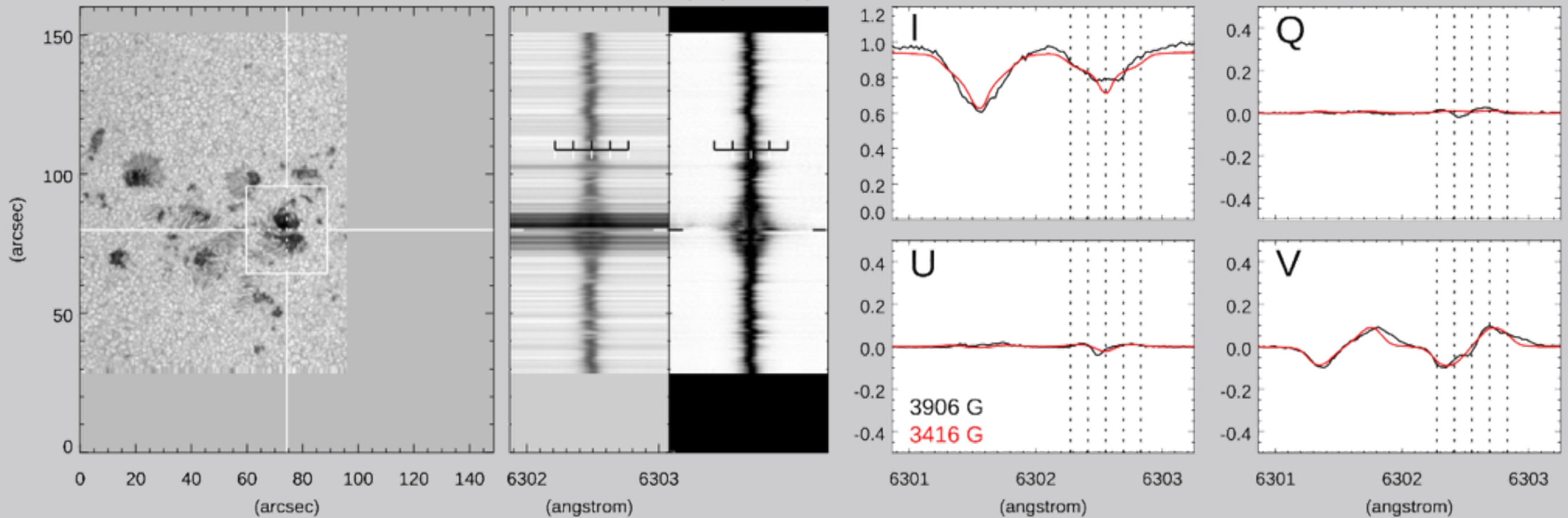
[20151103_225005]

Loc L Spec _/ PIL O Red O Flow O

Continuum

Stokes I (emphasized)

Full Stokes profiles at the location of the strongest field



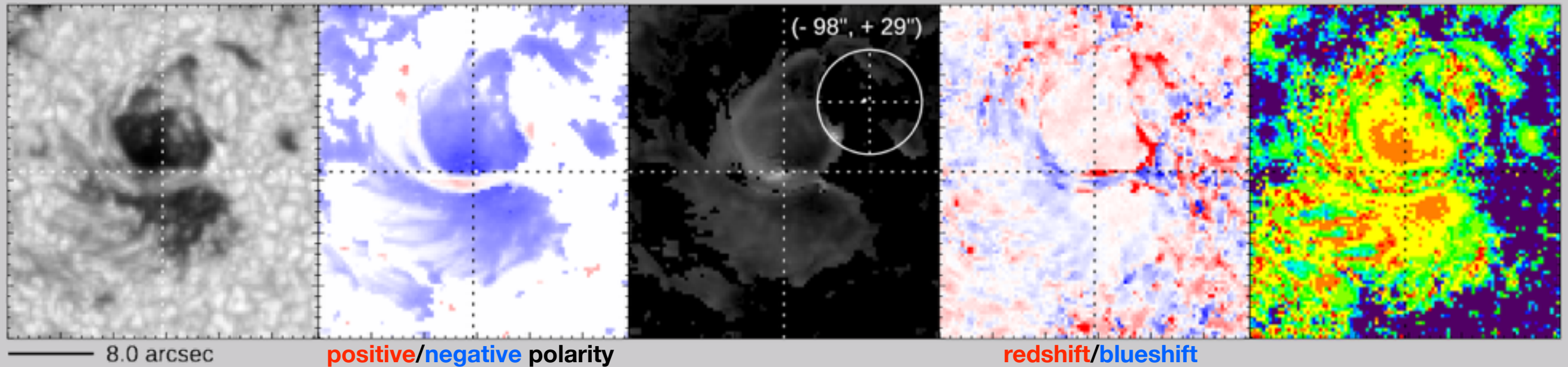
Continuum

B (LOS)

B (transverse)

Doppler velocity

Filling factor



8.0 arcsec

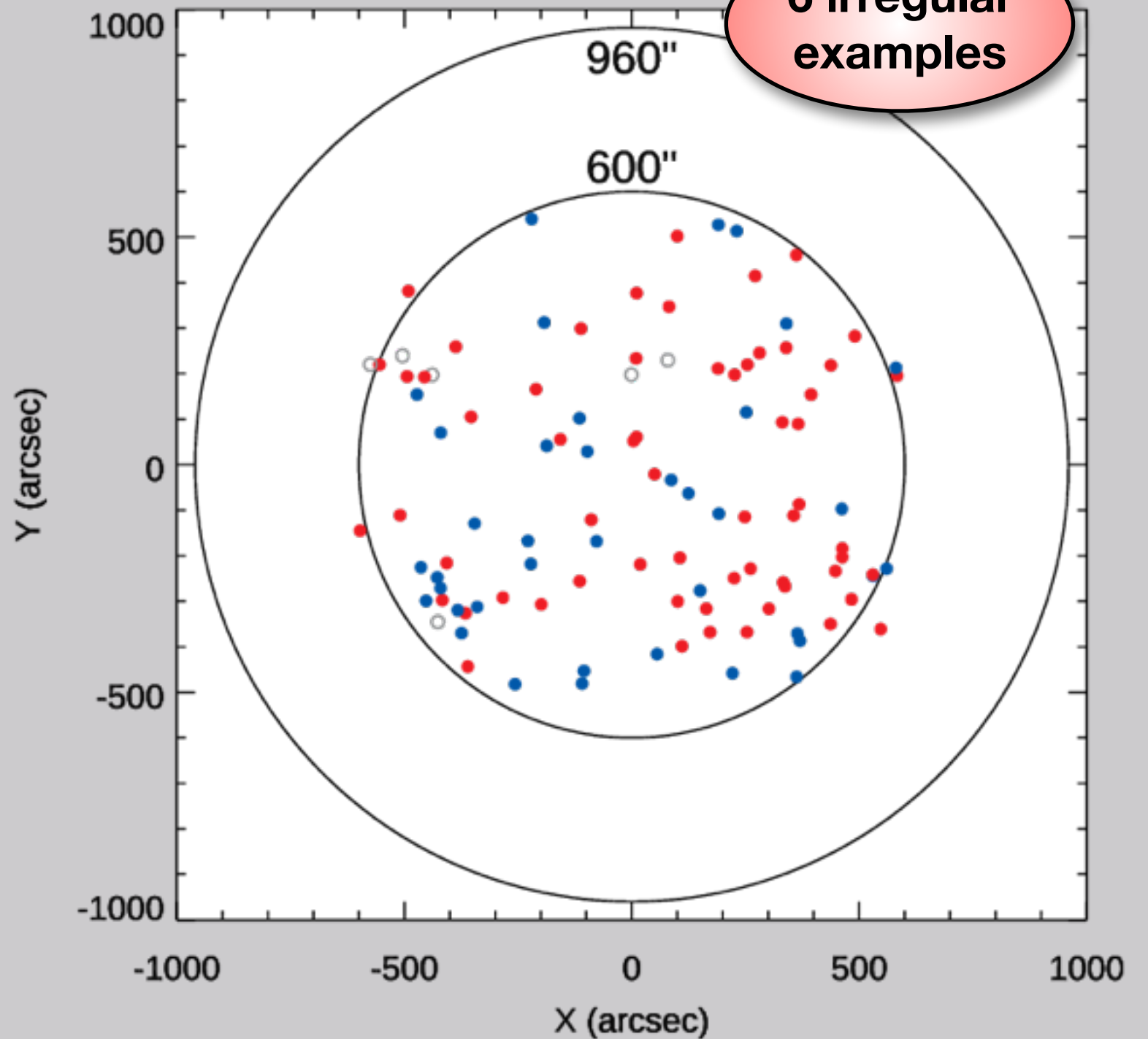
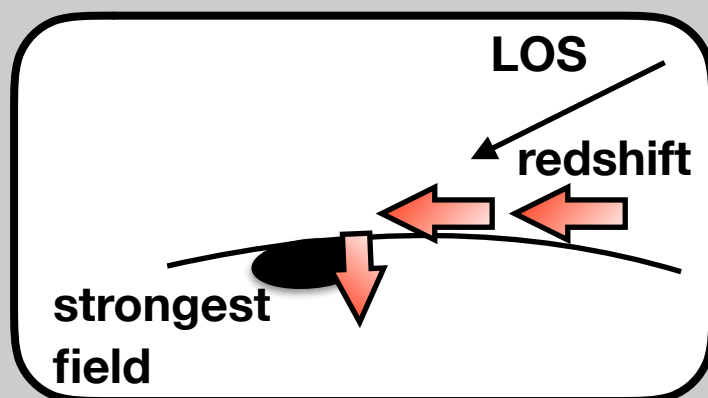
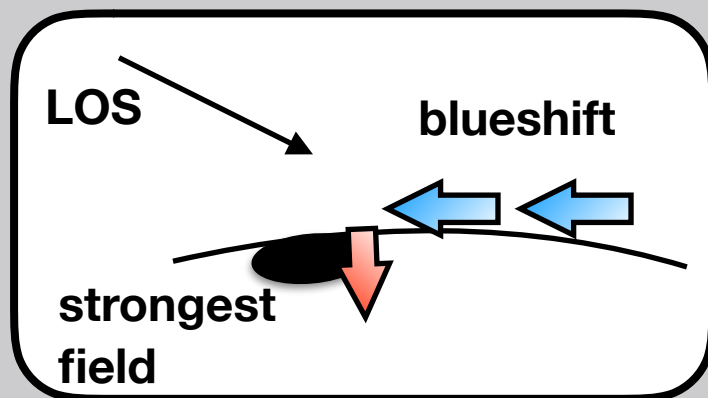
positive/negative polarity

redshift/blueshift

Distribution of Strongest Fields

non-umbra (105)

red/blue coloring —
redshift/blueshift consistent
with horizontal flows toward
the strong field region



In 94% of ARs with the strongest field in non-umbrae, the Doppler velocity can be interpreted as horizontal flows toward the strong field region.

Out of Theory (1/6)

(95) AR 11260

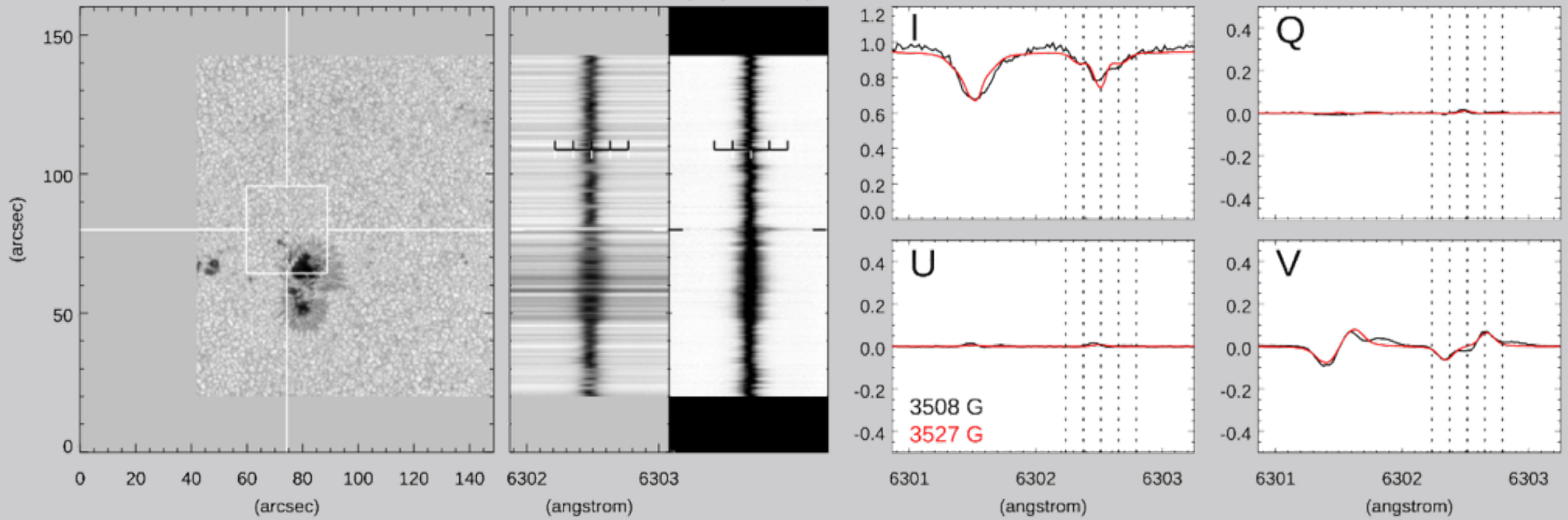
[20110730_140506]

Loc p Spec _/ PIL O Red O Flow -

Continuum

Stokes I (emphasized)

Full Stokes profiles at the location of the strongest field



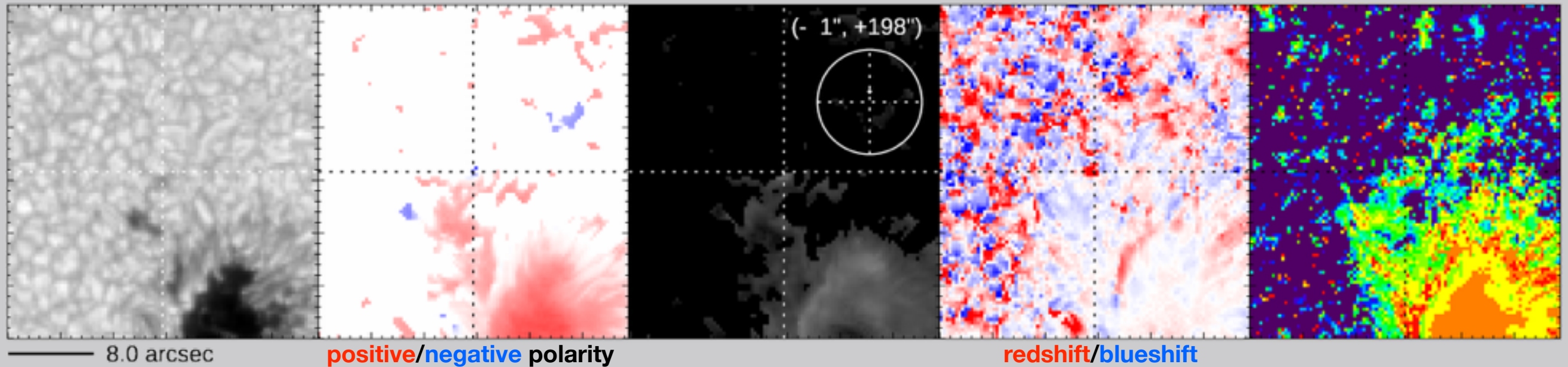
Continuum

B (LOS)

B (transverse)

Doppler velocity

Filling factor



8.0 arcsec

positive/negative polarity

redshift/blueshift

Out of Theory (2/6)

(105) AR 11301

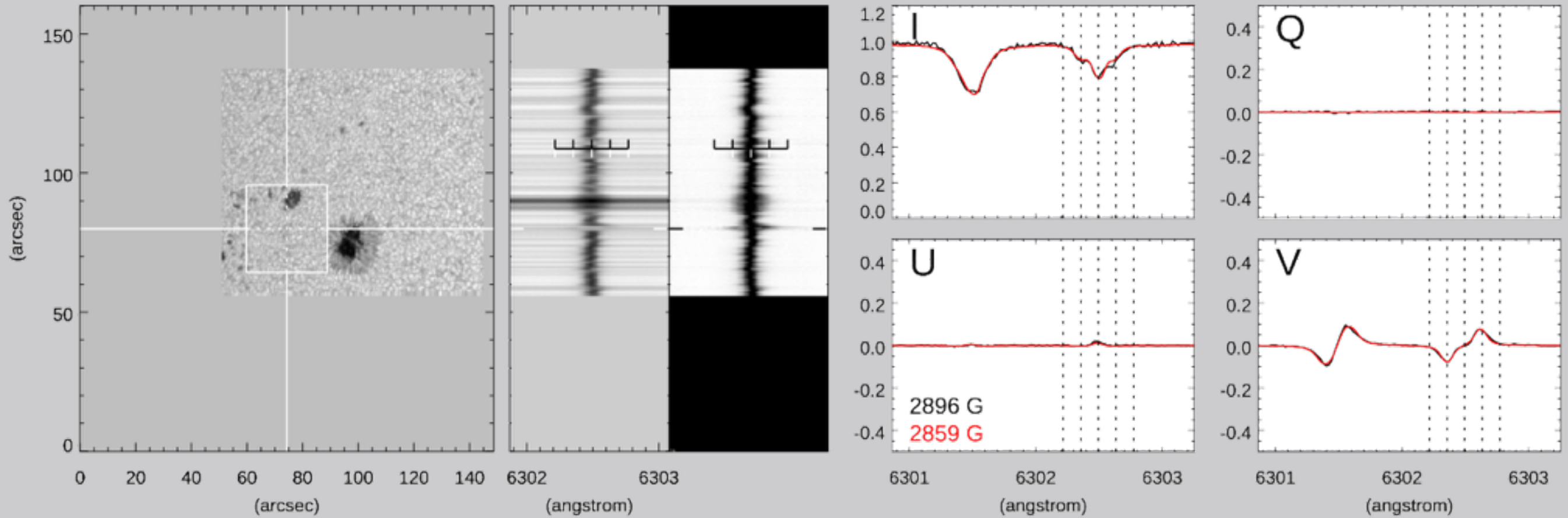
[20110923_072505]

Loc p
Spec V
PIL -
Red -
Flow -

Continuum

Stokes I (emphasized)

Full Stokes profiles at the location of the strongest field



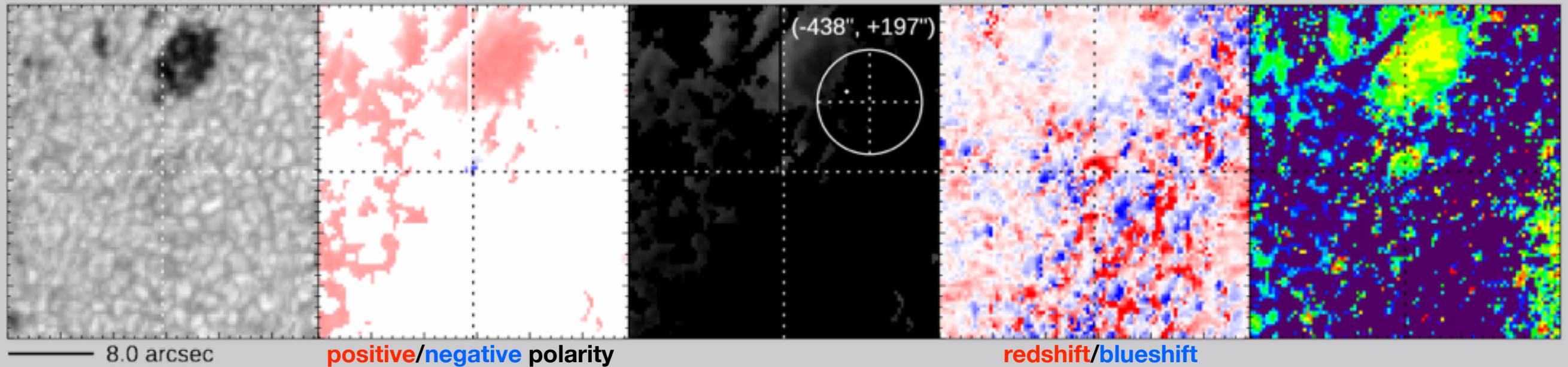
Continuum

B (LOS)

B (transverse)

Doppler velocity

Filling factor



Out of Theory (3/6)

(165) AR 11542

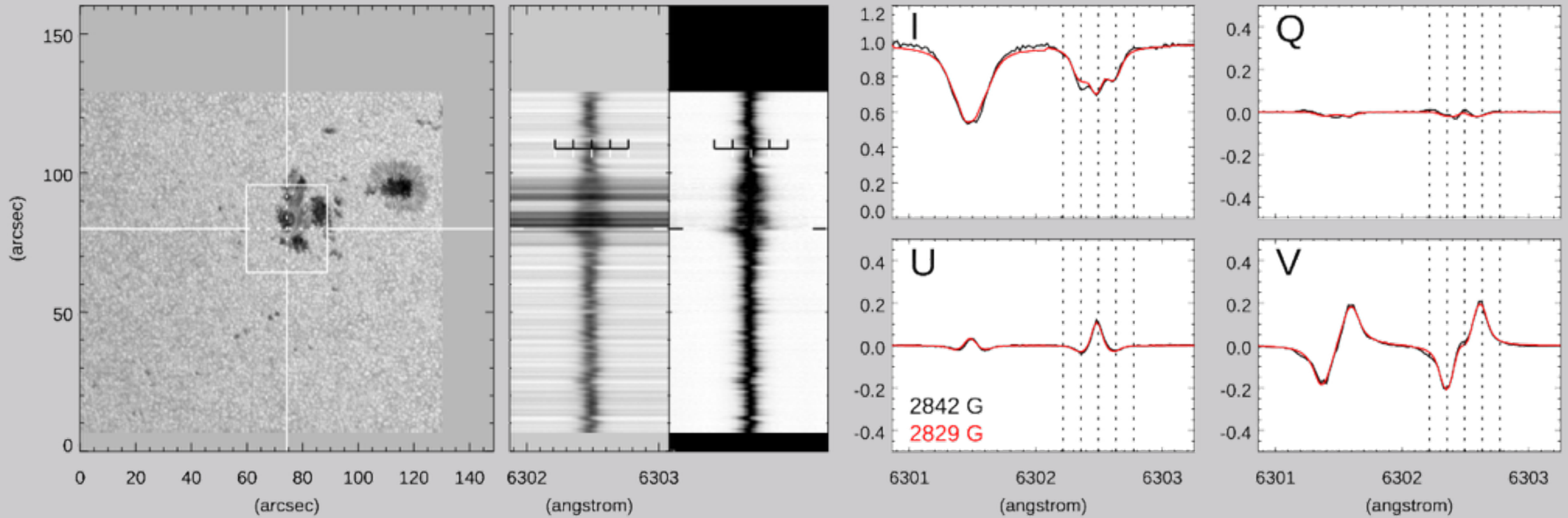
[20120810_193405]

Loc P Spec VVV PIL O Red - Flow -

Continuum

Stokes I (emphasized)

Full Stokes profiles at the location of the strongest field



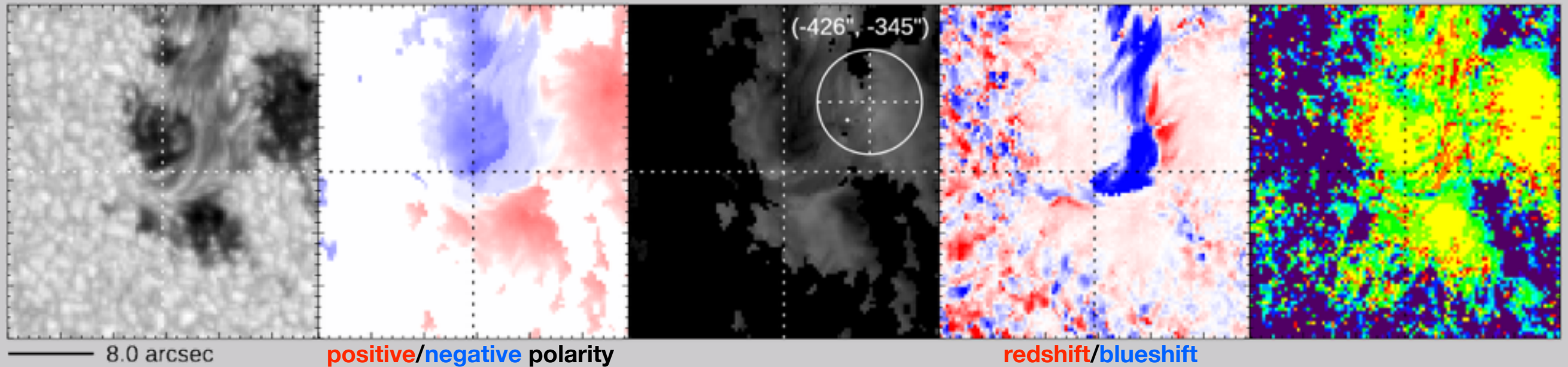
Continuum

B (LOS)

B (transverse)

Doppler velocity

Filling factor



8.0 arcsec

positive/negative polarity

redshift/blueshift

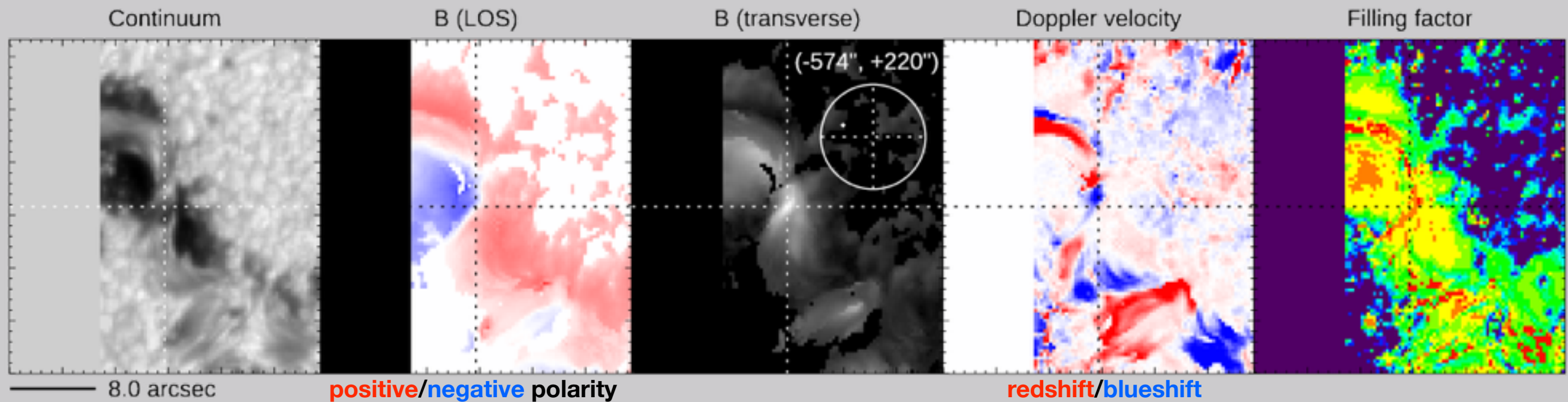
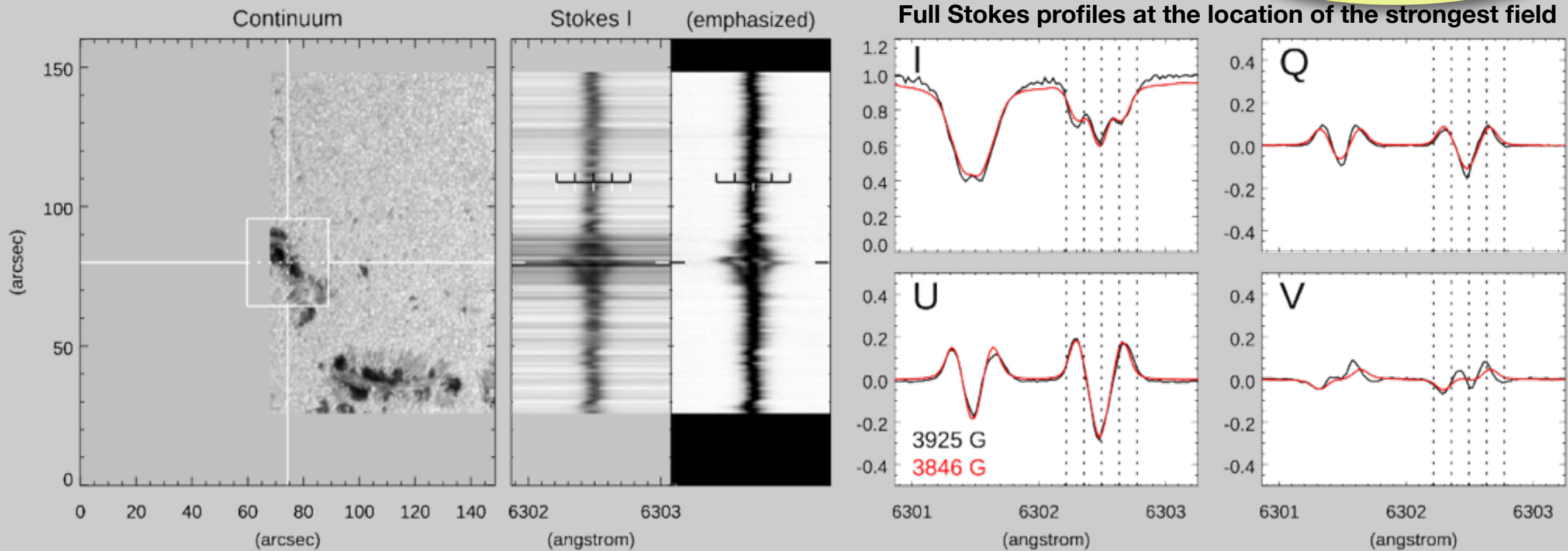
Out of Theory (4/6)

(316) AR 12205

[20141107_222544]

Loc
L

flux emergence ?



Out of Theory (5/6)

(330) AR 12277

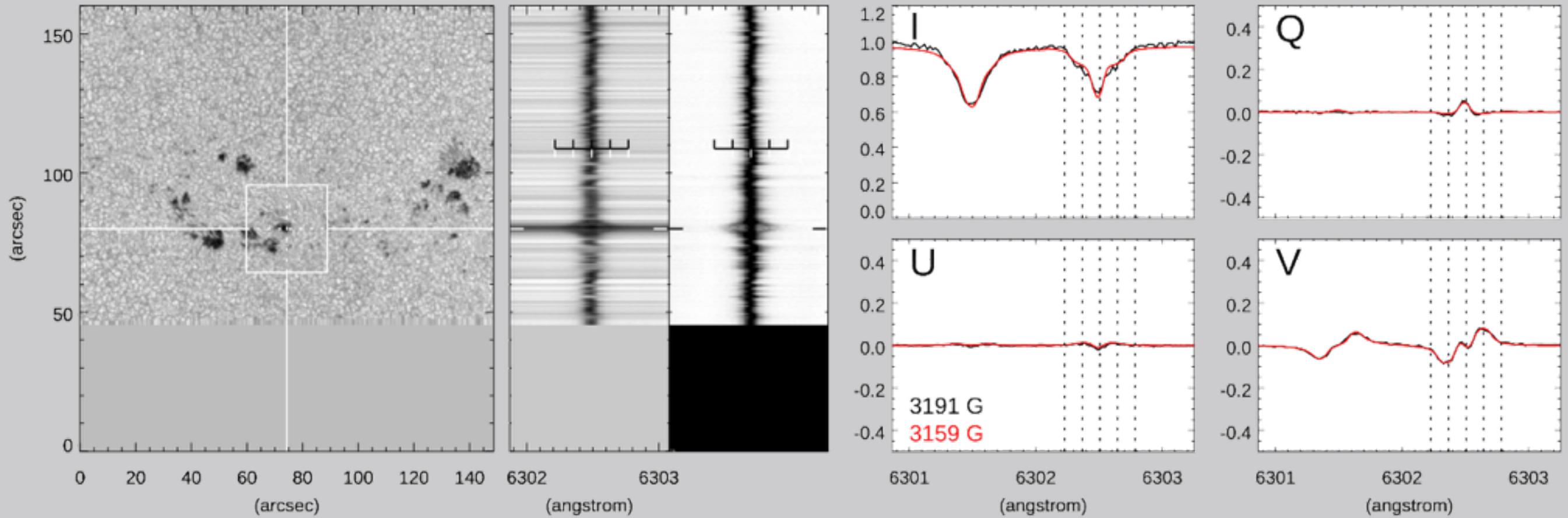
[20150203_132947]

Loc p
Spec V
PIL O
Red -
Flow -

Continuum

Stokes I (emphasized)

Full Stokes profiles at the location of the strongest field



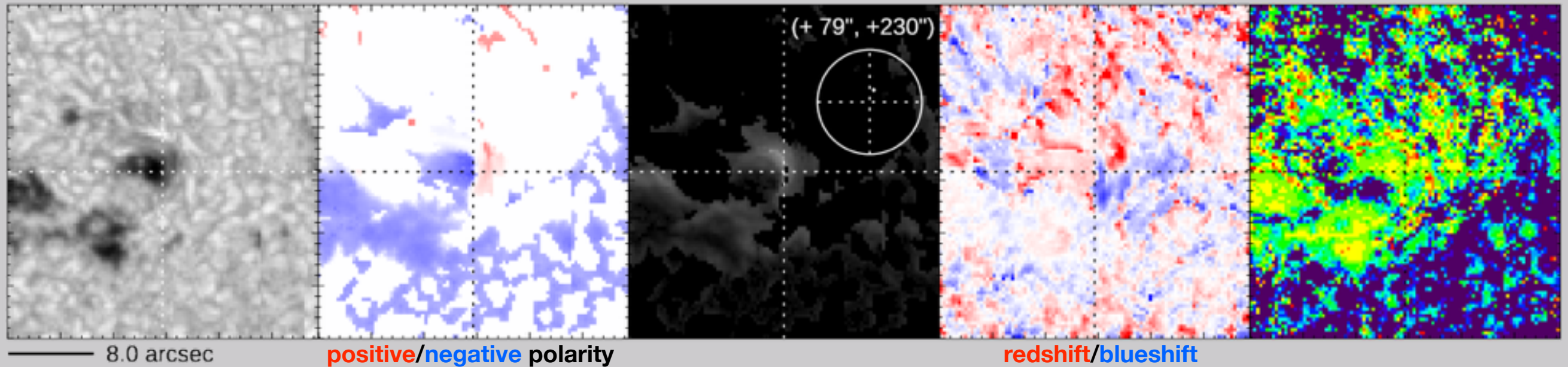
Continuum

B (LOS)

B (transverse)

Doppler velocity

Filling factor



Out of Theory (6/6)

(341) AR 12339

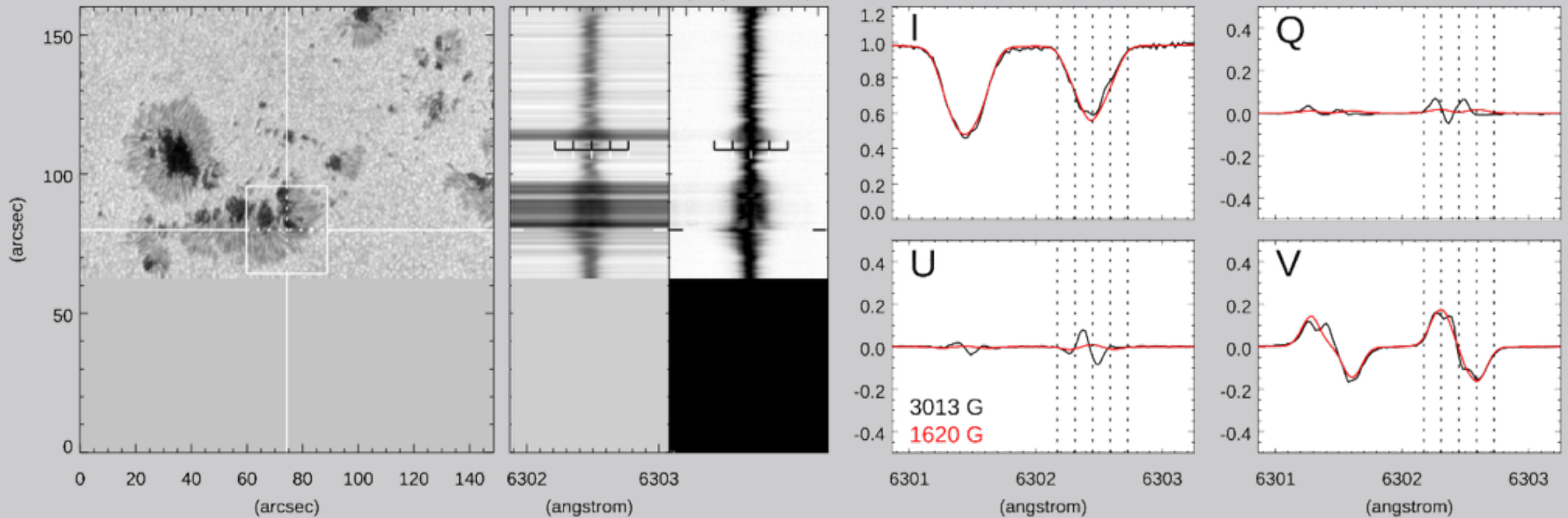
[20150509_123006]

Loc P Spec _/ PIL - Red - Flow -

Continuum

Stokes I (emphasized)

Full Stokes profiles at the location of the strongest field



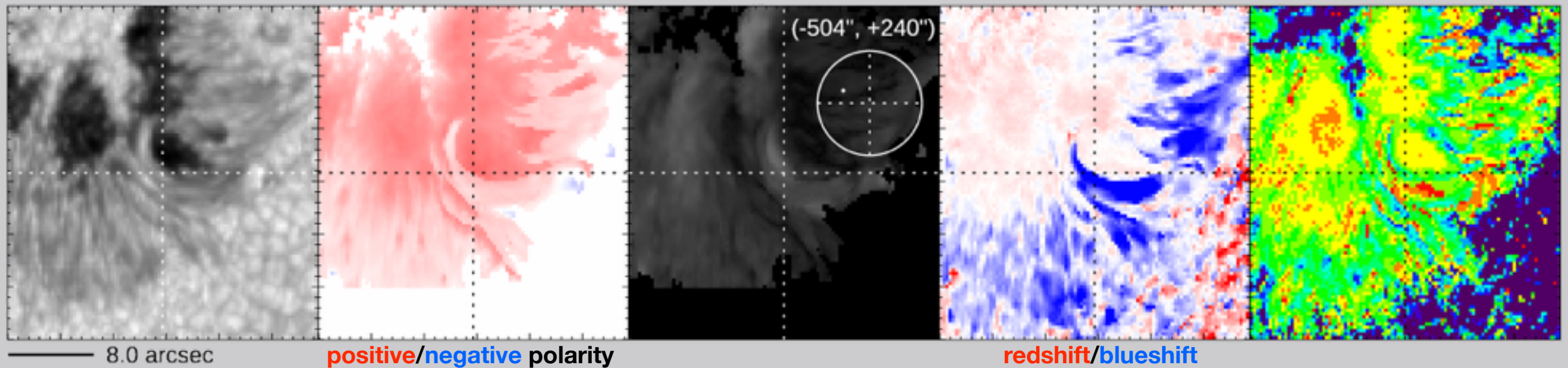
Continuum

B (LOS)

B (transverse)

Doppler velocity

Filling factor



Miscellaneous

Can a Flow Press Strong Fields ?

magnetic pressure

$$\frac{B^2}{8\pi}$$

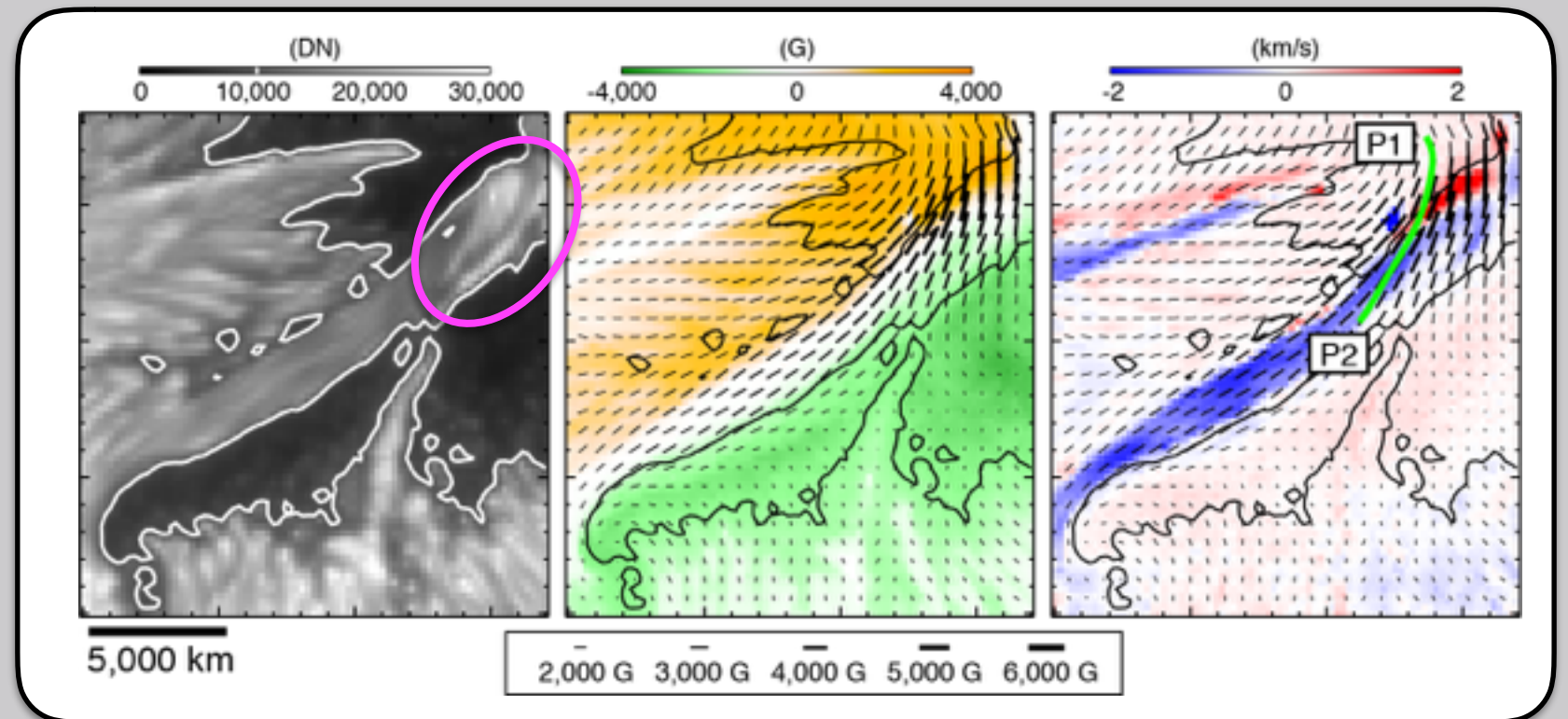
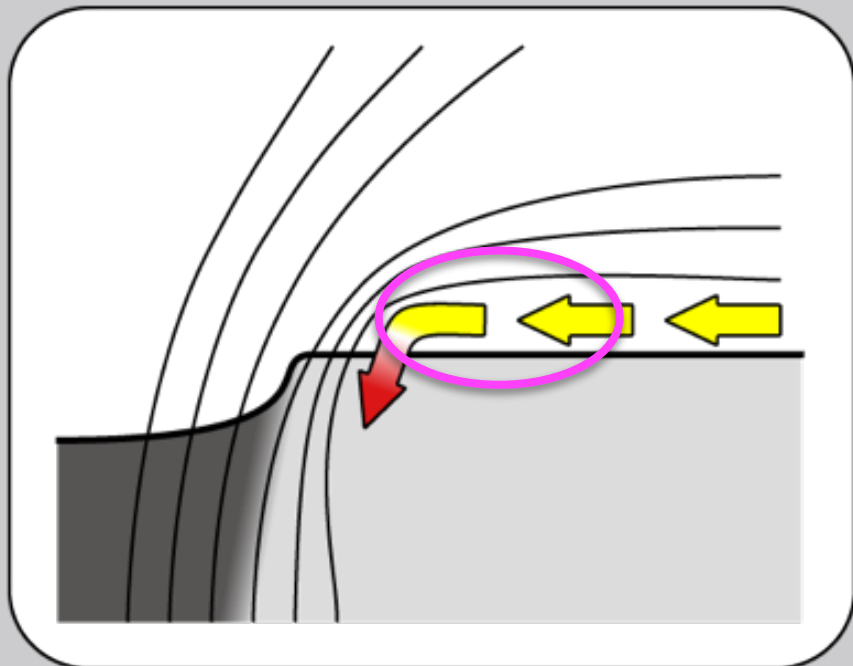
1 : 1

kinetic pressure

$$\frac{1}{2}\rho v^2$$

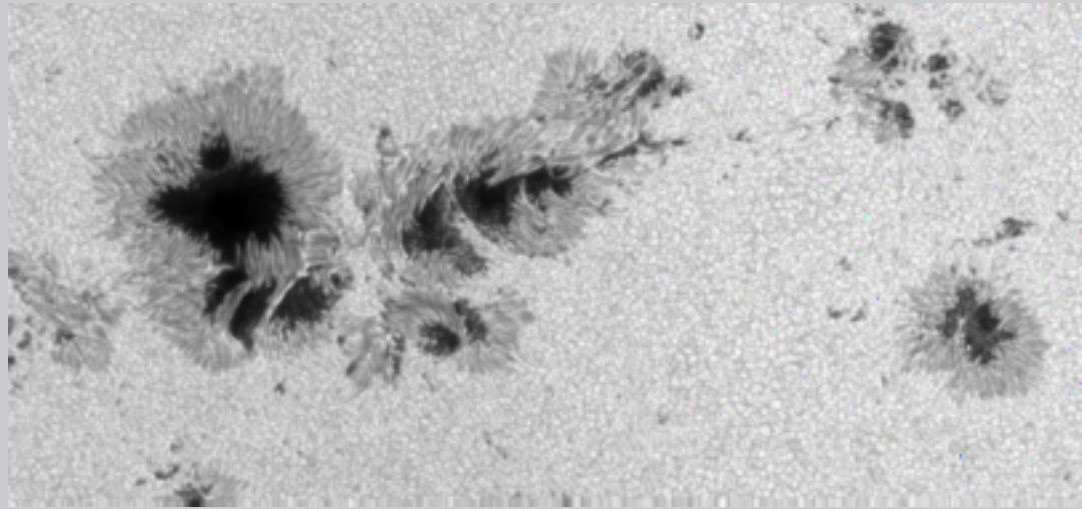
($B \sim 5,000$ G, $n \sim 10^{18}$ cm $^{-3}$, $v \sim 7$ km/s)

(number density: Model M of Maltby+1986)

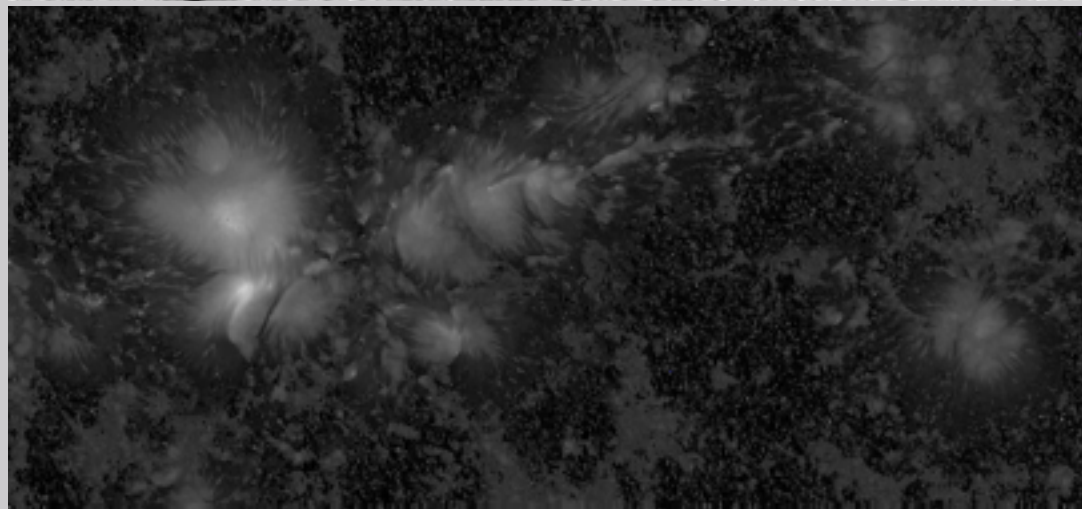


Dependence of Spatial Resolution in Inversion

original resolution
(0.32"/pix)



continuum



field
strength



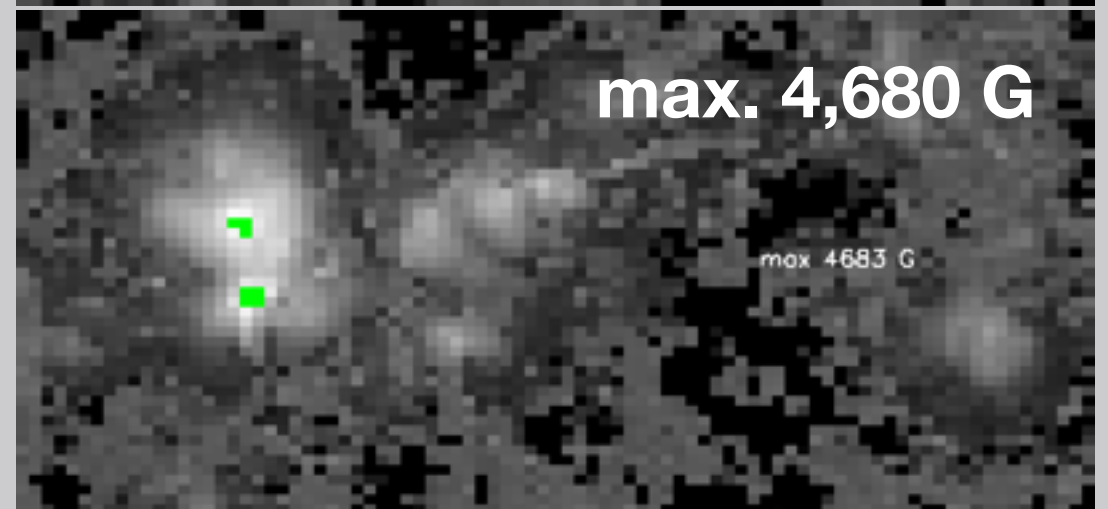
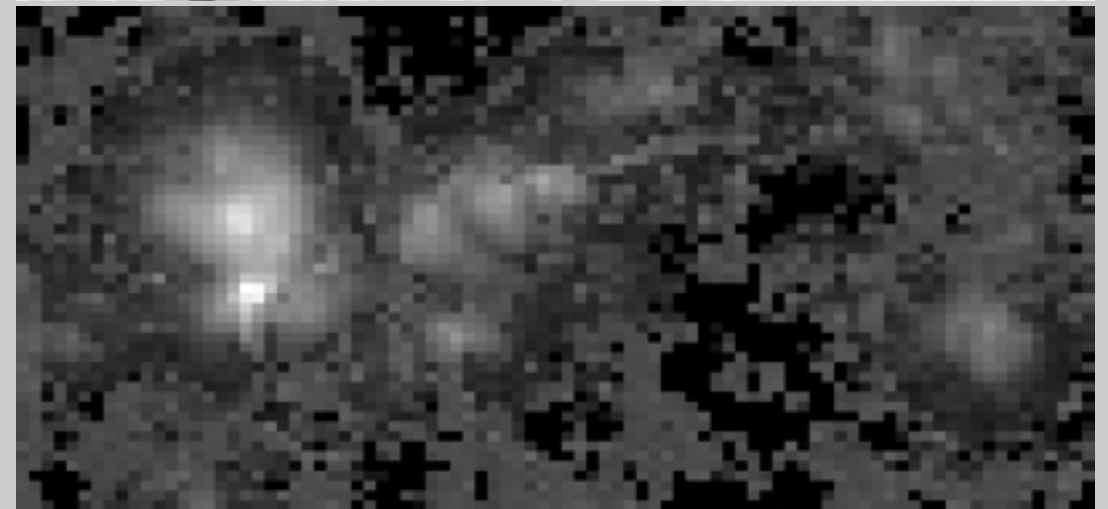
max. 5,390 G

colored
area

> 4,000 G

> 5,000 G

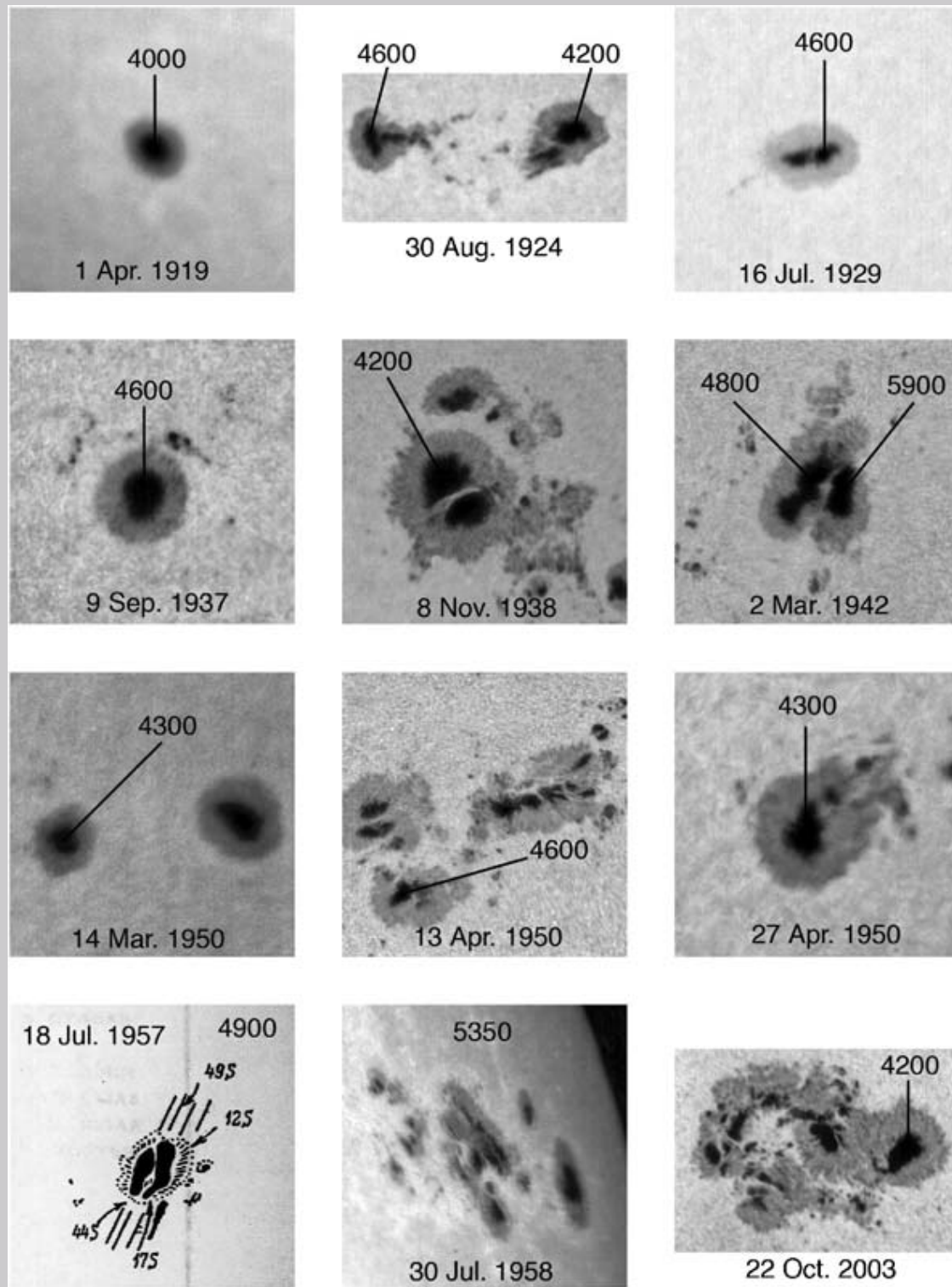
10 times coarser
(3.2"/pix)



max. 4,680 G

10x10 pix summing, without consideration of PSF

Spatial Resolution in Old Observations



Livingston+2006

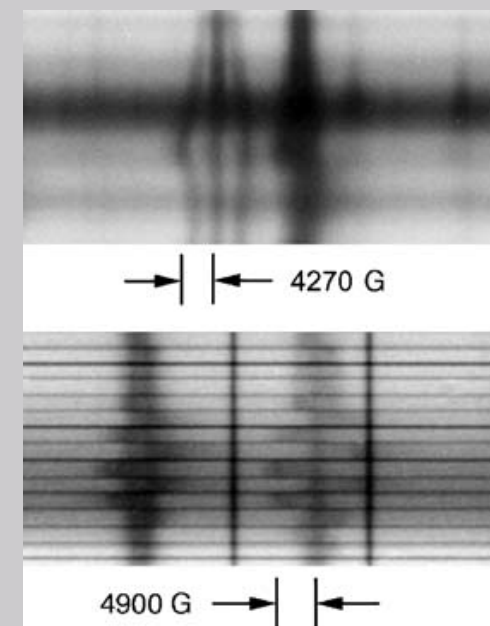


Figure 1. Examples of spectra. *Top* was obtained by J. Harvey (1986) using 525.0 nm on July 13, 1978 and refers to a light bridge in a complex sunspot. *Bottom* is from Baranovsky and Petrova (1957) using 630.2 nm on July 18, 1957. Field strengths are based on the total separation of the sigma components.

Figure 2. White light photographs (and a drawing) of strong-field spots. The width of the photographic panels is about 3.2 arc min.

All Sunspots with More Than 4,000 G

Livingston+2006

TABLE III

Sunspot groups with at least one measured magnetic field ≥ 4000 G.

<i>N</i>	Group	Date	<i>B</i> (G)	Lat	Obs	Observer	Ref	<i>N</i>	Group	Date	<i>B</i> (G)	Lat	Obs	Observer	Ref
1	1402	1919 Apr 1	4000	-20	M	Rodés	1	23	9199	1948 May 10	4200	-24	M	Hickox	2, 3
2	2095	1924 Aug 30	4200	22	M	Humason	1, 4		"	1948 May 12	4100	"	M	"	3
	"	"	4600	"	M	"	1, 4		"	"	3200	"	P	"	6
3	3726	1929 Jun 24	4300	-10	M	Hickox	2	24	9275	1948 Jun 28	4200	12	M	Hickox	2, 3
4	3754	1929 Jul 16	4600	-17	M	Richardson	2		"	1948 Jun 30	4100	"	M	"	3
5	5548	1937 Sep 9	4600	11	M	Hickox	2, 3	25	9317	1948 Jul 22-29	4300	12	M	Richardson	2, 3
6	6192	1938 Nov 8	4200	-9	M	"	2, 3		"	1948 Jul 26	2800	"	P	"	6
7	6725	1940 Jan 5	4100	12	M	"	2, 3	26	10027	1949 Oct 5, 8	4200	7	M	Hickox	2, 3
8	7297	1941 Oct 1	4100	2	M	"	3		"	1949 Oct 8	2800	"	P	"	6
9	7315	1941 Oct 31	4200	14	M	"	2, 3	27	10087	1949 Nov 6	4300	-10	M	Hickox	2, 3
10	7378	1942 Feb 28	6100	8	M	"	2, 3	28	10262	1950 Mar 14	4300	-16	M	"	2, 3
	"	1942 Mar 2	5900	"	M	"	3		"	"	2700	"	P	"	6
	"	"	4800	"	M	"	3	29	10303	1950 Apr 13	4600	13	M	Roques	2, 3
	"	1942 Mar 3	4300	"	P	Haffner	5		"	"	2500	"	P	"	6
	"	1942 Mar 4	4500	"	M	Hickox	3	30	10314	1950 Apr 25, 30	4200	-12	M	Hickox	2, 3
11	7550	1943 Feb 10	4500	5	M	"	2, 3		"	1950 Apr 26	2800	"	P	"	6
	"	1943 Feb 11	4200	"	M	"	3		"	1950 Apr 27	4300	"	M	Hickox	2, 3
12	7569	1943 Apr 3	4200	33	M	"	2, 3		"	1950 Apr 29	4100	"	M	"	2, 3
13	7617	1943 Oct 3	4300	16	M	"	2, 3	31	10347	1950 May 20	4300	-10	M	"	2, 3
14	7851	1945 Oct 4	4300	-22	M	"	2, 3	32	10382	1950 Jun 22, 23	4600	9	M	Roques	2, 3
15	8170	1946 Aug 29, 31	4200	9	M	"	2, 3	33	10384	1950 Jun 26	4600	9	M	"	2, 3
16	8319	1946 Dec 14, 16	4900	-6	M	"	2, 3	34	11352	1955 Oct 24	4100	28	M	Richardson	2, 3
	"	1946 Dec 18	4300	"	M	Richardson	3	35	11353	1955 Oct 24	4100	-23	M	"	2, 3
17	8707	1947 Jul 15	4300	13	M	"	2, 3, 4	36	11466	1956 Feb 20	4300	21	M	Cragg	2, 3
	"	1947 Jul 16	4100	"	M	Hickox	3	37	12417	1957 Jun 18	4100	18	M	"	2, 3
	"	1947 Jul 17	3700	"	P	"	6	38	12491	1957 Jul 17	5000	28	C	"	7
	"	1947 Jul 18	4100	"	M	Hickox	3		"	"	4900	"	C	"	8
18	8774	1947 Aug 15	4300	15	M	Richardson	2, 3, 4		"	"	2000	"	M	Hickox	3, 4
19	8833	1947 Sep 27	4200	17	M	Hickox	2, 3, 4		"	1957 Jul 18	4900	"	C	"	8
	"	1947 Sep 26	3000	"	P	"	6		"	"	4600	"	C	"	7
20	9086	1948 Mar 4	4200	17	M	Hickox	2, 3		"	1957 Jul 19	4700	"	C	"	7
	"	"	3200	"	P	"	6		"	"	4400	"	C	"	8
21	9150	1948 Apr 16, 17	4200	9	M	Hickox	2, 3		"	"	2300	"	M	Hickox	3, 4
	"	1948 Apr 17	3400	"	P	"	6	39	13388	1958 Jul 30	5350	-15	C	SS	9
22	9167	1948 Apr 26	4300	23	M	Hoge	2, 3	40	15733	1963 Jun 14	4000	11	C	"	7
	"	1948 Apr 25	2400	"	P	"	6	41	16150	1966 Oct 15	>4000	7	M	Cragg	3
									"	1966 Oct 19	4300	"	R	CCF	10

All Sunspots with More Than 4,000 G

Livingston+2006

<i>N</i>	Group	Date	<i>B</i> (G)	Lat	Obs	Observer	Ref
42	16387	1967 Jun 4	3600	23	M	Cragg	3
	"	1967 Jun 5	4000	"	R	CCF	10
	"	"	2800	"	C		7
	"	"	3000	"	M	Cragg	3
43	17196	1969 Mar 20	3600	22	M	Utter	3
	"	1969 Mar 22	4000	"	R	CCF	10
	"	"	2500	"	C		7
	"	1969 Mar 23	3000	"	M	Utter	3
44	17822	1970 Apr 7	4000	-12	M	Cragg	3
	"	1970 Apr 8	4300	"	R	CCF	10
	"	"	3100	"	C		7
	"	"	3400	"	M	Cragg	3
	"	1970 Apr 9	3800	"	M	"	3
	"	1970 Apr 10	3600	"	M	"	3
	"	1970 Apr 11	3800	"	M	"	3
45	18935	1972 Jul 31	3400	12	M	"	3
	"	1972 Aug 5	3200	"	M	"	3
	"	1972 Aug 7	4100	"	R	CF	10
	"	"	3100	"	C		7
	"	1972 Aug 8	5150	"	K		11
	"	"	2600	"	C	Shpitalnaya	7
	"	"	3000	"	R	CF	10
	"	"	2500	"	M	Cragg	3
46	19427	1974 Jul 3	4300	-14	O	Tanaka	17
	"	1974 Jul 4	4200	"	C		7
	"	"	3200	"	R	CC	10
	"	"	4130	"	N	Livingston	12
	"	"	3600	"	M	Cragg	3
47	19469	1974 Sep 11	4000	8	R	CC	10
	"	"	3200	"	C		7
	"	"	3200	"	M	Cragg	3
	"	1974 Sep 13	4000	"	R	CC	10
	"	"	3300	"	C		7
	"	"	3200	"	M	Cragg	3
48	19512	1974 Nov 19	4100	14	C		7
	"	"	3800	"	R	CC	10
	"	1974 Nov 21	3200	"	M	Adkins	3

<i>N</i>	Group	Date	<i>B</i> (G)	Lat	Obs	Observer	Ref
49	20123	1978 Jul 13	4300	18	N	Harvey	13
	"	"	3600	"	C		7
	"	"	2700	"	M	Gregory	3
	"	1978 Jul 14	3800	"	C		7
	"	"	2500	"	M	Gregory	3
50	21358	1980 Apr 8	3200	13	M	Webster	3
	"	1980 Apr 9	4000	"	C		14
	"	"	2800	"	M	Webster	3
51	21567	1980 Jul 6	4100	28	C		14
	"	"	2100	"	M	Webster	3
	"	1980 Jul 7	4600	28	C		14
	"	"	2100	"	M	Webster	3
52	24223	1985 May 11	>3800	-12	R	Croce	10
	"	1985 May 13	3500	"	C		7
53	26825	1991 Jun 6	3800	32	M	?	4
	"	1991 Jun 7	4100	"	C		7, 14
54	31909	2003 Oct 22	4200	4	C	Stepanian	15
	"	"	>3000	"	M	Padilla	4
55	32158	2004 Jul 23	4100	8	C		16
	"	"	>3000	"	M	Gilman	4

Notes. Group is the Mt. Wilson Observatory sunspot group number. *B* (G) is the magnetic field strength in Gauss. Lat is the latitude in degrees. Obs is the observatory abbreviated as follows: C = Crimean Astrophysical Obs., K = Kislovodsk, M = Mt. Wilson Obs., N = National Solar Obs., Kitt Peak, O = Okayama, P = Potsdam, R = Astro. Obs. of Rome. Observers are abbreviated as follows: CC = Casamassima and Croce, CCF = Cacciani, Croce and Flamini, CF = Croce and Flamini, SS = Stepanian and Selivanov. References: 1. Hale and Nicholson (1938). 2. *Pub. Astro. Soc. Pacific*, bi-monthly from 1920 to 1961. 3. Microfilm copies of original Mt. Wilson drawings. 4. <ftp://howard.astro.ucla.edu/pub/obs/drawings/>. 5. von Klüber (1947). 6. *Pub. Astro. Obs. Potsdam*. 7. <http://www.gao.spb.ru/database/mfbase/gmaps/krao/>. 8. Baranovsky and Petrova (1957). 9. Steshenko (1967). 10. *Solar Phenomena*, Astro. Obs. Rome, monthly. 11. Shpitalnaya, Makarov and Den (1973). 12. Livingston (1974). 13. Harvey (1986). 14. *Solar Data Bulletin*, Pulkovo Obs. 15. Personal communication. 16. <http://crao.crimea.ua/projects/solar/sunspot/DATA/>. 17. Tanaka (1991).

Histogram of Strongest Fields

Livingston+2006

The value of 6,100 G was not mismeasured, because 5,900 G was also detected 2 days later.

4.6% (>3,000 G)

1.5% (>3,500 G)

0.4% (>4,000 G)

0.09% (>4,500 G)

The abstract says that the rate of more than 4,000 G is 0.2%.

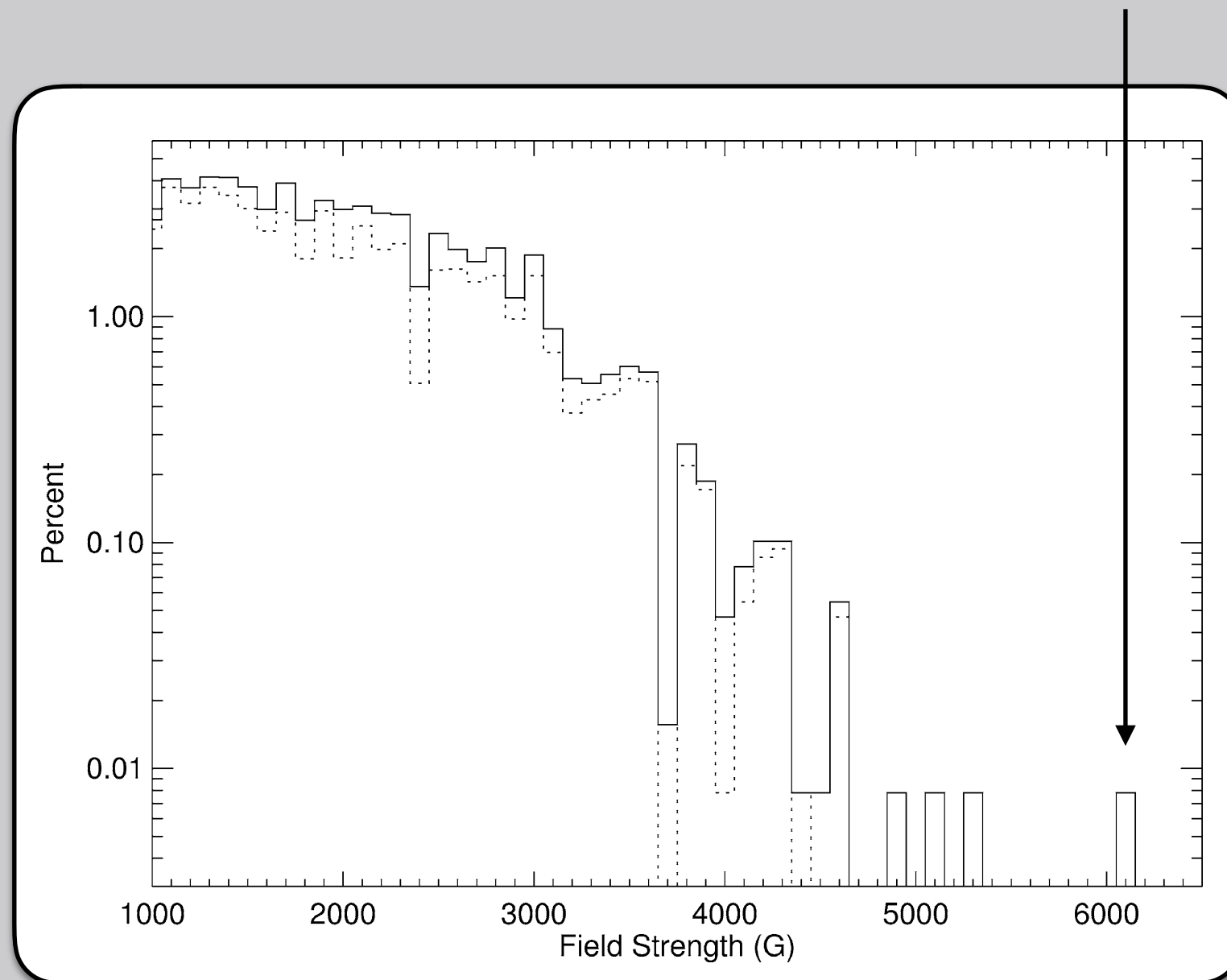


Figure 3. Distribution of maximum field strengths in 12 804 sunspot groups measured at Mt. Wilson (1917–1964) and Rome (1965–1974). Seven measurements from Table III not included in the Mt. Wilson and Rome data were added. The *dashed histogram* is only Mt. Wilson measurements.

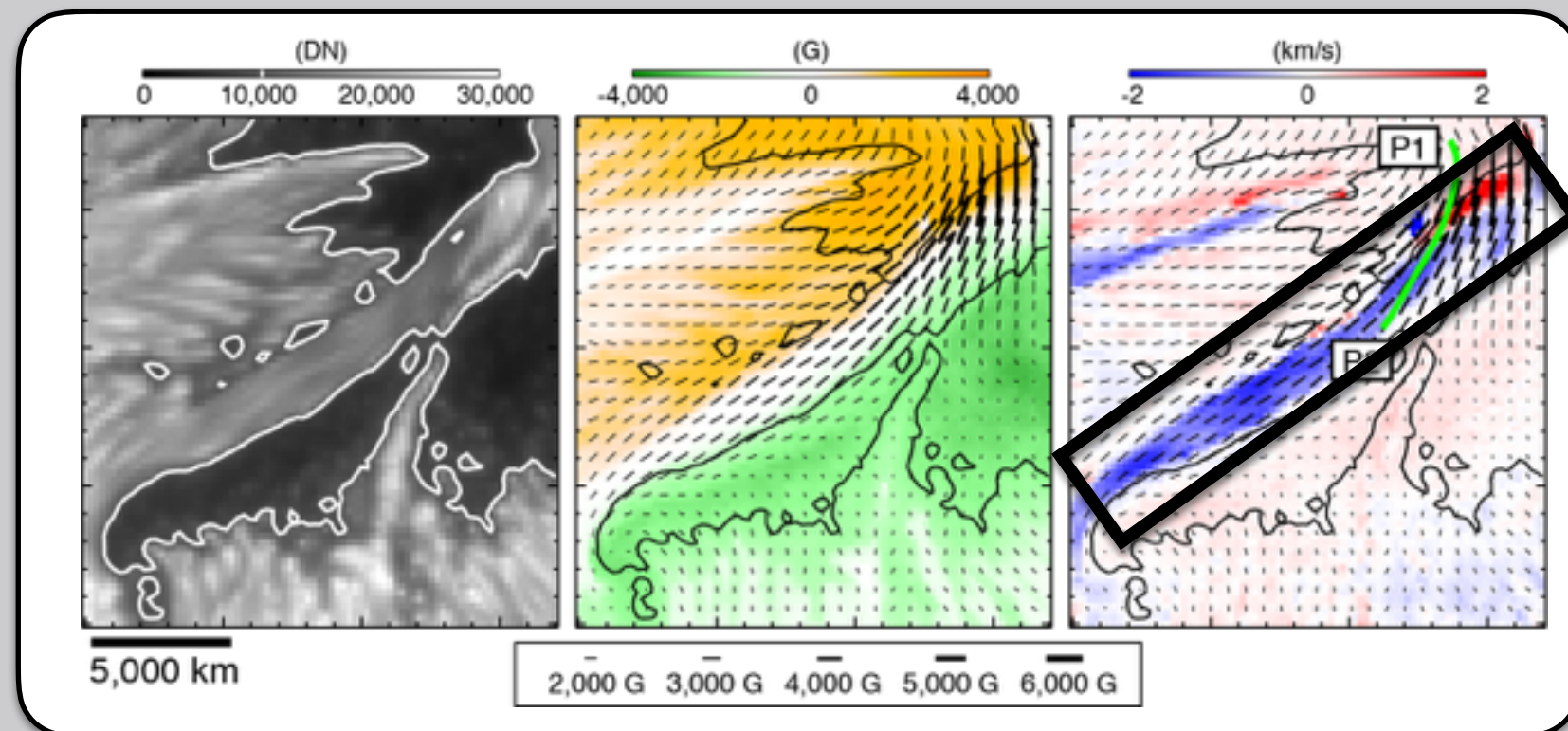
Comments

From Alberto Sainz Dalda

Penumbrae always have 2 components with different inclinations, and the observed spectra are complex. The ME inversion does not work for such spectra. The results based on the ME inversion are not reliable and not inappropriate to scientific discussion/papers.

Should check the results of 2-component inversion at least around the strong field regions in penumbrae/light bridges.

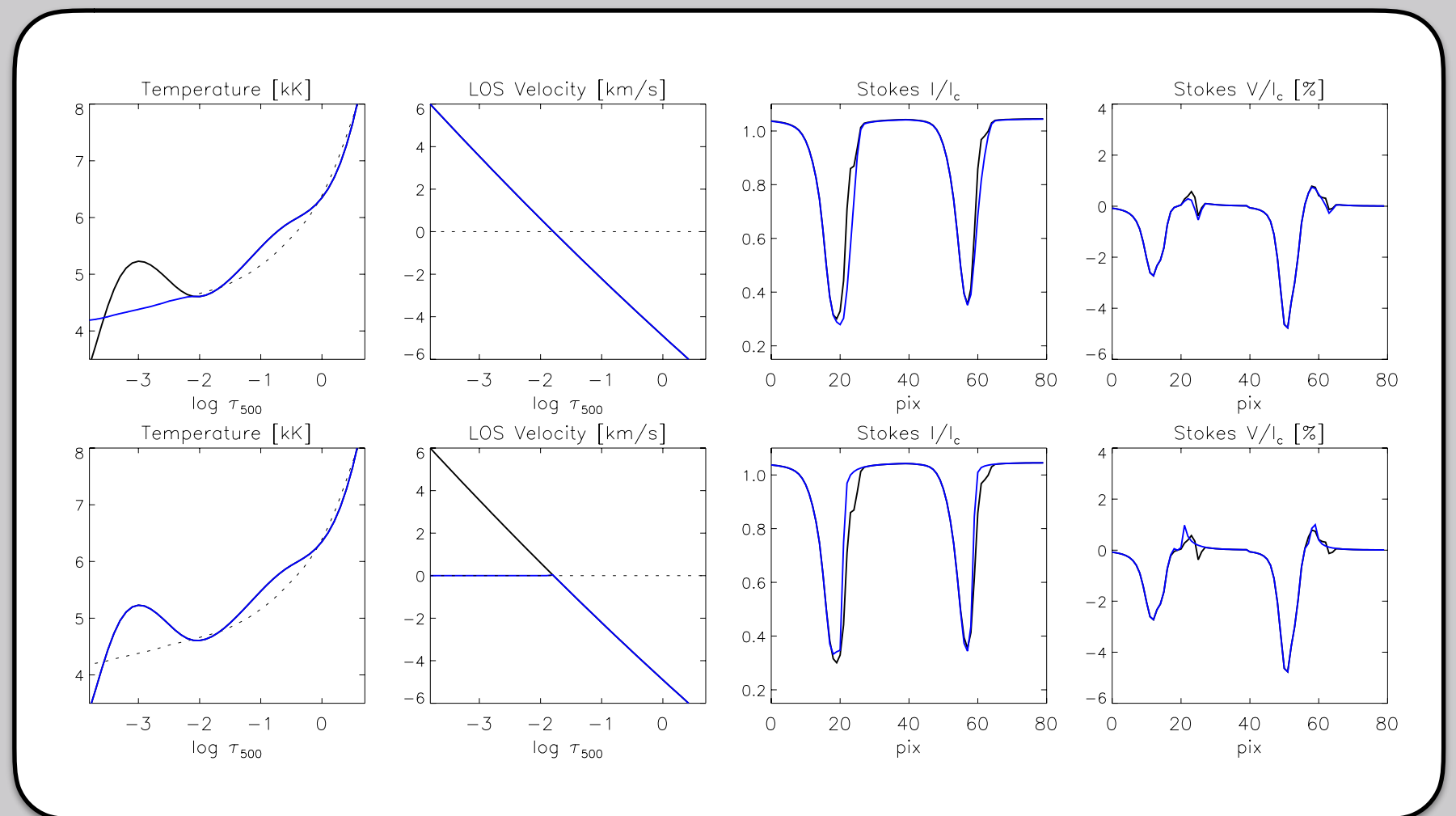
From Ted Tarbell,
the ME inversion is enough
for the statistics studied here.



Comments

From Carlos Quintero Noda,

Alberto's comment is too pessimistic. The statistics is good as the first step of this study. But, it is worth checking the LOS variation of physical parameters to fit the residual components from the ME results.



Comments

From Sacha Brun

Which phase in the sunspot evolution does the strongest field appear ?

It may provide some restrictions to the mechanism of sunspot emergence and occurrence of flares.

However, note that most of the ARs studied here already existed at the beginning of each observation. Large ambiguity needs be considered to count days after appearance.

Comments

From Alan Title

My presentation uses numerous color figures. Too colorful figures are problematic for color-blind people.

Method

screening → extract of strongest field → sort into AR

[used data] **SP level-2 data provided by HAO**

Oct. 25, 2006 – September 16, 2016

MERLIN inversion, limited field strength 5,000 G

partially used MEKSY inversion data (by NAOJ) for pixels > 5,000 G

= Milne-Eddington Katsukawa Shimojo Yokoyama

▶ **screening**

15,302 scans



< 600'' from the disk center

9,187 scans



selection of images having sunspots or pores by visual confirmation

4,566 scans

Method

screening → **extract of strongest field** → sort into AR

▶ searching for a pixel with the largest field strength in each scan dataset

- ignore pixels and fits files with obviously-strange profiles and polarization degree of less than 4%
- the pixel with the strongest field should have at least one surrounding pixel with less-than-500-G difference from the largest value
 - if not, delete the pixel, and then repeat the process with a new pixel with the strongest

removed

3,000	3,000	3,000
3,000	4,100	3,000
3,000	3,000	3,000

accepted

3,000	3,000	3,000
3,000	4,100	3,900
3,000	3,000	3,000

Method

screening → extract of strongest field → **sort into AR**

- ▶ sorting all scans by AR number (by hand)

419 ARs

12 – 2 ARs in one FOV
7 – unnamed AR

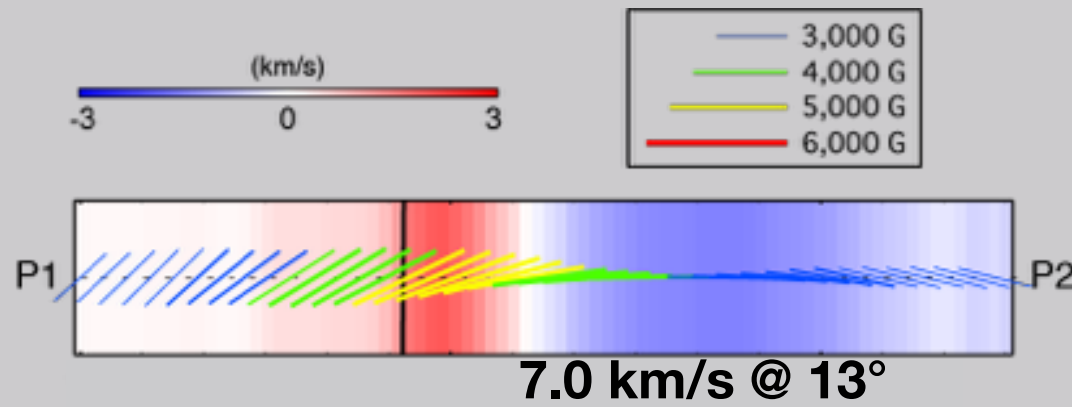
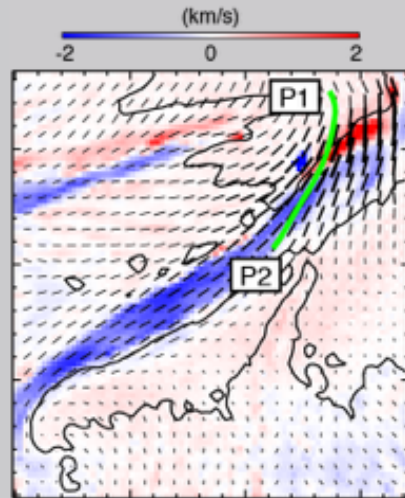
- ▶ investigating physical parameters and locations of the strongest field in each AR

- location
- spectral shape
- close to PIL
- redshift at the location
- horizontal flow toward the location
- fitting result
- filling factor

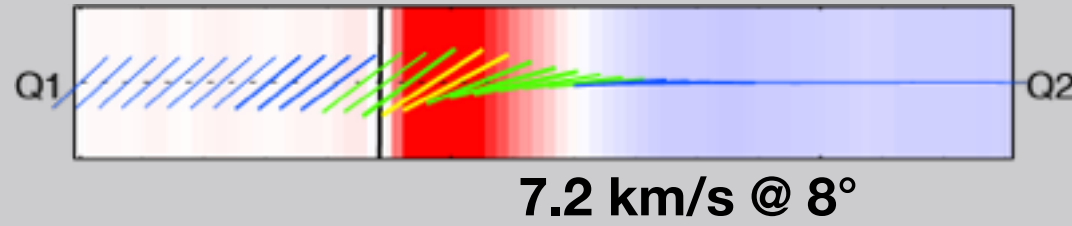
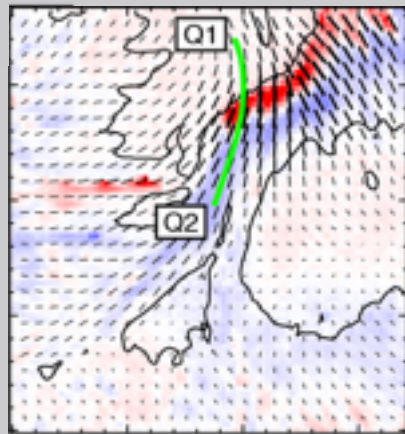
[umbra] [penumbra] in large sunspot
[umbra] [outside umbra] in small ss.
[light bridge]

Doppler Velocity and Field Strength

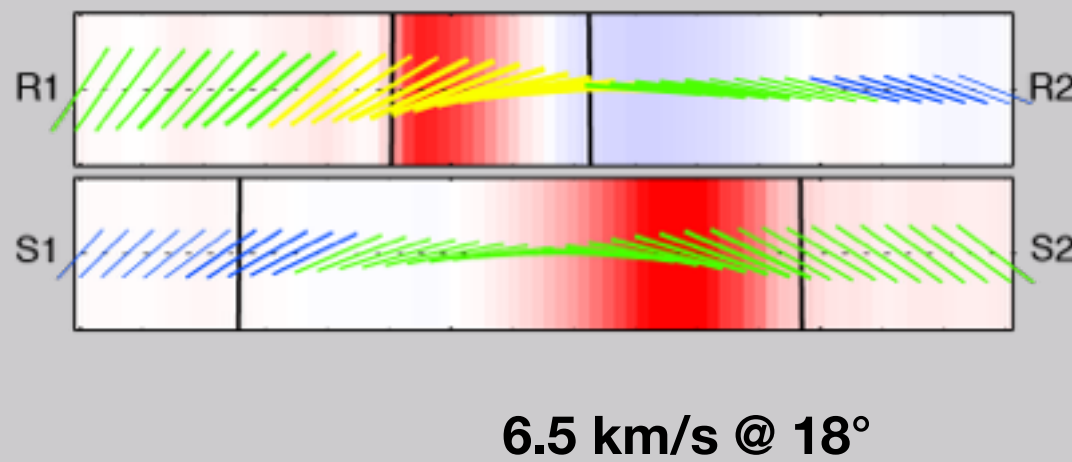
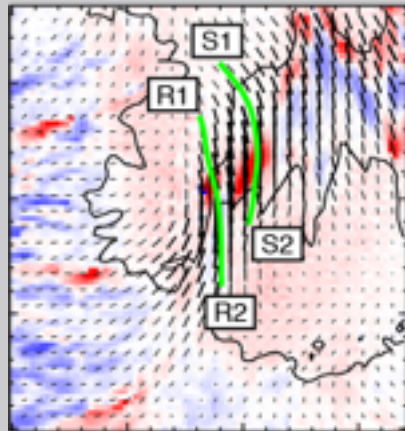
Feb. 02
16:11 UT



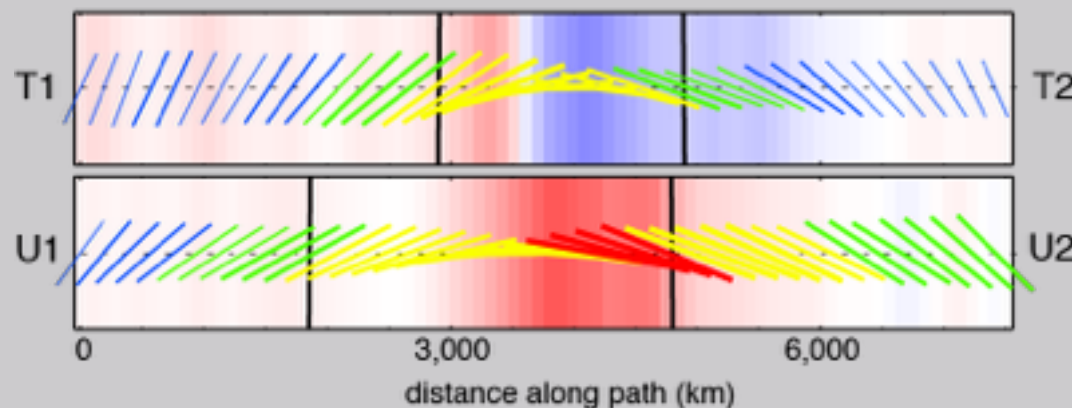
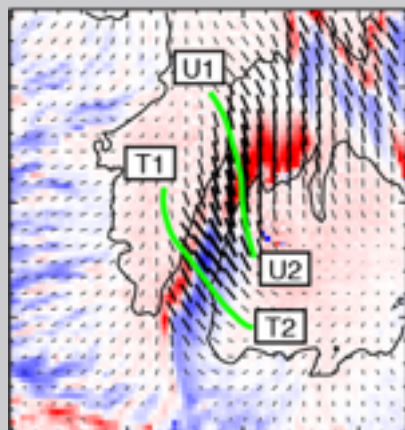
Feb. 03
18:34 UT



Feb. 04
15:54 UT



Feb. 04
19:11 UT



similar features seen during the observations

at the boundary

- blueshift → redshift
- inclination increased
- field strength enhanced

key structures